Aus dem Max von Pettenkofer-Institut für Hygiene und Medizinische Mikrobiologie

Lehrstuhl für Bakteriologie

der Ludwig-Maximilians-Universität München

Vorstand: Prof. Dr. Dr. Jürgen Heesemann

The role of the tumor suppressor CYLD in *Yersinia enterocolitica* infection

Dissertation
zum Erwerb des Doktorgrades der Humanbiologie (Dr. rer. biol. hum.)
an der Medizinischen Fakultät der
Ludwig-Maximilians-Universität zu München

vorgelegt von
Liu Yunying
aus V.R. China
2013

Mit Genehmigung der Medizinischen Fakultät
der Universität München

Berichterstatter: Prof. Dr. Dr. Jürgen. Heesemann

Mitberichterstatter: Prof. Dr. Simon. Rothenfußer
Prof. Dr. Thomas. Löscher

Mitbetreuung durch den promovierten Mitarbeiter: Dr. Hicham. Bouabe

Dekan: Prof. Dr. med. Dr. med. h.c. M. Reiser, FACR, FRCR

Tag der mündlichen Prüfung: 28. 02. 2013

CONTENTS

1. Introduction

1.1 *Yersinia enterocolitica*

1.1.1 *Yersinia* species and infection

*Yersinia*e are gram-negative bacteria that belong to the family of Enterobacteriaceae. They are facultative anaerobes with an optimal growth temperature of 27°C. There are 11 known species and 3 of them are pathogenic for humans: the genetically closely related *Y. pseudotuberculosis* and *Y. pestis* and the more distantly related *Y. enterocolitica*. These bacteria share a common tropism for lymphoid tissues and the ability to resist the host protective innate immune responses, even though their routes of transmission are quite different. *Y. enterocolitica* and *Y. pseudotuberculosis* infections typically result in gastroenteritis and lymphadenitis while *Yersinia pestis* is the causative agent of pneumonic plagues and bubonic plagues. *Y. enterocolitica* are commonly transmitted via the fecal-oral route (Putzker et al., 2001). Humans usually get infected by the consumption of contaminated food (in particular pork) or water. After ingestion, the bacteria survive passage through the stomach and enter the small intestine where they cross the intestinal barrier probably through specialized epithelial cells called M cells to disseminate into mesenteric lymph nodes, liver and spleen (Fig.1) (Hanski et al., 1989). M cells are dispersed among the villi of the small intestine in non-follicle-associated epithelium or associated with follicle-associated epithelium where they overlay lymphoid follicles such as Peyer's patches (Siebers and Finlay, 1996).

Y. pestis is commonly transmitted through flea bites or by inhalation and then invades and multiplies in regional lymph nodes corresponding to the infection point (Achtman et al., 1999; Brubaker, 1991). Subsequent dissemination via the lymphatic system and bacteremia with necrotic and hemorrhagic lesions in many organs lead to death of humans or rodents (mice, rats) within 2 to 3 days after infection.

1.1.2 Virulence factors of *Y. enterocolitica*

Common to all three human pathogenic Yersinia species is the presence of a 70-kb virulence plasmid (pYV) (called pCD1 in *Y. pestis*) that encodes the nonfimbrial Yersinia adhesin YadA (*Y. pestis* does not express YadA as a result of inactivating gene mutation), a type III secretion system (T3SS; also known as the injectisome, for Yersinia: Ysc-T3SS), and several secreted and translocated host cell injected effector proteins called Yersinia outer proteins
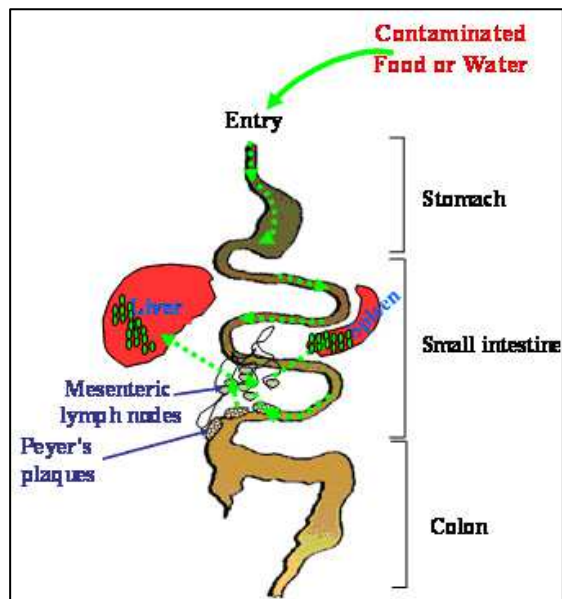
Fig. 1. Scheme of infection route of *Y. enterocolitica*. *Y. enterocolitica* are commonly transmitted to humans by the consumption of contaminated food or water. After ingestion, the bacteria survive passage through the stomach and enter the small intestine, where they cross the intestinal barrier through M cells to multiply in the PPs and mesenteric lymph nodes, and finally disseminate into liver and spleen.

(Yops) (Cornelis, 2002). Besides the pYV plasmid, enteropathogenic yersiniae also carry two chromosomally-located virulence determinants which support the intestinal invasion and virulence in mice: the *inv* gene, encoding an outer membrane protein called invasin (Inv) (*Y. pestis* does not express Inv as a result of inactivating gene mutation), which mediates the penetration of enterophatogenic yersiniae across the mucosal barrier by targeting M-cells (Clark et al., 1998; Hanski et al., 1989; Isberg et al., 2000; Isberg and Leong, 1990), and the high pathogenicity island (HPI), which comprises genes involved in the synthesis of the siderophore yersiniabactin (Ybt) (Carniel, 2001; Schubert et al., 2004). The HPI is also present in *Y. pestis* and other members of Enterobacteriaceae (e.g. extraintestinal *E. coli*, pathotype ExPEC).

The plasmid-encoded Ysc–T3SS allows *Yersinia* to deliver Yops into the cytosol of targeted phagocytes and other hematopoetic cells. These Yop effectors could disturb the dynamics of the cytoskeleton and block the phagocytosis by macrophages and polymorphonuclear leukocytes (PMNs) (Ruckdeschel et al., 1995; Fallman et al., 1995; Persson et al., 1997; Rosqvist et al., 1990; Visser et al., 1995). They could also impair the production of reactive oxygen/nitrogen species (ROS/RNS), pro-inflammatory cytokines, chemokines as well as adhesion molecules (Boland and Cornelis, 1998; Denecker et al., 2002; Palmer et al., 1998; Schulte et al., 1996). These actions allow the invading *Yersinia* to survive and multiply extracellularly, mainly in lymphoid tissues such as lymph nodes, spleen and liver (Cornelis et al., 1989; Simonet et al., 1990).

The Ysc–T3SS includes the Ysc (Yop secretion) needle-like apparatus — called the Ysc injectisome — and about 6 Yop effector proteins that are secreted by this apparatus. The tip protein LcrV (*Yersinia* V antigen) together with YopB and YopD act as transmembrane channel (translocon) by forming pores in the host cytoplasma membrane, whereby Yops are translocated into the cytosol of target cell (Fig.2) (Hakansson et al., 1996; Neyt and Cornelis, 1999; Rosqvist et al., 1991; Sory and Cornelis, 1994). Upon delivery into a host cell, Yop effectors modulate eukaryotic signaling pathways for the benefit of the pathogen (Fig.2) (Viboud and Bliska, 2005).
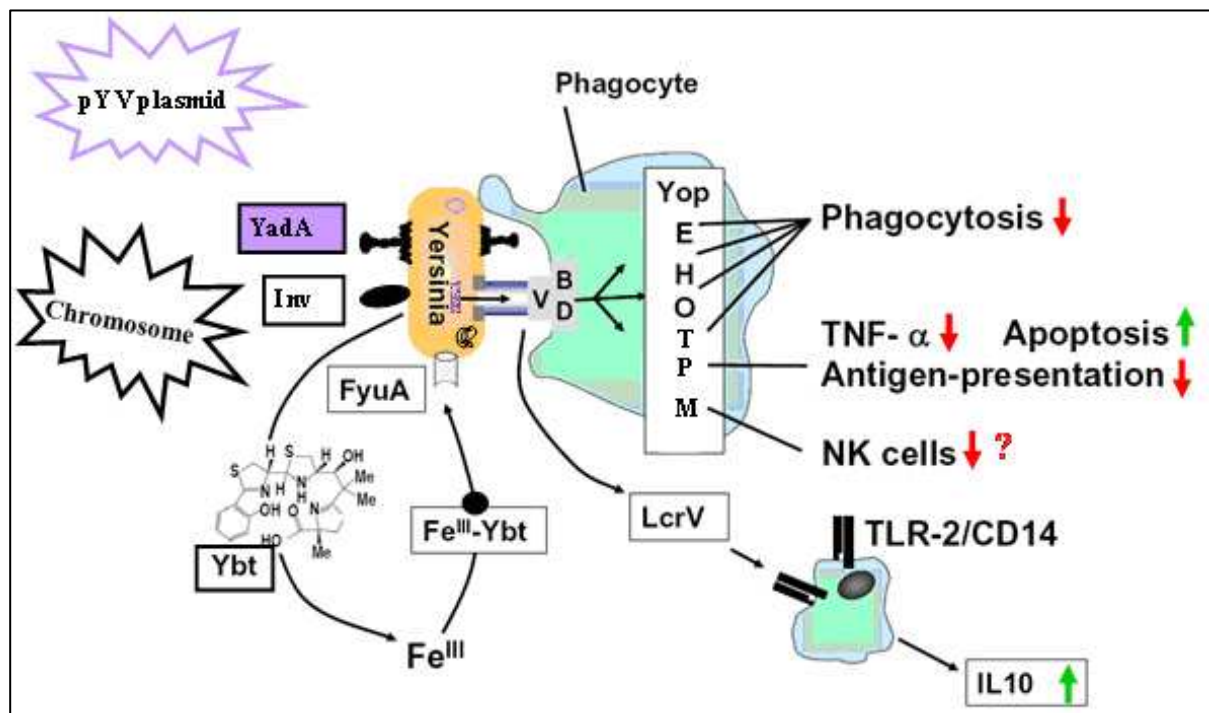
Fig. 2. Offense weapons of *Yersinia*. (Modified from Heesemann et al., 2006). Yersiniae harbor pYV-plasmid- and chromosomally-encoded virulence factors. pYV encodes the T3SS, a set of about six anti-host effector proteins (Yersinia outer proteins YopE, YopP, YopT, YopH, YopO and YopM) which are microinjected into contacted host cells to play their roles, and the nonfimbrial Yersinia adhesin YadA. With this armament, yersiniae replicate extracellularly in lymphatic tissue and encounter the immune defenses of the host. The chromosomally-encoded virulence factors include the *inv* gene, encoding an outer membrane protein called invasin (Inv), which mediates the penetration of yersiniae across the mucosal barrier by targeting M-cells, and the high pathogenicity island (HPI), which encodes the yersiniabactin (Ybt) iron-uptake system.

So far, six Yop effectors have been identified and functional characterized: YopH, YopE, YopT, YopO / YpkA, YopP/YopJ and YopM. A short summary of the functions of Yops is given bellow:

YopE is a GTPase-activating protein that acts preferentially on RhoG and with lower activity on Rac1 and RhoA, which may explain the YopE-associated effect of actin stress fiber destruction (Black and Bliska, 2000; Roppenser et al., 2009; Rosqvist et al., 1991; Von Pawel-Rammingen et al., 2000). Recent research showed that YopE could also inhibit reactive oxygen species (ROS) production by inactivating Rac2 (Songsungthong et al., 2010).

YopH contains a C-terminal catalytic domain that is very similar to eukaryotic protein tyrosine phosphatase (PTPase) enzymes (Zhang et al., 1994) and is involved in resistance to phagocytosis and inhibition of oxidative busrt (Guan and Dixon, 1990). YopH affects phosphotyrosine proteins associated with signalling from the ß1-integrin receptor, such as focal adhesion kinases, p130Cas, and the immune-cell-specific Fyn-binding protein (Fyb, also called ADAP or SLAP-130) (Black and Bliska, 1997; Hamid et al., 1999; Persson et al., 1997). YopH also downregulates the expression of monocyte chemoattractant protein 1 (MCP-1), a chemokine that is involved in the recruitment of macrophages to lymph nodes (Sauvonnet et al., 2002). In addition, YopH also contributes to the modulation of the adaptive immune response by impairing T- and B-cell activation (Alonso et al., 2004; Yao et al., 1999).

YopM is still enigmatic. It is a leucine-rich repeat (LRR) protein that can traffic to the nucleus of infected cells (Boland et al., 1996), but its function is as yet unclear. YopM has been shown to causes a decrease in NK cell populations in spleens (McCoy et al., 2010). YopM forms a protein complex with two cellular kinases, protein kinase C-like 2 (PRK2) and ribosomal S6 kinase 1 (RSK1) (McDonald et al., 2003). The interaction of YopM with RSK1 seems to be essential for virulence of Yersinia (McCoy et al., 2010). Recently, it was shown that the LRR6-15 region of the YopM of *Y. pseudotubeculosis* is required for PRK2 binding, whereas the C-terminal domain of YopM (from LRR12 to C-terminus) is required for binding to RSK1. Deletion of either of these domains from YopM resulted in increased production of IFN-γ and decreased levels of IL-18 and IL-10 in serum of infected mice, and subsequently to the abrogation of the virulence of *Y. pseudotuberculosis* via the orogastric route of infection (McPhee et al., 2010).

YopO (YpkA in *Y. pseudotuberculosis* and *Y. pestis*) is a multidomain protein that contains an N-terminal serine/threonine kinase domain, a C-terminal guanine nucleotide dissociation inhibitor (GDI) domain Rho-GTPase, followed by a domain required for binding to actin. The GDI domain of YopO binds to and prevents nucleotide exchange in Rac and RhoA that results in the inhibition of stress fiber formation (Barz et al., 2000; Dukuzumuremyi et al., 2000;). However, YopO seems to specifically block Rac-dependent Fc-receptor internalization pathway but not complement receptor 3-dependent uptake, which is controlled by Rho activity (Groves et al., 2010).

Actin binding to YopO is necessary for effective autophosphorylation of YopO at amino acids serin (S) 90 and S95 and subsequent activation of YopO's kinase activity (Trasak et al., 2007). The kinase activity of YopO regulates rounding/arborization and is specifically required for inhibition of Yersinia YadA-dependent phagocytosis (Trasak et al., 2007). Previously, a

molecular target for the serine/threonine kinase domain of *Yersinia* protein kinase A (YpkA) has been discovered. Navarro et al. demonstrated that YpkA phosphorylates Gαq at Ser47, a key residue located in the diphosphate binding loop that is important for GTP binding, and thus resulting in the impairment of guanine nucleotide binding by Gαq and subsequent inactivation of multiple Gαq-mediated signalling pathways (Navarro et al., 2007). Interestingly, Gαq knockout mice have increased bleeding times and defective platelet activation (Offermanns et al., 1997). Bleeding abnormalities are, remarkably, also the hallmark phenotype of the plague, suggesting that YpkA-mediated inhibition of Gαq may contribute to the most documented symptoms of *Yersinia pestis* infection, extensive bleeding (Laskowski-Arce and Orth, 2007; Navarro et al., 2007).

YopQ (YopK in *Y. pseudotuberculosis* and *Y. pestis*) has been shown to control the translocation of Yop effectors into eukaryotic cells by regulating the size of the translocation pore (Holmstrom et al., 1997). Recently, YopK has been shown to inhibit NLRP3/NLRC4 inflammasome recognition of TTSS by yet unknown mechanism (Brodsky et al., 2010).

YopT is a cysteine protease that preferentially inactivates Rho GTPases, including RhoA, Rac1 and Cdc42, by cleaving the C-terminal geranylgeranylated-cysteine methyl ester and thereby releasing the GTPases from the membrane and leading to their inactivation (Fueller and Schmidt, 2008; Shao et al., 2002; Zumbihl et al., 1999).

YopP (YopJ in *Y. pseudotuberculosis* and *Y. pestis*) induce apoptosis in macrophages and dendritic cells (DCs), but not in human neutrophils (Spinner et al., 2010), and inhibit the activation of the mitogen-activated protein kinases (MAPKs), like extracellular signal-regulated kinase (ERK), c-Jun N-terminal Kinase (JNK) and p38, and the Nuclear factor-kappa B (NF-κB), thereby inhibiting the release of inflammatory cytokines, such as tumor necrosis factor alpha (TNF-α) and interleukin-8 (IL-8) (Ruckdeschel et al., 1997, 1998, Boland and Cornelis, 1998; Denecker et al., 2001; Denecker et al., 2002).

However, the molecular function of YopP/J is controversial. Whereas some reports have shown that YopJ has acetyltransferase activity and prevent activation of IKK and MAPKK family members by acetylating serine and threonine residues in the activation loop of MAPKKs and IKKs (Mittal et al., 2006; Mukherjee et al., 2006), other studies showed that YopJ acts as a cysteine protease and, similarly deubiquitinates proteins by cleaving of lysin (K)48- and K63-linked (poly)ubiquitin chains from proteins involved in the signal transduction cascade, such as TRAF2, TRAF6, IKKα, IKKß, and IκBα and thereby inhibiting activation of NF-κB (Haase et al., 2005; Sweet et al., 2007; Thiefes et al., 2006; Zhou et al., 2005a). This attenuation of signal transduction is clearly observed when YopP/YopJ is

overexpressed. Whether YopP/YopJ is involved in attenuation of the ubiquitination of cellular proteins by direct deubiquitination remains to be elucidated (Haase et al., 2005; Mukherjee et al., 2007), because both ubiquitination and phosphorylation are essential post-translational modifications that are involved in the activation of MAPK and NF-κB signaling pathways (Perkins, 2006). Furthermore, phosphorylation is often a prerequisite for subsequent substrate recognition by the ubiquitin-conjugating machinery to dock with and ubiquitinates substrates (Adhikari et al., 2007; Perkins and Gilmore, 2006; Yamamoto et al., 2006). Thus, YopJ-mediated acetylation of MKKs that competes with phosphorylation targeted to the same serine and threonine residues would result in the attenuation of ubiquitination and, subsequently, alter the course of MAPK and NF-κB signaling pathways.

There are yet no known eukaryotic functional homologs of YopJ that have executed serine and threonine acetylation. In contrast, many cellular deubiquitinating enzymes are known, which attenuates NF-κB signalling by selectively removing K48-linked monoubiquitin and/or K63-linked polyubiquitin chains (Sun, 2008).

1.2 The NF-κB family

NF-κB was first identified as a DNA-binding complex governing transcription at the immunoglobulin light chain gene intronic enhancer over 25 years ago (Lenardo et al., 1987; Sen and Baltimore, 1986). Later on, it was identified as a principal transcriptional regulator that plays a pivotal role in innate and adaptive immunity, inflammation, development, cell proliferation and survival. In mammals, the NF-κB family consists of five members called RelA (p65), RelB, c-Rel, NF-κB1 (p50/p105), and NF-κB2 (p52/p100) (Gilmore and Herscovitch, 2006). RelA, RelB, and c-Rel are synthesized as mature proteins associated with inhibitory proteins termed IκBs (inhibitors of NF-κB), while NF-κB1 and NF-κB2 are first synthesized as large precursors, p105 (105kDa) and p100 (100kDa), which are posttranslationally processed to the DNA-binding subunits p50 and p52, respectively.

NF-κB proteins are characterized by the presence of a conserved 300-amino acid Rel homology domain (RHD) that is located toward the N terminus of the protein. The RHD contains a nuclear localization sequence (NLS) and is responsible for dimerization, interaction with IκBs, and binding to DNA. Besides to the RHD, RelA or RelB and c-Rel also contain a transactivation domain through which they activate transcription (Ghosh and Karin, 2002). In contrast, p50 and p52 have only a DNA binding domain and lack the transactivation domain. Therefore, p50 and p52 are only able to promote gene transcription if they either form a

heterodimer with RelA, RelB, or c-Rel or recruit other coactivators, like Bcl-3 (a member of the IκB family) (Massoumi et al., 2006), which contains a transactivation domain that switches the transcriptional properties of NF-κB p50 or p52 homodimers from a repressive state to an activating state.

Generally, in normal resting cells, NF-κB members are sequestered within the cytoplasm in a latent form as a homo- and heterodimeric complex through its association with the inhibitory IκB proteins, which consists of IκBα, IκBβ, IκBε, IκBγ and Bcl-3 (Hayden and Ghosh, 2004). IκBs contain multiple ankyrin repeats that interact with and mask the NLS of associated Rel proteins, and thus prevent nuclear translocation of Rel subunits. IκBs contain also an N-terminal regulatory domain, which controls their inducible degradation. The precursor NF-κB proteins, NF-κB1 (p105) and NF-κB2 (p100), also function as IκBs as a result of ankyrin repeat regions in their C-termini and of which must be degraded in order to generate the mature Rel subunits. Upon exposure to pro-inflammatory agents such as TNF-α, IL-1, B-cell mitogens, bacterial lipopolysaccharide (LPS), or viral infection, IκB kinase (IKK) complex are activated and subsequently lead to the phosphorylation of IκBs on two conserved serine residues, which result in the subsequent ubiquitination and degradation of the IκBs by the 26S proteasome (Nishikori et al., 2005; Verma et al., 1995). NF-κB is thus liberated by this cytoplasmic "switch" and subsequently translocates into the nucleus, where it acts as a transcription factor by binding to regulatory DNA sequences known as κB sites (Chen et al., 1998), thereby initiating transcription of target genes that encode cytokines, chemokines, adhesion molecules and cell survival proteins.

The NF-κB activation pathways are broadly classified as the canonical and non-canonical pathways, depending on whether activation involves IκB degradation or p100 processing (Fig.3).
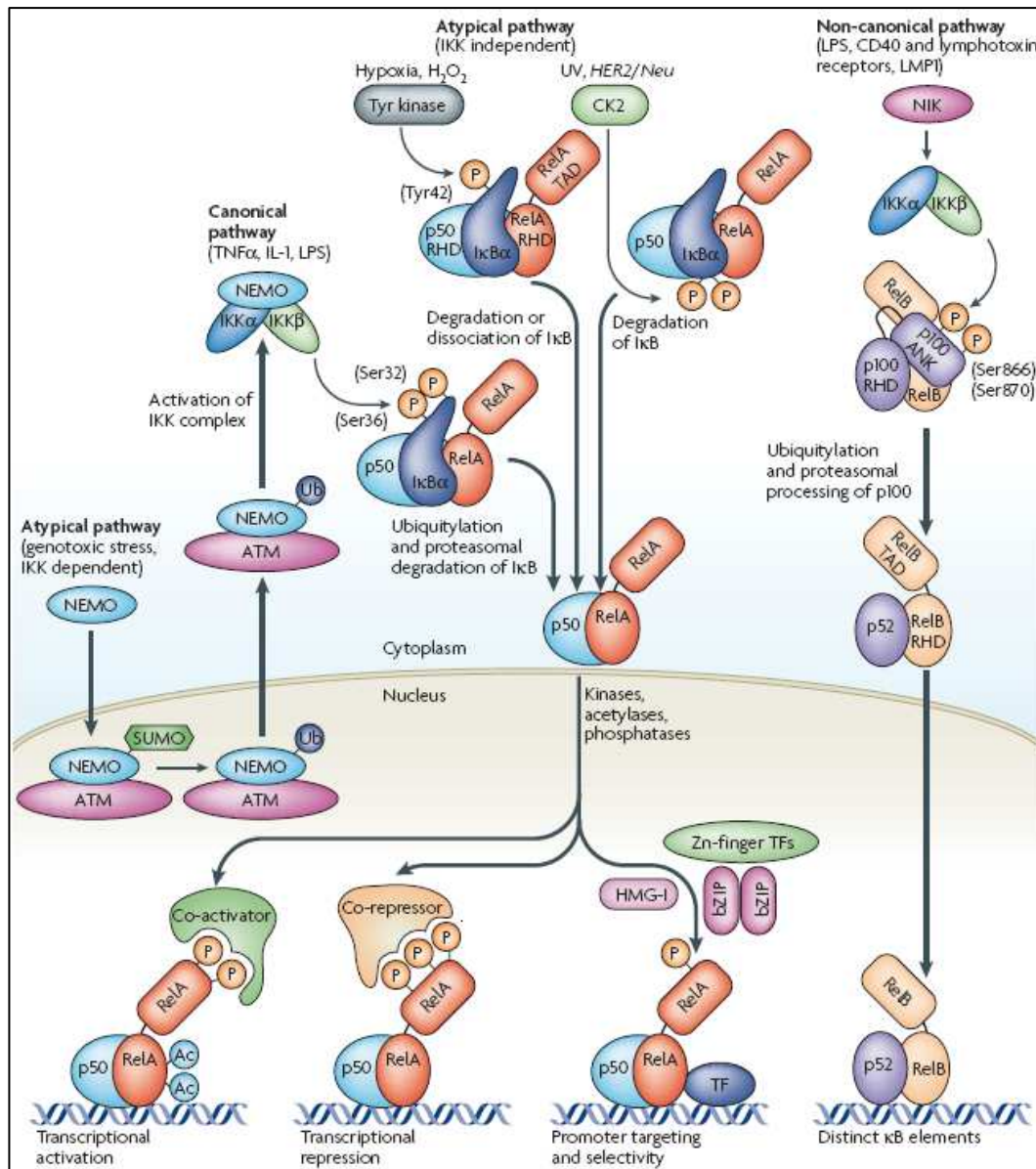
Fig.3. Pathways leading to the activation of NF-κB. (Adapted from Perkins, 2007). The canonical pathway is induced by TNF-α, IL-1 and many other stimuli, and is dependent on activation of IKKβ. This activation results in the phosphorylation (P) of IκBα at Ser32 and Ser36, leading to its ubiquitination (Ub) and subsequent degradation by the 26S proteasome. Release of the NF-κB complex allows it to relocate to the nucleus. Under some circumstances, the NF-κB – IκBα complex shuttles between the cytoplasm and the nucleus (not shown). IKK-dependent activation of NF-κB can occur following genotoxic stress. Here, NF-κB essential modifier (NEMO, aka IKKγ) localizes to the nucleus, where it is sumoylated and then ubiquitinated, in a process that is dependent on the ataxia telangiectasia mutated (ATM) checkpoint kinase. NEMO relocates back to the cytoplasm together with ATM, where activation of IKKβ occurs. IKK-independent atypical pathways of NF-κB activation have also been described, which include casein kinase-II (CK2) and tyrosine-kinase-dependent pathways. The non-canonical pathway results in the activation of IKKα by the NF-κB-inducing kinase (NIK), followed by phosphorylation of the p100 NF-κB subunit by IKKα. This results in proteasome dependent processing of p100 to p52, which can lead to the activation of p52 – RelB heterodimers that target distinct κB elements. Phosphorylation of NF-κB subunits by nuclear kinases, and modification of these subunits by acetylases and phosphatases, can result in transcriptional activation and repression as well as promoter-specific effects. Moreover, cooperative interactions with heterologous transcription factors can target NF-κB complexes to specific promoters, resulting in the selective activation of gene expression following cellular exposure to distinct stimuli. Ac, acetylation; bZIP, leucinezipper-containing transcription factor; HMG-I, high-mobility-group protein-I; IκB, inhibitor of κB; IKK, IκB kinase; LMP1, latent membrane protein-1; LPS, lipopolysaccharide; NF-κB, nuclear factor-κB; RHD, Rel-homology domain; TAD, transcriptional activation domain; TF, transcription factor; UV, ultraviolet; Zn-finger TF, zinc-finger-containing transcription factor.

1.2.1 The canonical NF-κB pathway

In the canonical pathway, which is the predominant NF-κB signaling pathway, stimulating cells with agonists like TNF-α, LPS or IL-1β activate the IKK complex that is composed of two catalytic subunits IKKα and IKKβ and a regulatory subunit IKKγ (also known as NF-κB essential modulator, NEMO). Activated IKK phosphorylates IkBα, predominantly via the action of IKKβ, triggering its lysine-48–linked polyubiquitination and proteasomal degradation, releasing associated NF-κB subunits to translocate into the nucleus. Studies with knockout mice have shown that IKKβ is the dominant kinase in regulating pathogen-associated molecular patterns (PAMPs)-, TNF-, and IL-1-induced activation of NF-κB (Li et al., 1999; Tanaka et al., 1999), whereas IKKα revealed an opposing role to IKKβ in the control of inflammation and innate immunity. IKKα contributes to suppression of NF-κB activity by accelerating both, the turnover of the NF-κB subunits RelA and c-Rel, and their removal from pro-inflammatory gene promoters (Lawrence et al., 2005).

1.2.2 The non-canonical pathway

In contrast to receptor-mediated activation of the canonical NF-κB pathway, which occurs within minutes and does not require new protein synthesis, activation of the noncanonical NF-κB pathway takes several hours and requires new protein synthesis (Zarnegar et al., 2008).

The non-canonical pathway of NF-κB activation operates mainly in B cells in response to stimulation of a subset of the TNF receptor superfamily, including B cell activated factor (BAFF), lymphotoxin-β (LTβ) and CD40 ligand that mediate secondary lymphoid organogenesis, maturation of B cells, adaptive humoral immunity, and promotion of cell survival (Zarnegar et al., 2004). Stimulation of these receptors leads to the recruitment of multiple adaptor proteins, such as TNF receptor-associated factor (TRAF) 2, TRAF3, TRAF6 (Hinz et al., 2010; Zarnegar et al., 2008) that recruit cellular inhibitor of apoptosis 1 and 2 (cIAP1 and cIAP2) and NF-κB inducing kinase (NIK). Subsequently, NIK is activated through a currently unknown mechanism, which in turn selectively phosphorylates and activates the IKKα catalytic subunit independent of IKKβ and NEMO (Mahoney et al., 2008; Zarnegar et al., 2008). IKKα homodimer then phosphorylates NF-κB2/p100 at two C-terminal serine residues leading to the selective degradation of its IκB-like domain by the proteasome. The mature p52 subunit and its binding partner Rel-B translocate into the nucleus to regulate gene expression (Belich et al., 1999).

The physiological role of p52 is highlighted by the association of mice lacking p52 (NF-κB2) with their impairment to develop normal B cell follicles and germinal centers (Caamano et al.,

1998; Franzoso et al., 1998; Paxian et al., 2002).

1.2.3 Atypical NF-κB activation pathway

Like the canonical and non-canonical pathways, the atypical NF-κB pathway also plays an important part in immune functions (Beinke and Ley, 2004). But unlike the noncanonical pathway, constitutive processing of NF-κB1/p105 to produce p50 subunit by the 26s proteasome is not regulated by the agonists stimulation. In fact, p105 is phosphorylated by IKK after activation of the canonical pathway, targeting it for partial degradation by the proteasome to release p50 for RelA association. Because the inducible degradation of p105 regulates NF-κB as well as the activation of Tpl-2 kinase (Beinke and Ley, 2004), therefore, it is considered to be an atypical pathway (Sun and Ley, 2008). Tpl-2 is a mitogen-activated protein (MAP) 3-kinase that regulates inflammatory responses by mediating Toll-like receptor (TLR)-stimulated activation of ERK and production of TNF-α in macrophages (Beinke and Ley, 2004).

1.3 Ubiquitination and deubiquitination

1.3.1 Ubiquitin and ubiquitination

Ubiquitin (Ub) is a highly conserved 76-amino-acid polypeptide that is covalently, but reversibly, attached to one or more lysine (Lys) residues of target proteins through an enzymatic cascade involving three classes of enzymes termed Ub-activating (E1), Ub-conjugating (E2 or Ubc) and Ub-ligating (E3) enzymes (Fig.4) (Hershko and Ciechanover, 1998). In the first step, ubiquitin is activated by E1 in an ATP-dependent reaction. Secondly, the activated ubiquitin is transferred to E2, forming an E2-Ub thioester. Finally, in the presence of E3, ubiquitin is attached to a target protein through an isopeptide bond between the carboxyl terminus of ubiquitin and the ε-amino group of a lysine residue in the target protein.

The types of Ub modification of proteins are diverse. In the simplest form, a single Ub molecule is attached, which is defined as monoubiquitination (Fig.4) (Hicke and Dunn, 2003). Alternatively, several Lys residues can be tagged with single Ub molecules, giving rise to multiple monoubiquitination, also referred to as multiubiquitination (Fig.4) (Haglund et al., 2003). Since Ub contains seven Lys residues itself (Lys6, Lys11, Lys27, Lys29, Lys33, Lys48 and Lys63), Ub molecules can form different types of chains in an iterative process, known as polyubiquitination, and each Lys residue is possibly involved in chain formation *in vivo*.

However, Ub chains linked via Lys48 or Lys63 are the best characterized so far (Hicke et al., 2005). Generally, polyubiquitin chains linked through lysine at position 48 of ubiquitin (Lys 48) target protein substrates for degradation by the 26S proteasome (Hershko and Ciechanover, 1998; Hochstrasser, 1995), whereas K63-linked polyubiquitin chains regulate many functional activities, such as protein trafficking, protein–protein interactions, DNA repair and regulation of signal-transduction events, independently of proteolytic degradation (Adhikari et al., 2007; Chen, 2005; Hershko and Ciechanover, 1998; Liu et al., 2005; Pickart and Eddins, 2004).

Like phosphorylation, ubiquitination is a reversible process that is counter-regulated by deubiquitinating enzymes (DUBs).

1.3.2 Deubiquitinating enzymes and Deubiquitination

Deubiquitinating enzymes (DUBs) form a large group of proteases that hydrolyze ubiquitin chains from proteins, peptides, or small molecules, a process that is known as deubiquitination to oppose the functions of their counteractive ubiquitinases, which play an important role in regulating ubiquitin-dependent pathways. The existence of close to 100 DUBs in the human genome implies that DUBs may possess certain levels of substrate specificity and participate in specific biological functions. DUBs can be divided into five families according to their catalytic domains: the ubiquitin carboxy-terminal hydrolases (UCHs), the ubiquitin-specific proteases (USPs), the ovarian tumour-related proteases (OTUs), the Machado–Joseph disease protein domain proteases (MJDs), and the Jab1/Pab1/MPN-domain-containing metallo-enzymes (JAMMs) (Nijman et al., 2005; Sun, 2008).

The UCH family consists of a small number of structurally related DUBs that are known to cleave short ubiquitinated peptides, which play an important role in the recycling of free ubiquitin. The physiological role of UCHs is highlighted by the association of one member, UCH-L1, one of the most abundant proteins in the mammalian nervous system, with the development of neurodegenerative diseases (Chen et al., 2010; Gong and Leznik, 2007; Sun and Ley, 2008).

USPs are characterized by the presence of two conserved sequence motifs — the cysteine and histidine boxes — in their catalytic domain (Gong and Leznik, 2007) and form the largest family of DUBs with 53 and 54 USP genes that have been so far identified in the human and mouse genome, respectively (Gong and Leznik, 2007). Although the function of most DUBs is yet to be characterized, one USP-family member, CYLD, has been extensively studied in
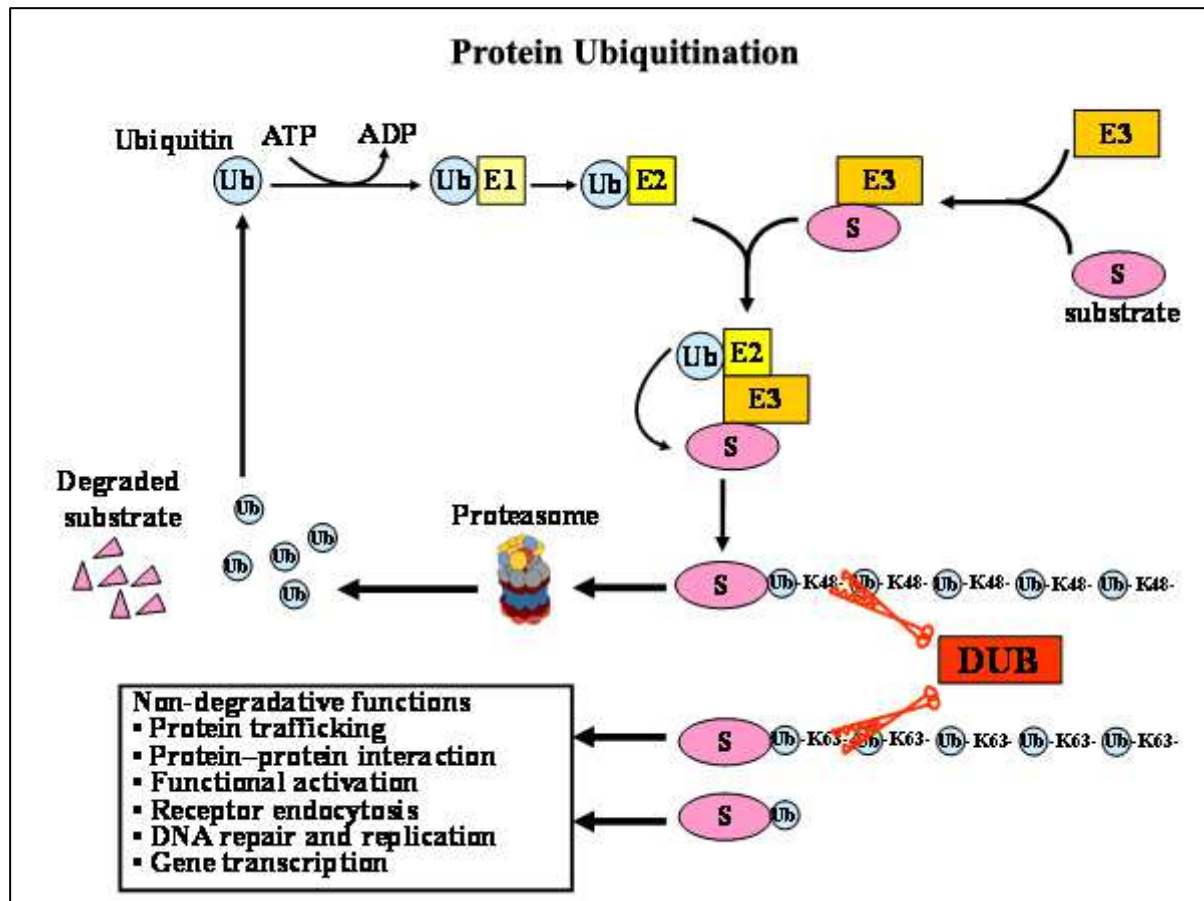
Fig. 4. Scheme of the protein ubiquitination process. (Modified from Sun, 2008). The ubiquitination reaction is catalysed by the sequential and cooperative actions of three enzymes: the ubiquitin-activating enzyme (E1), the ubiquitin-conjugating enzyme (E2) and the ubiquitin ligase (E3). In the first step, ubiquitin is activated by E1 in an ATP-dependent reaction. Secondly, the activated ubiquitin is transferred to E2, forming an E2-Ub thioester. Finally, in the presence of E3, ubiquitin is attached to a target protein through an isopeptide bond between the carboxyl terminus of ubiquitin and the ε-amino group of a lysine residue in the target protein. Since Ub contains Lys residues itself, Ub molecules can form different types of chains in an iterative process, known as polyubiquitination. The K48-linked polyubiquitin chains generally mark substrate proteins for proteasomal degradation and to release free ubiquitin molecules, whereas the K63-linked polyubiquitin chains together with monoubiquitin mediate various non-degradative functions, including protein trafficking, protein–protein interactions, functional activation of signalling factors, receptor endocytosis, DNA repair and DNA replication, and gene transcription. DUBs can deconjugate the ubiquitin chains from ubiquitinated proteins and proteasomal degradation products, thereby reversing the ubiquitination process and regenerating free ubiquitin molecules.

both patients and animal models.

OTUs, being composed of about 24 members in the human genome, form the second largest mammalian DUB family (Gong and Leznik, 2007; Makarova et al., 2000). The first OTU gene was identified in *Drosophila melanogaste* and it was found to regulate the development of the ovaries of the *Drosophila melanogaste*; mammalian OTUs were later discovered based on OTU-domain homology (Makarova et al., 2000). Several OTU-family members, such as

A20, Cezanne, DUBA and otubain-1, are involved in the regulation of immune responses. Until now, little is known about the MJD and JAMM families of DUBs, and it is still unclear whether they also have a role in immune regulation.

Although the role of DUBs in the immune system has been less well studied, accumulating evidence has provided important information about how Ubiquitination/deubiquitination regulates signal transduction from different immune receptors of both the innate and adaptive immune system, such as TLRs, TNFR, and T and B cell receptors (TCR, BCR).

1.4 The role of Ubiquitination in innate immune signaling pathways

Upon exposure to PAMPs, the innate immune response and the subsequent inflammation reaction rely on evolutionarily conserved receptors termed pattern-recognition receptors (PRRs) (Lee and Kim, 2007). These signaling receptors, such as TLRs, and the nucleotide-binding oligomerization domain (NOD) receptors, have the ability to activate several phosphorylation-dependent signaling cascades that lead to the activation of transcription factors, such as NF-κB, activator protein-1 (AP1), IFN-regulatory factor 3 (IRF-3), and IRF-7. In regard of the aforementioned information the IKK complex (two catalytic subunits, IKKα and IKKβ, and a regulatory subunit IKKγ, also known as NEMO) phosphorylates IκBs and p105, which triggers K48-linked ubiquitination and proteasomal degradation of these inhibitors and release of p50 from p105, leading to the nuclear translocation of canonical NF-κB complexes (e.g. p50/RelB).

IKK activation by TLRs and cytokine receptors requires members of the TRAF (TNF receptor-associated factor) family, which belongs to another family of adaptor proteins that bridge the intracellular domains of multiple receptors, such as TNFR, IL1R, and TLRs, to downstream effectors involved in the inflammatory and innate immune signaling pathways. The TRAF family consists of seven members, TRAF1 through TRAF7. TRAF3 and TRAF6 are most important in PRR signaling among TRAF family members. The TRAF6-dependent pathway engages MAPKs and IKK, which activate transcription factors, such as AP-1 and NF-κB that participate in proinflammatory cytokine induction (Fig.5a). Unlike TRAF6, TRAF3 is required for the activation of IRF-3 and the induction of type I interferons but not NF-κB. IRF-3 regulates e.g. the transcription of IFNα/β genes in response to viral infection (Hacker et al., 2006; Oganesyan et al., 2006) (Fig.5b). TLR signaling is transduced through nondegradative K63-linked polyubiquitination of adapter proteins, such as TRAF6 and TRAF3. Polyubiquitinated TRAFs recruit downstream signalling molecules that function as

both adaptors and E3 ubiquitin ligases by catalysing K63-linked self-ubiquitination and the ubiquitination of other signalling molecules. For instance, the ubiquitin-dependent IKK-activating kinase, TAK1 (transforming-growth factor-β- activated kinase 1) which recognizes the K63-linked ubiquitin chains through its partner protein, TAB2 (TAK1-binding protein 2) or TAB3, is recruited and activated (Fig.5a). IKKγ also has ubiquitin-binding function and recognizes K63-linked ubiquitin chains (Ea et al., 2006; Wu et al., 2006). Together, the ubiquitinated TRAFs form a platform that recruits TAK1 and IKK complexes and thus leading to their activation (Adhikari et al., 2007).

This whole activation process is subject to tight regulation by negative mechanisms, and accumulating evidence indicates that the DUBs have a crucial role in this control of innate immune-receptor signalling. It is reported that CYLD, a member of the USP family of DUBs, could target multiple ubiquitinated signalling molecules and thus regulates diverse biological functions. As the role of CYLD in *Yersinia* infection is the focus of this thesis, a more detailed description is presented in the next section.
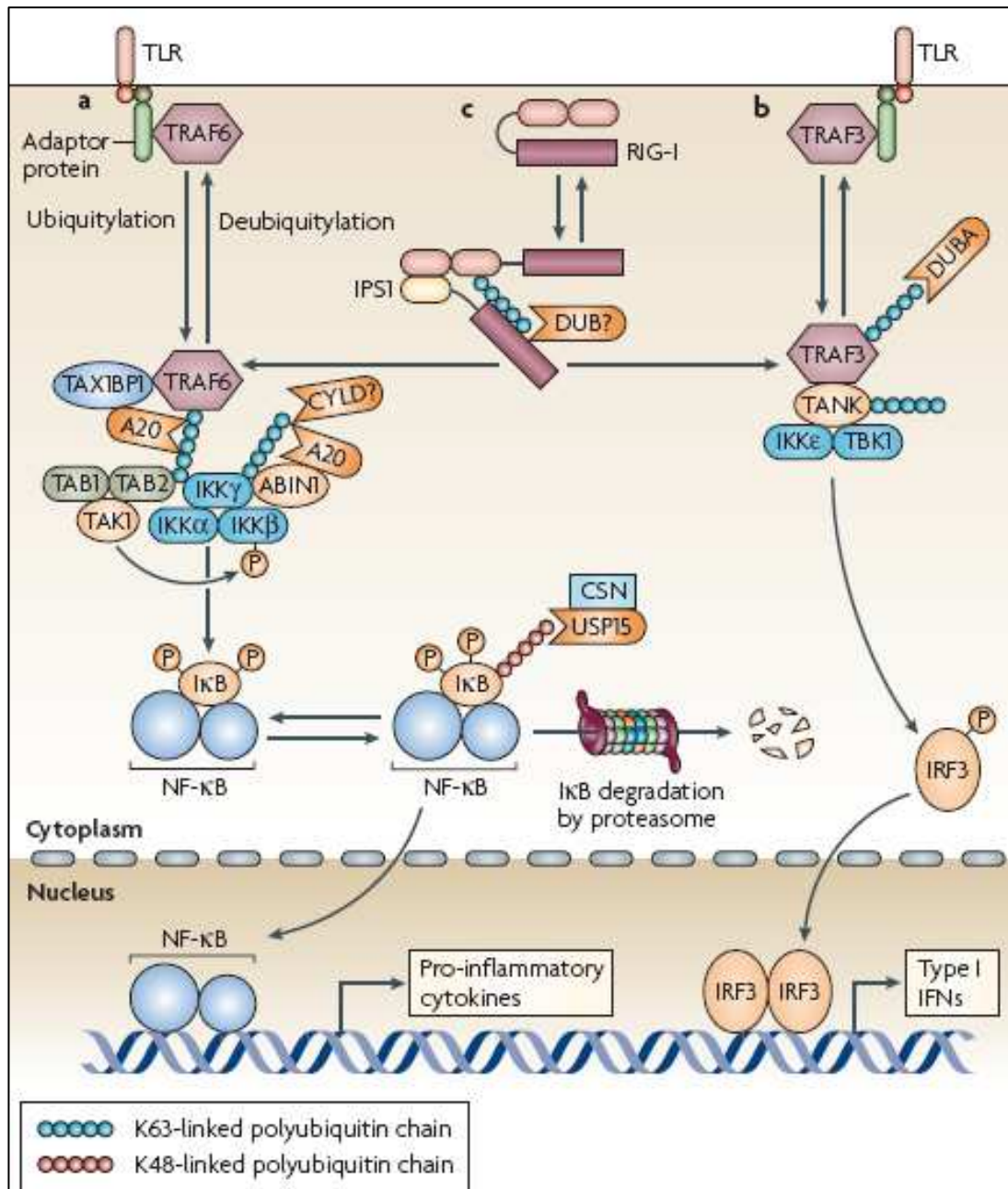
Fig. 5. Regulation of innate immune-receptor signalling by deubiquitinating enzymes (DUBs). (Adapted from **(Sun, 2008).** Toll-like receptors (TLRs) stimulate the K63-linked ubiquitination of TRAF6 and TRAF3, which leads to the recruitment of downstream signalling molecules. **(a)** Ubiquitinated TRAF6 recruits the IKK complex and its activating kinase, transforming growth factor-β-activated kinase 1 (TAK1) in association with TAK1-binding protein 1 (TAB1) and TAB2 through the ubiquitin-binding function of IKKγ and TAB2, leading to activation of these kinases. The IKK complex phosphorylates IκB, triggering its K48-linked ubiquitination and proteasomal degradation. Through TAX1-binding protein 1 (TAX1BP1) and A20-binding inhibitor of NF-κB 1 (ABIN1), A20 binds to and deubiquitinates TRAF6 and IKKγ, respectively, thereby negatively regulating NF-κB signalling. CYLD is also involved in the negative regulation of NF-κB signaling by deubiquitinating TRAFs (see the following chapter). Deubiquitination of IκB, which is another mechanism for the negative regulation of NF-κB, involves USP15 (ubiquitin-specific protease 15), a DUB that is associated with the COP9 signalosome (CSN). **(b)** Ubiquitinated TRAF3 recruits the IKK-related kinases, TANK-binding kinase 1 (TBK1) and IKKε, through the adaptor protein TANK (TRAF-family-member-associated NF-κB activator). Similar to IKKγ, TANK is ubiquitinated in the signalling complex. Deubiquitination of TRAF3 is mediated by DUBA, a crucial and specific negative regulator of type I interferon (IFN) induction. **(c)** The cytoplasmic RNA sensor, retinoic-acid-inducible gene I (RIG-I), undergoes ubiquitination on binding to viral RNA, which is required for its association with the adaptor, IPS1 Interferon β-promoter (*IFNB*-promoter stimulator 1), and activation of downstream signalling events. It is currently unclear which DUB regulates the deubiquitination of RIG-I.

1.5 Cylindromatosis (CYLD)

1.5.1 The discovery of CYLD

CYLD was originally identified as a gene mutated in familial cylindromatosis (FC, OMIM 132700), an autosomal dominant predisposition to multiple neoplasms of the skin appendages and it was termed cylindroma because of their characteristic microscopic architecture (Bignell et al., 2000) (Fig.6A). Cylindromas are benign tumours that typically appear on the scalp and are thought to be derived from hair follicle stem cells (Massoumi and Paus, 2007). The development of many tumours on the scalp sometimes leads to the formation of a confluent mass which may ulcerate or even get infected, and which has led to the designation 'turban tumour syndrome' (Fig.6B).

(A)   **(B)**
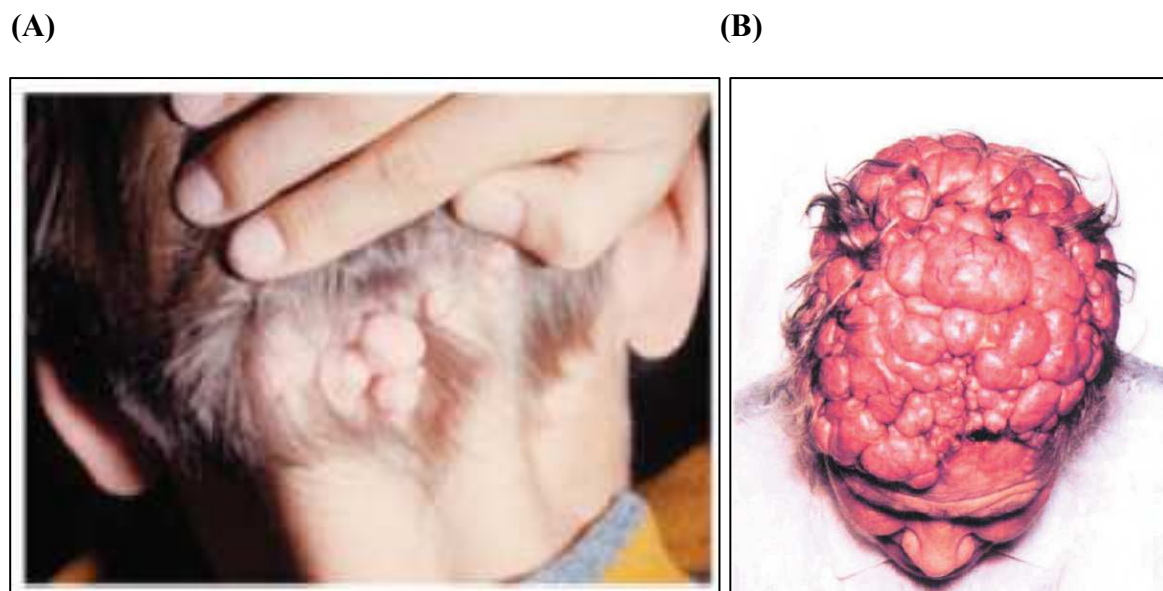
Fig. 6. Macroscopic pictures of two patients with cylindromatosis. A was adopted from Massoumi et al. (Massoumi and Paus, 2007) . B was adpted from Biggs et al. (Biggs et al., 1995).

In familial cylindromatosis, the cylindromas usually begin to appear in the second or third decades, accumulating in number and growing slowly in size throughout the adult life and it seems that women are more frequently affected than men.This disease can cause considerable discomfort and disfigurement and, in severe cases, removal of the scalp and reconstruction using skin grafts is required. Malignant change with distant metastasis is unusual despite the profusion of benign lesions.

Linkage analysis in families with multiple cylindromas mapped the susceptibility gene (CYLD) to a single locus on chromosome 16q12-13 (Biggs et al., 1995). Loss of heterozygosity at the same locus was reported in a large number of these tumors suggesting that CYLD may function as a tumor suppressor (Biggs et al., 1996; Biggs et al., 1995;

Takahashi et al., 2000). Most of the mutations, which are mainly located at the C-terminal of the CYLD coding sequence, lead to the formation of truncated proteins (Bignell et al., 2000). Besides to its role in the etiology of cylindromatosis, CYLD also acts as a tumor suppressor in multiple types of human cancer, which includes melanoma (Massoumi et al., 2009), colon carcinoma (Hellerbrand et al., 2007), lung cancer (Zhong et al., 2007) and multiple myeloma (Annunziata et al., 2007; Keats et al., 2007).

CYLD expression is highest in the human brain, skeletal muscles, and testes (Bignell et al., 2000), whereas in mouse, the highest expression levels of CYLD are detected in the brain, thymus, testes, and skin (Massoumi et al., 2006).

1.5.2 Functional domains of CYLD

Full-length CYLD is composed of 20 exons (the smallest being 9 bp), of which the first 3 are untranslated (UTR) (Fig.7), and extends over approximately 56 kb of genomic DNA. Exon 3 (in the 5′ UTR) and the 9-bp exon 7 (which is coding) both show alternative splicing. Overlapping exon 1 is a GC-rich region where there are many CpG dinucleotides and which has the properties of a CpG island. CYLD protein is predicted to be approximately 956 aa long (molecular weight approximately 120kDa).

CYLD protein contains several functional domains (Fig.7) (reviewed e.g. in Massoumi, 2010). Motif analysis revealed that the C-terminal region of CYLD displayed good sequence similarity to ubiquitin-specific proteases (USP) (Nijman et al., 2005). Like other members of the DUB enzymes, CYLD also exhibits a catalytic domain composed of two conserved subdomains at the C terminus that contains the active cysteine and histidine which form the catalytic pocket. The B-box-type zinc finger domain within UCH is found in TRIM (tripartite motif) proteins that are E3 ligases. Although in vitro ubiquitination assays demonstrated that CYLD lacks ubiquitin ligase activity, it appears that the B-box plays an important role in CYLD cellular localization and deletion of the CYLD B-box resulted in sustained nuclear localization. In addition, CYLD contains within its N-terminal section three cytoskeletal-associated-protein glycine-(CAP-Gly) motifs that have been proposed to participate in binding to microtubules (Weisbrich et al., 2007). Indeed, recent studies could show that CYLD associates with microtubules, and the first CAP-Gly domain of CYLD is mainly responsible for the interaction (Gao et al., 2008).

Comparison of the CYLD sequence with itself reveals a short, repeated segment of approximately 25 amino acids (aa 388–413 and 446–471) that is rich in proline residues. This proline-rich region may constitute an SH3-binding domain, which mediates protein-protein

interactions in signal transduction or vesicle-transport pathways (Feng et al., 1994).
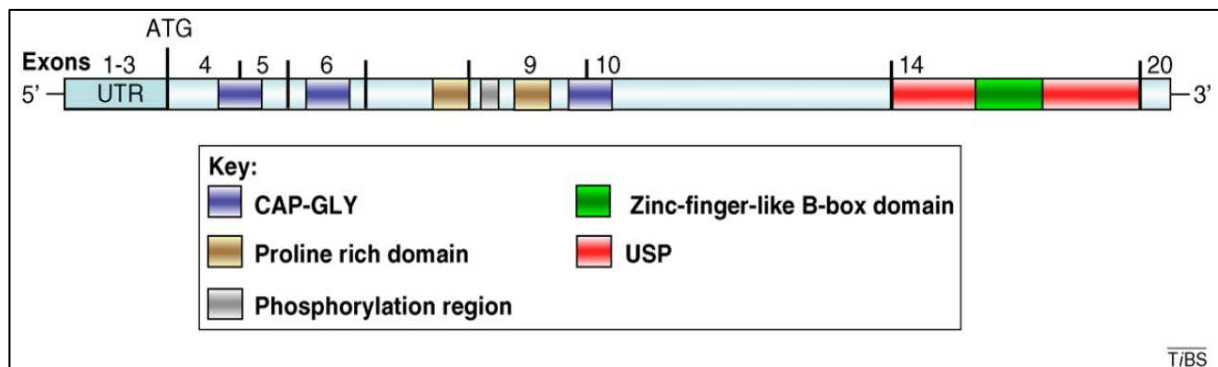
Fig. 7. The structure of the CYLD protein (figure was taken from Massoumi 2010). The CYLD protein contains three CAP-Gly repeats (blue), two proline-rich segments (gold), a phosphorylation region (gray), and a zinc-finger-like B-box motif (green) within the UCH (or USP) domain (red). The first three exons are untranslated (UTR).

1.5.3 CYLD substrates and their reported functions

Many different cellular functions have been ascribed to CYLD and the loss of CYLD expression promotes cell survival (Brummelkamp et al., 2003; Kovalenko et al., 2003; Trompouki et al., 2003), cell proliferation (Massoumi et al., 2006), and migration (Gao et al., 2008). Moreover, the study of *Cyld*$^{-/-}$ animals highlights the importance of CYLD in regulating diverse physiological processes, including spermatogenesis (Wright et al., 2007), osteoclastogenesis (Jin et al., 2008), and the immune response (reviwed e.g. in Sun, 2008). In the following the functions of CYLD being identified so far and the substrates involved will be described.

Proliferation and cell cycle: the CYLD–BCL3 association leads to a significant reduction in the Lys-63-polyubiquitination of BCL3, a process that is important for BCL3 nuclear translocation and cyclin D1 upregulation (Massoumi et al., 2006). Midbody localization of CYLD induces inactivation of HDAC6 and a delay in cytokinesis, owing to an increase in acetylated α-tubulin (Gao et al., 2008; Wickstrom et al., 2010). Deubiquitination of polo-like kinase1(PLK1) by CYLD promotes cell division, and is required for entry into mitosis (Stegmeier et al., 2007).

Ca^{2+} channel signaling: Deubiquitination of the Ca^{2+} TRPA1 (Transient receptor potential cation channel, subfamily A, member 1) channel by CYLD increases the cellular pool of TRPA1 proteins (Stokes et al., 2006).

Survival and apoptosis: The removal of the Lys-63-linked polyubiquitin chains from TRAF2, TRAF6 or NEMO by CYLD attenuates TNF-α-induced classical NF-κB signaling, and leads to programmed cell death (Brummelkamp et al., 2003; Kovalenko et al., 2003;

Trompouki et al., 2003). In addition, CYLD enhances cell survival by deubiquitinating TRAF2 which leads to subsequent JNK activation and induction of apoptosis (Reiley et al., 2004). CYLD can also remove Lys-48-linked polyubiquitin chains from drosophila (d) TRAF2, thereby preventing the proteolytic degradation of TRAF2 (Xue et al., 2007). A direct interaction between TRIP and CYLD is necessary for downregulation of NF-κB activity after TNF-α stimulation and subsequent cell survival (Regamey et al., 2003).

Inflammation: CYLD negatively regulates pathogen-induced inflammation and NF-κB signaling via TRAF6 and TRAF7 deubiquitination (Lim et al., 2007).

T-cell development and activation: CYLD-mediated Lys-48- and Lys-63-deubiquitination of the tyrosine kinase Lck blocks downstream TCR signaling (Reiley et al., 2006). CYLD-mediated TAK1 deubiquitination prevents the spontaneous activation of TAK1 and its downstream signaling. This activity prevents sustained inflammation (Reiley et al., 2007).

Antiviral response: CYLD can negatively regulate innate antiviral responses through RIG-I deubiquitination (Friedman et al., 2008; Zhang et al., 2008).

Spermatogenesis: CYLD deubiquitinates receptor-interacting protein 1 (RIP1) in wild-type germ cells and blocks the aberrant expression of survival genes via NF-κB signaling (Wright et al., 2007).

1.5.4 Cyld-deficient mice

In order to unravel the *in vivo* role of CYLD, a series of CYLD-deficient mice have been recently engineered and characterized (Hovelmeyer et al., 2007; Massoumi et al., 2006; Reiley et al., 2006; Trompouki et al., 2009; Zhang et al., 2006). Generally, these studies have confirmed the physiological importance of this enzyme and provided interesting insights into new putative functions of CYLD. However, also contradictory phenotypes were reported.

Here is a short summary of the initial phenotypic characterization of $Cyld^{-/-}$ mice and their engineering stratigies reported by the five groups mentioned above. The engineering strategies could so far be relevant; diverse cyld gene targeting strategies and/or genetic background of used embryonic stem (ES) cells or mice could be the reason for contradictory results obtained from the different knockout mice.

1. Massoumi et al. reported in their CYLD knockout mice that tumors are only formed by this $Cyld^{-/-}$-mice after treating animals with a two-stage carcinogenesis protocol (Massoumi et al., 2006). This group went on to show that the development of skin tumors in $Cyld^{-/-}$ mice is associated with elevated cyclin D1 expression in $Cyld^{-/-}$ keratinocytes, which is dependent on

the alternative NF-κB pathway. So far no alterations in T and B cell development or abnormalities of the secondary immune organs in these knockout mice have been reported.

Their $Cyld^{-/-}$ mice (Massoumi et al., 2006) were generated using a targeting construct in which the ATG-containing exon 4 of the $Cyld$ gene was disrupted with a lacZ reporter and a neomycin gene. The targeting vector was electroporated into R1 ES cells (passage 13), and two independently targeted ES cell clones were injected into C57Bl/6 blastocysts to generate germline chimeras. The chimeric founders were crossed to C57Bl/6 females to establish heterozygous $Cyld^{+/-}$ and subsequently homozygous $Cyld^{-/-}$ mice.

2. Reiley et al. (Jin et al., 2007; Reiley et al., 2007; Reiley et al., 2006) identified, in contrast to Massoumi et al. (Massoumi et al., 2006), a critical role for CYLD in thymocyte development, and T and B lymphocyte activation.

$Cyld^{-/-}$ mice from Reiley et al. were generated as follows: PCR with the high-fidelity Takara LA DNA polymerase was used to amplify 5-kilobase and 2.75-kilobase DNA fragments of Cyld from 129 x 1/SvJ genomic DNA. The 5-kilobase fragment (part of exon 1 and its upstream sequence) and the 2.75-kilobase fragment (part of exon 1, the entire exon 2 and intron sequences) were cloned into the pPNT targeting vector upstream and downstream of the neomycin-resistance gene, respectively. This targeting vector was partially sequenced, was linearized and electroporated into R1 mouse ES cells (Nagy et al., 1993). Recombinant embryonic stem cells were injected into C57BL/6 x DBA/2 blastocysts.

3. Zhang et al. (Zhang et al., 2006) reported increased colonic inflammation and colon cancer incidence in their $Cyld^{-/-}$ mice compared with wild-type mice, after azoxymethane and dextran sulfate sodium administration.

Their $Cyld^{-/-}$ mice (Zhang et al., 2006) were generated by Lexicon Genetics Inc. In general, the ATG start codon is in exon 2, and a gene-targeting construct was designed to delete exons 2 and 3 and replace them with a $lacZ$ reporter and a neomycin resistance gene. The targeting vector was linearized and electroporated into Lex-1 ES cells. Clones resistant to G418 were selected and screened for homologous recombinants by Southern blot analysis. Two targeted ES cell clones were microinjected into C57BL/6-albino blastocysts, and the resulting chimeras were mated to C57BL/6-albino females to generate mice heterozygous for the $Cyld$ mutation.

4. The three aforementioned groups all inactivated $Cyld$ by disrupting the translation-initiation-ATG–containing exon (exon 1, 2 or 4). A fourth research group (Hovelmeyer et al., 2007) reported recently the disruption of B-cell homeostasis in mice overexpressing solely an

alternatively spliced CYLD product, which is catalytically active but lacks the TRAF2 and IKKγ–interacting domains.

The *Cyld* mutant mice (Hovelmeyer et al., 2007) were generated by applying standard gene targeting techniques in mouse ES cells. Using *Cre/loxP* technology, three different mouse strains were generated. The first strain, *Cyld^neo^*, contains the neo resistance gene upstream of exon 7, decreasing transcription of *Cyld*. The second strain, *Cyld^FL^*, harbors two *loxP* sites flanking exon 7 of *Cyld*. Finally, *Cyld^ex7/8^* mice lacking exon7 after Cre-mediated recombination through transient transfection of the targeted ES cells with a Cre-expressing plasmid, or by crossing *Cyld^FL^* with CD19-Cre mice, in order to delete exon7 solely in B cells. *Cyld^ex7/8^* mice were born at the expected Mendelian frequencies and survived normally when housed under specific pathogen-free conditions. Germline deletion of exon 7 should lead to splicing from exon 6 to 8 resulting in an out-of-frame translation of CYLD. RT-PCR was applied to cDNA from mouse embryonic fibroblasts (MEFs) of the indicated genotypes using primers located in exon 6 and 9 of the CYLD transcript to verify the absence of the WT allele in *Cyld^ex7/8^* MEFs. This analysis revealed an unexpected shorter amplified product besides the expected band from the full-length transcript (FL-CYLD) in WT MEFs. This shorter product represents an alternative splice variant of CYLD lacking exons 7 and 8, termed sCYLD. *Cyld^ex7/8^* MEFs are devoid of the fulllength transcript, but express the sCYLD splice variant excessively. sCYLD protein is a naturally occouring splice variant that could be detected in different tissues and cells of WT animals.

5. However, none of the targeting approaches mentioned above mimic the identified mutations of *Cyld* in human tumors, which leads to truncation of the catalytic domain of CYLD. Trompouki and collegues used a conditional approach to introduce and characterize phenotypically a carboxyl-terminal truncating mutation of *Cyld* that mimics the characterized oncogenic human mutations (Trompouki et al., 2009). However, their approach revealed a previously unidentified role of *Cyld* in lung maturation. The lungs of these mice demonstrated an immature phenotype resulting in respiratory dysfunction and perinatal lethality. However, because a Cre-loxP‒based conditional approach was used for *Cyld* inactivation, this mouse model will enable to study the biological role of *Cyld* in specific tissues.

To generate targeting construct, Trompouki et al. (Trompouki et al., 2009) used genomic DNA from a 129Ola mouse. The targeting vector was designed to flank an exon 9–containing 0.95-kb HgaI-SalI genomic fragment with loxP sites (flx). The vector also consisted of a 4.95-kb BamHI-HgaI genomic fragment as the 5′ arm of homology then a loxP-flanked neomycin resistance gene expression cassette, followed by a second 2.65-kb SalI-ClaI genomic

fragment as the 3′ arm of homology and a thymidine kinase expression cassette. The neomycin resistance gene was used for the positive selection of correctly targeted stem cells, and the thymidine kinase gene was used for the negative selection of incorrectly targeted ES cells. Correctly targeted ES cell clones were injected onto C57BL/6 blastocysts for chimera production and germ line transmission. Mice carrying the recombined *Cyld*^{flx} locus in the germ line were crossed with *Cre* transgenic mice expressing the *Cre* recombinase.

1.6 Objectives of the doctoral project

CYLD is suggested as a key negative regulator for NF-κB signaling by deubiquitinating TRAFs and IKK-γ subunit (Brummelkamp et al., 2003; Kovalenko et al., 2003; Yoshida et al., 2005). Furthermore, CYLD inhibits also indirectly the activation of c-Jun N-terminal kinase (JNK) and p38 (Reiley et al., 2004; Yoshida et al., 2005). *Yersinia* has also evolved strategies to selectively target signaling pathways of NF-κB and MAPKs (such as p38, ERK and JNK), allowing them to interfere with the transcription of immune response genes (reviewed in Navarro et al., 2005; Ruckdeschel et al., 1997).

Because of the overlapping functions of CYLD and virulence factors of *Yersinia*, and given that many infections are known to induce or promote cell transformation e.g. by inducing constitutive NF-κB activation (Lax and Thomas, 2002; McLaughlin-Drubin and Munger, 2008; McNamara and El-Omar, 2008), it is worthwhile to explore whether, conversely, mutations in tumor suppressor genes, especially those that interfere with NF-κB and MAPK signalling, would benefit or detriment pathogens.

Therefore, the aim of this study was to investigate the role of CYLD in regulation of innate immune responses to the enteric pathogen, *Yersinia enterocolitica* by comparing *Cyld*$^{+/-}$-C57Bl/6 mice with *Cyld*$^{-/-}$-C57Bl/6 mice in regard of

(i) control of the bacterial burden in spleen

(ii) cytokine/chemokine response

(iii) MAP kinase- and NF-κB signality pathway

(iv) in vitro bacterial killing

(v) in comparison with Salmonella infection

2. Materials and Methods

2. 1 Materials

2.1.1 Chemicals and media

Table 1- Chemicals and media

Name	Company
Acrylamide/Bisacrylamide	National Diagnostics, Atlanta, USA
Agar	Roth GmbH & Co. KG, Karlsruhe, Germany
Agarose	Biozym, Hess. Oldendorf, Germany
Albumin Fraction V	Roth GmbH & Co. KG, Karlsruhe, Germany
Ammoniumsulfate	Applichem
Ampicillin	Sigma-Aldrich, Taufkirchen, Germany
Ampuwa®	Fresenius Kabi, Bad Homburg, Germany
APF	Invitrogen, Karlsruhe, Germany
APS	Sigma-Aldrich, Taufkirchen, Germany
Aqua bidest, DNase- free	Gibco-Invitrogen, Karlsruhe, Germany
Bacto-Agar	Difco
Bacto-Hefeextrakt	MP Biomedicals Inc.
Bacto-Trypton	Difco
Bench Mark Prestained Protein Ladder	Invitrogen, Karlsruhe, Germany
BHI (Brain Heart Infusion)-Medium	Oxoid, Hampshire, England
Brilliance *Listeria* agar	Oxoid Germany GmbH, Wesel, Germany
Brilliance *Salmonella* agar	Oxoid Germany GmbH, Wesel, Germany
Bis-Acrylamide	SERVA, Heidelberg, Germany
BSA (bovine serum albumine)	Biomol, Hamburg, Germany
Calciumchlorid	Roth GmbH & Co. KG, Karlsruhe, Germany
CCF2/4	Invitrogen, Karlsruhe, Germany
Chloramphenicol	Sigma-Aldrich, Taufkirchen, Germany
Chloroform	Roth GmbH & Co. KG, Karlsruhe, Germany
CIN-Agar	Oxoid Germany GmbH, Wesel, Germany
Coomassie Brilliant Blue™ R250	Biomol, Hamburg, Germany
D-+-Glucose	Sigma
DMEM	Gibco-Invitrogen, Karlsruhe, Germany

DMSO	Sigma-Aldrich, Taufkirchen, Germany
DNA-size standard (DNA-ladder) (Ready Load™ 1 kb)	Invitrogen, Karlsruhe, Germany
DTT	Applichem, Darmstadt, Germany
EDTA	Sigma
EGTA	Sigma
Ethanol (~99.8 %)	Roth GmbH & Co. KG, Karlsruhe, Germany
Ethidiumbromide	Roth GmbH & Co. KG, Karlsruhe, Germany
FBS (Fetal Bovine Serum)	Gibco-Invitrogen, Karlsruhe, Germany
Formaldehyde 37 %	MERCK, Darmstadt, Germany
Geneticin (G418)	Gibco-Invitrogen, Karlsruhe, Germany
Gentamicin solution	Invitrogen
Glutamine	PAA Laboratories GmbH
Glycerine	Roth GmbH & Co. KG, Karlsruhe, Germany
Glycine	MP Biomedicals Inc.
HBSS (Hanks Balanced Salt Solution)	PAA Laboratories GmbH
HEPES (N-2 [Hydroxyethyl] piperazine-N'-[2-Ethanesulfonic acid])	Gibco-Invitrogen, Karlsruhe, Germany
H_2O_2	Merck
HCl	Roth GmbH & Co. KG, Karlsruhe, Germany
IL-2 recombinant	ImmunoTools, Friesoythe, Germany
Immersion oil	Zeiss
IPTG	Applichem
Iso-propanol	Roth GmbH & Co. KG, Karlsruhe, Germany
Kanamycin	Sigma-Aldrich, Taufkirchen, Germany
KCl	Merck
KH2PO4	Sigma
K2HPO4	Sigma
LB (Luria Bertani)-Agar	Oxoid, USA
LB (Luria Bertani)-Medium	Oxoid, USA
L-Glutamine (200 mM)	Gibco-Invitrogen, Karlsruhe, Germany
Liquid Nitrogen	Linde
LPS	Quadratech Diagnostics, England
Luminol (3-Aminophthalhydrazide)	Fluka (Sigma), Artikelnr.0925321

2-Mercaptoethanol	Applichem
Milk powder (Blotting grade)	Roth GmbH & Co. KG, Karlsruhe, Germany
Moviol 4-88	Sigma-Aldrich, Taufkirchen, Germany
NaCl	Roth GmbH & Co. KG, Karlsruhe, Germany
Na$_2$HPO$_4$ (water free)	Applichem
NaH$_2$PO$_4$	Applichem
NaOH	Sigma
Paraformaldehyde	Fluka
PBS	Gibco-Invitrogen, Karlsruhe, Germany
Peptone	Merck
Penicillin-Streptomycin-Solution	Gibco-Invitrogen, Karlsruhe, Germany
pH-Meter Calibration-solution (pH 4.0, 7.0, 10.0)	Applichem
PMSF (Phenylmethylsulfonylfluoride)	Applichem
Poly-L-Lysine	Sigma-Aldrich, Taufkirchen, Germany
Ponceau S-Concentrate	Sigma-Aldrich, Taufkirchen, Germany
Protease Inhibitor Cocktail Tablets	Roche Diagnostics GmbH, Mannheim, Germany
Proteose Peptone	Difco Laboratories, Detroit
Saponin	Applichem
SDS (sodium dodecyl sulfate)	Roth Diagnostics GmbH, Mannheim, Germany
Sodium acetate	Roth GmbH & Co. KG, Karlsruhe, Germany
Sucrose	Applichem
TEMED	Biomol, Hamburg. Germany
Tris	MP Biomedicals Inc.
Triton X-100	Sigma-Aldrich, Taufkirchen, Germany
TrypanBlue	SERVA, Heidelberg, Germany
Trypsin-EDTA	Gibco-Invitrogen, Karlsruhe, Germany
Trypton	MP Biomedicals Inc.
Tween 20	Sigma-Aldrich, Taufkirchen, Germany
Yeast-Extract	Difco

2.1.2 Enzymes and markers

Table 2- Enzymes and markers

Name	Company
Bench Mark ^{TM} Prestained Protein Ladder	Invitrogen, Karlsruhe, Germany
BioMix Red	Bioline, Luckenwalde, Germany
DNA-Ladder for Agarose gel	MBI Fermentas, St Leon-Rot, Germany
Pfu-Polymerase	MBI Fermentas, St Leon-Rot, Germany
Proteinase K	MBI Fermentas, St Leon-Rot, Germany
Protease Inhibitor Cocktail Tablet(complete)	Roche Diagnostics GmbH, Mannheim, Germany
Restriction enzymes	MBI Fermentas, St Leon-Rot, Germany
Shrimp alkaline phosphatase	MBI Fermentas, St Leon-Rot, Germany
T4-DNA-Ligase	MBI Fermentas, St Leon-Rot, Germany
Taq-Polymerase	MBI Fermentas, St Leon-Rot, Germany

2.1.3 Antibodies

Table 3- Antibodies

Name	Company
Anti-GFP	Santa Cruz Biotechnology, Heidelberg, Germany
Anti-Actin	Santa Cruz Biotechnology, Heidelberg, Germany
Rabbit Anti-Listeria ActA	This institute
Rabbit Anti-Salmonella enterica, Serotype Enteritidis	This institute
Rabbit Anti-Yersinia (WA-vital, serovar O:8)	This institute
HRP-conjugated anti-Rabbit IgG (Horseraddish-peroxidase)	Santa Cruz Biotechnology, Heidelberg, Germany
FITC-conjugated anti-Rabbit IgG	Sigma-Aldrich, Taufkirchen, Germany
FITC-conjugated anti-Mouse IgG	Sigma-Aldrich, Taufkirchen, Germany
PE-Cy7-conjugated anti-CD45	eBioscience, NatuTec GmbH, Frankfurt, Germany

PE-conjugated anti-B220 (CD45R)	BD, Heidelberg, Germany
PE-conjugated anti-CD4	BD, Heidelberg, Germany
FITC-conjugated anti-CD4	BD, Heidelberg, Germany
APC-H7-conjugated anti-CD4	eBioscience, NatuTec GmbH, Frankfurt, Germany
PE-conjugated anti-CD8alpha (Ly2)	BD, Heidelberg, Germany
PerCP-conjugated anti-CD8alpha (Ly2)	eBioscience, NatuTec GmbH, Frankfurt, Germany
FITC-conjugated anti-CD8alpha (Ly2)	BD, Heidelberg, Germany
PE-conjugated anti-Gr1 (Ly6G)	BD, Heidelberg, Germany
APC- conjugated anti-CD11b	eBioscience, NatuTec GmbH, Frankfurt, Germany
PE-conjugated anti-CD11c	BD, Heidelberg, Germany
APC-Alexa750-conjugated anti-CD11c	eBioscience, NatuTec GmbH, Frankfurt, Germany
Rat Anti-Mouse CD16/CD32	eBioscience, NatuTec GmbH, Frankfurt, Germany
FITC-conjugated anti-NK-1.1	BD, Heidelberg, Germany
APC-conjugated anti-CD49b	eBioscience, NatuTec GmbH, Frankfurt, Germany
PE-Texas Red conjugated F4-80	Caltag Laboratories
PE-Cy5-conjugated F4-80	eBioscience, NatuTec GmbH, Frankfurt, Germany

2.1.4 Kits

Table 4- Kits

Name	Company
Mouse Cytokine Flex Set (CBA)	BD, Heidelberg, Germany
FACE^{TM} STAT4 Chemi ELISA Kits	Active Motif
Mouse TLR1-9 Agonist Kit	InvivoGen/Cayla SAS
Mouse Cell Signaling Flex Set (CBA)	BD, Heidelberg, Germany
pJNK1/2 (T183/Y185), p38 (T180/Y182), and pERK1/2 (T202/Y204), tolal JNK(1/2),	BD, Heidelberg, Germany

total p38α multiplex Flex Set Cytometric
Bead Array (Cat. No. 560213, 560010,
560012, 560214 and 560145, respectively)

Nuclear extraction Kit	Active Motif
TransAM™ NFκB Family Kits	Active Motif

2.1.5 Consumables

Table 5- Consumables

Name	Company
Pipettes 5 ml, 10 ml und 25 ml (sterile, Plastic)	Greiner
Falcon-tubes, 15 ml und 50 ml	Greiner
Gloves	Flexam
Microtiter plates, Maxisorp F96	Nunc
Paper napkins	ZVG
Parafilm "M"$^®$	ANC
Pasteur-Pipettes	Brand
Petri-dishes for Bacterial culture	Greiner
Petri-dishes for cell culture	Greiner
Pipette Tips 10 μl, 200 μl and 1000 μl	Sarstedt
Plastic cuvettes 1 ml	Greiner
PVDF-Membrane	Millipore
Reaction tubes 0.5 ml	ABgene
Reaction tubes 1.5 ml und 2 ml	Eppendorf
X-ray films	Amersham
Safeseal Tips 10μl, 100μl and 1250μl	Biozym, Hess. Oldendorf, Germany
Scalpel	Braun
Sterile-Filter (0.2 μm)	Schleicher & Schuell
Vinyl-gloves	Sempermed
Whatman-Filter paper	Schleicher & Schuell
Cell culture flasks, 25 cm^2 und 75 cm^2	Greiner
Cell culture plates (6 and 24 well)	Greiner
Centrifugation tubes 14 ml	Greiner

2.1.6 Instruments and devices

Table 6- Instruments and devices

Instruments and devices	Company
Agarose Gel-Electrophoresis apparatus	Peqlab and Gibco
Autoclave	Varioklav, Germany
Centrifuge:	
Eppendorf 5417R	Hamburg, Germany
Sigma 3K30B and 1K15B	Braun Biotech International, Osterode in Harz, Germany
CO2-Incubator (37°C, 5 % CO2)	Heraeus
FACS-Canto II	BD, Heidelberg, Germany
Gel documentation	Bio-Rad
Gel Drying System	Bio-Rad
Glass wares	Schott, VWR Brand
Heat block (Thermomixer 5436)	Eppendorf
Ice machine	Sierra
Ice machine	Scotsman
Incubator BBD 6220	Heraeus, Hanau, Germany
Incubator shaker	B. Braun Biotech
Magnetic stirrer heat able	Labortechnik
Microscope:	
- Phase contrast microscope ID 02	Zeiss
- Fluorescence microscope Olympus BX61	Olympus, Hamburg, Germany
Microwave	AEG
Microplate reader Fluostar Optima	BMG Labtech, Jena, Germany
Neubauer chambers	Josef Peske Gmbh, Germany
PCR-Thermocycler Gene Amp® PCR System 2400	Perkin Elmer, Foster City, CA, USA
pH-Meter	Hanna Instruments, Kehl am Rhein, Germany
Pipettes	Gilson
Pipettes Eppendorf Power Supply 200/2.0	
Thermoshaker Thermomixer compact	Eppendorf, Hamburg, Germany

SDS-Gel electrophoresis apparatus	Peqlab
Shaking incubators:	
Certomat® R, B. and BS-1	B Braun Biotech International, Osterode am Harz, Germany
Spectrophotometer Ultrospec 3000,	Pharmacia Biotech, Freiburg, Germany
Sterile Working bench	Heraeus, HS12, Hanau, Germany
Transblot SD Semidry Transfer Cell	Bio-Rad
Sonificator (Sonifier 250)	Branson
UV-Transilluminator	BIO- RAD Laboratories, München, Germany
Vortex Genie 2	Scientific Industries
Voltage devices Power Pac 1000,	Bio-Rad Laboratories, München, Germany
Weighing balance	Kern & Sohn
Water bath GFL®	

2. 2 Methods

2.2.1 Microbiology

2.2.1.1 Bacteria strains

Yersinia enterocolitica **serotype O:8, wild type strain WA-314**, this is a clinical isolate harbouring the virulence plasmid pYV (Heesemann and Laufs, 1983; Heesemann et al., 1986). In this thesis, this strain is denoted WA(pYV).

WA-C: pYV cured strain obtained from WA-314

WA-C (pYV::CM) is an isogenic derivative of *Yersinia enterocolitica* serotype O: 8 strain WA(pYV), which contains a chloramphenicol resistance (Cmr) cassette in a noncoding region of the pYV plasmid, upstream of *yadA*-gene (Trulzsch et al., 2004).

WA-C (pYVΔH): WA(pYV) with deleted *yopH*-gene (Trulzsch et al., 2004)).

WA-C (pYVΔP): WA(pYV) with deleted *yopP*-gene (Trulzsch et al., 2004).

WA(pYVΔLcrD): WA(pYV) with inactivated lcrD gene, Ysc-T3SS defect (Ruckdeschel et al, 1996)

Yersinia pseudotuberculosis **serotype O3 wild type strain YPIII pIB1**, is a virulent clinical isolate that naturally lacks yopT and its chaperone, sycT (Viboud et al., 2006).

***Salmonella typhimurium* mutant SB300** (streptomycin resistance: StrR) (SL1344) (Hoiseth and Stocker, 1981).

***Listeria monocytogenes* serotype 1/2a** streptomycin resistant mutant obtained from strain 10403. The parental strain 10403 was first reported by Edman et al. (Edman et al., 1968) as an isolate from a human skin lesion and is further described by Bishop et al. (Bishop and Hinrichs, 1987).

Escherichia coli* strain K12 (JM109)* is a non-pathogenic laboratory strain (Kuhnert et al., 1997; Yanisch-Perron et al., 1985).

2.2.1.2 Bacteria culture medium

Table 7- Culture medium for the bacteria

Medium or Agar	Application
LB medium:	*E.coli*
10 g Peptone, 5 g Yeast-extract, 10 g NaCl were dissolved with	*Yersinia*
distilled water to 1000 ml and then autoclaved.	*Salmonella*
LB-Agar:	
10 g Peptone, 5 g Yeast-extract, 10 g NaCl and 15 g Agar were dissolved with distilled water to 1000 ml and then autoclaved.	
BHI-Medium:	*Listeria*
37 g BHI-powder was dissolved in distilled water to 1000 ml and then autoclaved.	
BHI-Agar:	
37 g BHI-powder and 15 g Agar were dissolved in distilled water and filled up to 1000 ml and then autoclaved.	

Table 8- Antibiotics used in the study

antibiotic	bacteria strain	working concentration	stock solution	dissolved in
Chloramphenicol (Cm)	WA-C (pYV::CM**)** WA314-Yops-Bla-Reporter strains (defined in chapter 2.2.1.1.)	30 µg/ml	30 mg/ml	70% Ethanol

Kanamycin (Km)	WA-C(pYVΔH)	100 µg/ml	50 mg/ml	H₂O dest.
	WA-C(pYVΔP)			
Streptomycin (St)	*Salmonell*	100 µg/ml	100 mg/ml	H₂O dest.
	Listeria			
Gentamycin (Gt)	depends	depends	10 mg/ml	Commercial product
Ampicillin (Amp)	depends	100 µg/ml	100 mg/ml	H₂O dest.

2.2.1.3 Bacteria mouse passage and storage

Prior to use for infection experiments, the pathogenic strains of *Yersinia*, *Salmonell*a and *Listeria* were passaged through mice by intraperitoneal infection with 5×10^5-5×10^6 colony forming unit (CFU). After 18-20 h, peritoneal lavage was plated on selective agars, *Yersinia*-selective CIN-agar, Brilliance *Salmonella* agar or Brilliance *Listeria* agar, respectively (Oxoid Germany GmbH, Wesel, Germany). One single colony from each strain was picked to inoculate an overnight liquid culture in Luria-Bertani (LB)- or brain heart infusion (BHI)-medium, supplemented with antibiotics (chloramphenicol, 30 µg/ml; kanamycin, 50 µg/ml or streptomycin, 100 µg/ml) where appropriate, and incubated at 27°C (*Yersinia*) or 37°C (*Salmonella*, *Listeria*). Bacteria in the stationary phase were sedimented and resuspended in LB-medium (*Yersinia*, *Salmonella*) or BHI-medium (*Listeria*) containing 15-20 % glycerol. 1 ml aliquots were frozen immediately in liquid nitrogen and stored at -80°C (stock aliquots). Serial dilutions from stock aliquot were plated to determine the CFU per ml for pathogens used for mouse infection. Mouse passage was performed every 3 to 6 months.

2.2.1.4 Bacteria culture and CFU determination

For mouse infection experiments with *Yersinia*, the appropriate concentration was prepared by diluting a frozen stock with PBS.

For mouse experiments with *Salmonella* and *Listeria*, or *in vitro* infection experiments, overnight cultures were prepared by inoculating the bacteria stocks in LB-medium (for *Salmonella* and *E. coli*) or BHI-medium (for *Listeria* and *Yersinia*), supplemented with 100 µg/ml streptomycin in the case of *Salmonella* and *Listeria*, 100 µg/ml Kanamycin in the case of WA-C (pYVΔH) and WA-C (pYVΔP), or 30 µg/ml chloramphenicol in the case of WA-C (pYV::CM), and incubated at 27°C (for *Yersinia* strains) or 37°C (for all the other strains).

Thereafter the overnight cultures were diluted 1:50 in fresh medium, supplemented with 0.3 M NaCl in the case of *Salmonella* to allow the expression of TTSS encoded by the *Salmonella* pathogenicity island 1 (SPI-1) which supports the invasion of *Salmonella* into host cells. The cultures were incubated for further 1.5 h (*Yersinia*) or 2.5-3 h (*Listeria*, *Salmonella*) at 37°C. Bacteria were then sedimented, resuspended in 1 ml cold PBS (in the case of Yersinia) or in 5-10 ml cold PBS (*Listeria*, *Salmonella*) and the OD_{600} was determined. The OD_{600} of *Yersinia* suspension was adjusted to 0.36 with PBS that corresponds to a concentration of ca. $3x10^9$ CFU/ml. The OD_{600} of 0.1 corresponds to ca. $5x10^7$ CFU of *Salmonella*/ml, 10^8 CFU of *Listeria*/ml or ca. $2.5x10^7$ CFU of *E. coli* K12/ml, respectively. The appropriate concentration for infection was then prepared by dilution with cell culture medium (with or without FCS) for *in vitro* infection or with PBS for mouse infection.

The equation that was used to adjust *Yersinia* CFU was as follows:

(Volume of Yersinia (in µl) x OD_{600} measured / 0.36) - Volume of Yersinia (in µl) = the volume (µl) that should be added or removed from the Yersinia culture, in order to reach a concentration of $3x10^9$ CFU *Yersinia* /ml.

2.2.2 Mouse experiments

2.2.2.1 Mouse infection

Cyld$^{-/-}$-knockout mice were generated by R. Massoumi as previously described (Massoumi et al., 2006). The mice are on a C57Bl/6J X 129Sv genetic background. All mice were bred under specific pathogen-free conditions. Female mice were used for infection experiments at 7–12 wk of age and the actually administrated dose was determined by plating serial dilutions on the appropriate agar plates.

For mouse infection experiments with *Yersinia*, the appropriate concentration was prepared from frozen stock suspensions by two times washing with PBS and then diluted with PBS. Stock suspensions were prepared as mentioned before by growing bacteria to stationary phase in LB medium at 27°C, followed by freezing in 15% glycerol. For oral infection, mice were subjected to fasting 16 h prior to the infection and $5 x 10^8$ CFU/20µl was administrated by peroral feeding through a pipette or by injection of an approximate volume and CFU.

For mouse infection with *Salmonella* and *Listeria*, overnight cultures were prepared by inoculating the bacteria stocks in LB-medium (for *Salmonella*) or BHI-medium (for *Listeria*), supplemented with 100 µg/ml streptomycin in the case of Salmonella and Listeria and incubated at 37°C. Thereafter, the overnight cultures were diluted 1:50 in fresh medium,

supplemented with 0.3 M NaCl in the case of *Salmonella* to allow the expression of TTSS encoded by the Salmonella pathogenicity island 1 (SPI-1) which mediates the invasion of *Salmonella* to the host cells. The cultures were incubated for further 2.5-3 h at 37°C. Bacteria were then sedimented, resuspended in 10 ml cold PBS and the OD_{600} was determined. The appropriate concentration for infection was then prepared by dilution with PBS (OD_{600} of 0.1 corresponds to ca. $5x10^7$ CFU of *Salmonella*/ml).

For intraperitoneal (i.p.) infection, mice were infected with the appropriate CFU in 500 µl DPBS. Syringe (1- or 3-ml syringe with 25-G needle) was filled with bacterial suspension, e.g. bacteria in DPBS and air bubbles were removed. The mouse was manually restrained with the abdomen being exposed, and the head was tilted backward. Needle was inserted into the lower left or right quadrant of the abdomen, avoiding the abdominal midline. The infection dose was injected with moderate pressure and speed.

Mice were sacrificed by CO_2 asphyxiation at indicated days. Organs (spleen, liver, Peyer's patches) were surgically removed and put in 2 mL tubes containing 1 ml PBS (for each liver, it was splited into three parts and put into three tubes) and 1 stainless steel bead (Ø 5 mm; Qiagen) and the organ was then homogenized in a mixing mill (Retsch, MM2000, Haan, Germany) by shaking 2-3 min at an oscillation frequency of 20 Hz. CFU were determined by first plating serial dilutions on LB- or BHI-plates supplemented with the appropriate antibiotics and then counting the CFU after incubation of ca. 40 h at 27°C (*Yersinia*) or 12-36 h at 37°C (*Listeria, Salmonella*). Statistical analysis of two mice groups was performed using a two-tailed Student's *t* test with Welch's correction. A *p-value* of less than 0.05 was considered to be statistically significant.

2.2.2.2 Saphenous vein puncture for blood sampling from mice

For the mouse, the circulating blood volume is about 5.5-7% of the body weight. For example a mouse with a weight of 25 g contains between 1.37 and 1.75 ml of circulating blood (Guidelines for the Survival Bleeding of Mice and Rats (NIH) http://oacu.od.nih.gov/ARAC/Bleeding.pdf).

Blood was collected from the lateral saphenous vein. This method yield enough blood for cytokine determination (0.1-0.2 ml), anaesthesia is not necessary, and enables serial blood collection from the same site without a need for new puncture wounds (Hem et al., 1998). The mouse was placed in a (perforated) restraining tube, so that its head was covered and the hind legs were free (Fig.8 Step1). The saphenous vein is found on the caudal surface of the thigh. Hair was removed from the area with scalpel (Fig.8 Step 2) to expose the saphenous vein

(Fig.8 Step3). The saphenous vein was punctured with a 22-gauge needle (Fig.8 Step4) and microvette collection tube (Sarstedt, Germany) was held against the blood drop that forms on the skin (Fig.8 Step5). When the needed blood volume was collected, the end of the microvette tube was sealed by a plastic cap (Fig.8 Step6) and the tube was inserted into the outer case (Fig.8 Step7). To stop the bleeding, pressure with cotton tissue was applied to the puncture site (Fig.8 Step8). The mouse was put back into the cage (Fig.8 step 9). Blood samples were incubated at 4°C for at least two hours and then centrifuged at ca. 5000 g for 10 min. Supernatants (serums) were transferred in new tubes and stored at -20°C. Blood collection from sacrificed mice was performed by puncture of the heart and collecting the flowing blood by using 1 ml pipette.
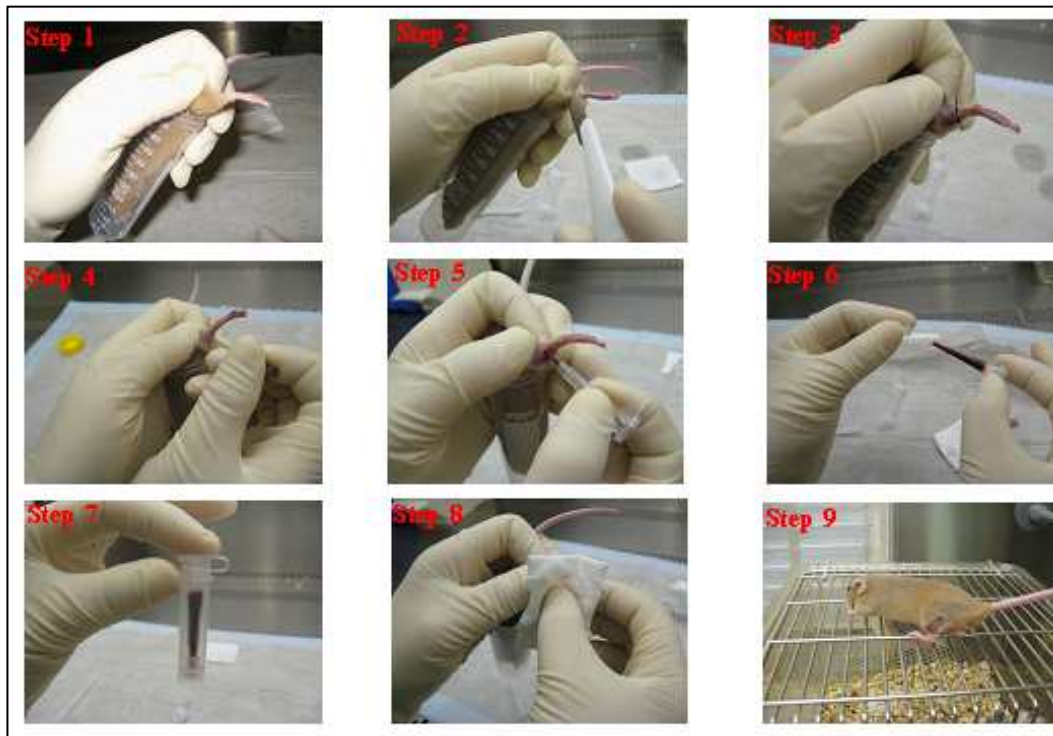
Fig. 8. Photographic documentation of blood sampling from the saphenous vein.

2.2.2.3 Proteose peptone elicitation of peritoneal exudate cells (PECs)

The murine peritoneal cavity provides a convenient site to obtain either resident or elicited macrophages and neutrophils (Edwards et al., 2006). Usually, the number of macrophages or neutrophils present in the peritoneum under nonelicited condition is insufficient for extensive cellular or biochemical studies. Therefore, eliciting agents, such as thioglycollate- Bio-Gel, or proteose peptone solutions have to be injected intraperitoneally several hours (for neutrophils) or days (for macrophages) prior to cell harvest to enrich the amount of phagocytes (Hoover

and Nacy, 1984). However, such elicitation will also alter the physiologic characteristics of the cells collected, such as the increased rate of plasma membrane turnover as well as increased phagocytic and respiratory burst capacity, and can exhibit variable responses to cytokine stimulation.

Considering that neutrophils are among the first cells to migrate into the inflammatory focus (within 2 to 4 hr) followed by a macrophage infiltrate, we prepared a differential elicitation procedure for neutrophils and macrophages, respectively.

For neutrophil elicidation, 3% (w/v) Proteose Peptone /D-PBS (without Ca^{++} or Mg^{++}) was freshly prepared and filtered through sterile 0.22 μm cartridge. 3 ml of this soltution were i.p injected. After 3 hours, PECs were isolated by lavage of the peritoneal cavity (2.2.2.4.) and used for in vitro infection experiments including respiratory oxidative burst or phagocytosis assay. Under theses conditions, neutrophils constituted about 60-90% of PECs. Since neutrophils are short-lived, they should be used within 2-4 hours after harvesting.

For macrophage elicitation, mice were i.p injected with 2 ml freshly prepared and sterile filtered (through 0.22 μm filter sterile cartridge) 10% (w/v) Proteose Peptone /D-PBS (without Ca or Mg). Three days later, PECs were isolated by lavage (2.2.2.4.) and used for in vitro infection experiments. Since macrophages are acutely sensitive to the biological effects of endotoxin, all reagents must be of high quality and endotoxin-free. If the yield of peritoneal cells seems unusually high, then the possibility of an ongoing low level of infection in the colon should be considered due to colon puncture during proteose/peptone injection.

Experienced yields of peritoneal cells were as follows:

Naive adult mice provided 1-3 x 10^6 cells per mouse (of which 20-30% were adherent cells, majority macrophages). Elicited mice provided 3-15 x 10^6 cells per mouse (60->80% were adherent cells).

3 ml 3% proteose peptone/DPBS i. p. injection resulted 3 hr later in 60-90% neutrophils (CD45+Ly6G+) and 10-30% macrophages (CD45+F4/80+) (Results are acquired by FACS analysis in this study).

2.2.2.4 Peritoneal lavage

This method was performed as mentioned by Stall et.al (Stall et al., 1988) and the website (http://icg.cpmc.columbia.edu/cattoretti/Protocol/MousePathology/CollectPerC.html)   with some minor modifications. It can be applied for peritoneal cells collection and bacteria mouse passage. In general, mice were sacrificed by CO_2 asphyxiation and immersed in 70% ethanol for ca. 5 min. The abdominal skin below the sternum was carefully nicked (taking care not to

nick the peritoneum). The abdominal skin was ripped apart with a firm but gentle movement by grabbing the two sides of the cut gently to expose the sternum and the pelvis (Fig.9 image A). Care should be taken not to rip the major abdominal vessels in order to avoid blood flow into the peritoneal cavity. The surface of the abdomen was again disinfected with 70% ethanol. 10ml syringe fitted with a 27-gauge short needle was prepared, first filled with 2 ml of air and thereafter with 5-6 ml of DPBS (Fig.9 image B). Air is very important in this step. The sternum was grabbed with the tweezers and the abdominal cavity was gently filled with DPBS. The needle was removed and followed by self-sealing of the peritoneum. The mouse was hold in the hand and shaken vigorously back and forth, left and right for about 15-20 times. The mouse was put back on the table. Pasteur pipette was prepared by attaching a rubber pipette. The sternum together with some peritoneum was grabbed with the tweezers and air-filled Pasteur pipette was inserted in the peritoneal cavity with a swirling movement (Fig.9 image C). The air was expressed in the cavity to distend the peritoneum and the peritoneal lavage fluid was aspirated. The success of peritoneal lavage depends on the distension of the peritoneum. The peritoneum was washed several times by injecting DPBS in the peritoneum with the Pasteur pipette and re-aspirating it.

Fig. 9. Collection of Peritoneal Cells. Images were adapted from the website
(http://icg.cpmc.columbia.edu/cattoretti/Protocol/MousePathology/CollectPerC.html)

2.2.3 Cell biology and Immunology

2.2.3.1 Poly-L-lysine treatment of well plates

Well-plates were coated with 0.01%, mol wt 150,000-300,000, sterile-filtered, cell culture tested Poly-L-lysine solution to let the cells attach to the bottom. In general, each well was covered with Poly-L-lysine (volume was depending on size of the well) and kept at room temperature for 1 hour under the culture hood. Poly-L-lysine solution was aspirated, and then washed with sterile water. The wash-step was repeated twice. The plates were allowed to dry completely (with the lids on) in the hood. Poly-L-lysine-coated plates could be stored at 4°C, wrapped in foil or applied for experiments directly.

2.2.3.2 Preparation of the splenocytes and determination of cell number

Mice were sacrificed by CO_2 asphyxiation. Spleen was surgically removed from the mouse and was put in a tube with 1 ml cold D-PBS. The spleen was placed into 40 μm cell strainer (BD). A plunger end of syringe was used to mash the spleen through the cell strainer into 50 ml Falcon tube. The cell strainer was rinsed with D-PBS to reach a final volume of ca.10 mL. The strainer was discarded. Cells suspension was spun at 300 x g/4°C for 5 minutes. Supernatants were discarded and cell pellet was resuspended in 5-10 mL erythrocytes lysis buffer, and incubated at RT for 5-10 minutes. 5 mL RPMI 1640 medium were added and cells were spun. Cell pellet was resuspended in 5 mL RPMI 1640 medium and any dead cell mass was discarded.

The estimation of the number of cells in a suspension was determined with a Neubauer counting chamber. 10 μL cell suspensions was mixed with 10 μL 0.4% trypan blue, and a drop of the mixed cell suspension was added on the top of the Neubauer count chamber covered by a cover-slip and the number of cells in the central largest square was counted under the light microscope. The exact number of cells per ml of the suspension was obtained by cells multiplying the number of cells in the large square x 10^4 (volume of the large square is 10^{-4} ml) x 2 (dilution number) = Cell number/ml suspension.

Erythrocyte lysis buffer (3/2 stock and store at 4°C)

Ammonium chloride 8.29 g/l; potassium hydrogen carbonate ($KHCO_3$) 1 g/l or $NaHCO_3$ 0.783 g/l; EDTA 0.0371 g/l, dissolved in 1 l Ampuwa and filter sterilized.

Working solution: mix 2 portions of Erythrocyte lysis buffer with 1 portion D-PBS.

2.2.3.3 Generation of BMDC from mice

The method to generate dendritic cells from mouse bone marrow was taken from Lutz. et al. with some minor modifications (Lutz et al., 1999). In general, mice were sacrificed by CO2 asphyxiation. All muscle tissues (rough tissue from the femurs, tibias and humerus) were removed with gauze. The bones were placed in a 60-mm dish with 70% ethanol for 5 min and then transferred into 60-mm dish with PBS. One or both ends of the bones were cut gently with scalpel, and then the bone marrow was flushed out by using a syringe and 27-gauge needle with 20 ml of RPMI 1640. Cells were centrifuged at 300 x g/ 4°C for 5 min.

Bone marrow cells from one mouse were resuspended in ca. 64 ml RPMI 1640 medium, containing 20 ng/ml GM-CSF, 10% fetal bovine serum (FCS), penicillin (P) (100

U/ml)/streptomycin (S) (100 mg/ml). The cell suspension was then split into eight Petri dishes (8 ml/dish) and incubated at 37°C (day 0).

On day 3, 8 ml RPMI 1640 medium, containing 20 ng/ml GM-CSF, 10% FCS, P/S, were added into each dish.

On day 6, 8 ml cell culture medium was collect from each dish and centrifuged at 300 x g, 4°C for 5 min. The supernatant was discarded, the cell pellet was resuspended in 64 ml RPMI 1640 medium, containing 20 ng/ml GM-CSF, 10% FCS, P/S, and split into the eight dishes.

On day 8 or 9, the BMDCs were ready to use. Non-attached cells were collected and centrifuged at 300 x g/4°C for 5 min. 6 ml cold PBS were added into each dish and incubated on ice for 300 x g/4°C ca. 20-30 min. Thereafter, cells were collected gently by using the cell scraper and centrifuged at 300 x g/4°C for 5 min. BMDCs were resuspended in RPMI 1640 medium (depending on subsequent experiments, with or without 5% FCS and/or penicillin/streptomycin) and counted.

2.2.3.4 Generation of BMDM from mice

Bone marrow cells were isolated from the mice as described before in chapter 2.2.3.3.

Bone marrow cells from one mouse were resuspended in ca. 64 ml RPMI 1640 medium, containing 10 ng/ml M-CSF, 10% FCS, penicillin (P) (100 U/ml)/streptomycin (S) (100 mg/ml). The cell suspension was distributed into eight Petri dishes and incubated at 37°C in 5% CO_2/air (day 0).

On day 3, 1 ml RPMI 1640 medium, containing 40 ng/ml M-CSF, 10% FCS, P/S, were added into each dish. The used M-CSF concentration allows to reach a final concentration of 5 ng/ml of M-CSF.

The BMDM were harvested as follows: the culture supernatant was discarded and ca. 5 ml cold PBS was put into each dish and incubated at 4°C for ca. 30 min. BMDM cells were then detached by pipetting up and down several times and centrifuged at 300 x g/4°C for 5 min. BMDM were resuspended in RPMI 1640 medium (depending on subsequent experiments, with or without 5% FCS and/or penicillin/streptomycin) and counted. Cell concentration was adjusted and cells were seeded on well plates. Generally, for the 48-well plate, 2×10^5 cells (in 100 µl medium) for each well were seeded.

2.2.3.5 Phagocytosis and intracellular growth assay

Phagocytosis assay was performed as mentioned by Hamrick et al. with some minor modifications (Hamrick et al., 2000). In general, mice were i.p. injected with 2 ml 10% sterile

proteose peptone/DPBS (0.22 µm filter-sterilized). Three days later, PECs were harvested and resuspended in RPMI 1640 medium containing 5% FBS and gentamicin (5 µg/ml) at a concentration of 5 x 10^5 cells/ml, and 0.5 ml of the cell suspension was placed into each well of a 48-well cell culture cluster plate (Costar, Cambridge, Mass.). Two hours later, the medium was removed and the plastic adherent cells were washed three times with 0.5 ml of Hanks balanced salt solution (HBSS) and then incubated in 0.5 ml of RPMI 1640 medium containing 5% FBS (without antibiotics) at 37°C in a humidified 5% CO2 incubator. Eighteen to twenty-four hours later, approximately 2.5 x 10^6 bacteria in 100 µl RPMI 1640 medium containing 5% FBS were added to the wells (this corresponded to MOI of 10). As control, some cell-free wells were seeded only by bacteria. The wells were mixed and centrifuged at RT, 300 x g /5 min. The well plate was incubated at 37°C in a humidified 5% CO2 incubator for 30 min. Thereafter the wells were washed gently three times with 0.5 ml of pre-warmed PBS, 500 µl RPMI 1640 medium containing 5% FBS and 100 µg/ml gentamicin were added to the cells and incubated for ca. 90 min at 37°C. The supernatants were then discarded and the wells were washed for three times with 0.5 ml of PBS each to eliminate loosely attached bacteria. Then, ca. 500 µl cold 0.1% Triton X-100/PBS were added into each well for cell lysis and incubated at 4°C for ca.15 min. Released bacteria were then collected by pipetting up and down very carefully and the wells were washed with ca.500 µl cold PBS. Both washes from each well were pooled together and serial dilutions were plated on LB-agar plates. After ca. 40 h/26°C (*Yersinia*) or 20 h/37°C (*E. coli* JM109) incubation, CFU were counted and documented. The gentamicin-protection assay was applied to determine the intracellular bacterial survivors.

After 30 min (or 60 min) of infection, the wells were gently washed three times with 0.5 ml of pre-warmed PBS and then 500 µl RPMI 1640 medium containing 5% FBS and 6 µg/ml gentamicin were added to kill the left extracellular bacteria at 37°C (time periods as indicated). Surviving intracellular bacteria were determined by plating serial dilutions of 0.1 % Triton R lysed infected cells as described above. The initial number of phagocytosed bacteria was defined as the CFU after 30 min of infection and 1 hr of gentamicin treatment.

For phagocytosis and intracellular growth assay with BMDMs, procedures were performed just exactly like that with PECs or splenocytes.

10% proteose peptone/DPBS:
Freshly prepared and sterile filtered through 0.22 µm cartridge.

0.1% Triton X-100/PBS:

100µl Triton X-100 were added to 100 ml PBS and stored for ca. 1 week at 4°C (the solution is stable during this short storage time).

2.2.3.6 *In vivo* phagocytosis assay

Mice were injected i.p. with 1 ml 10% proteose peptone. Ca. 40 h later the mice were infected i.p. with 500 µl PBS containing 5×10^7 CFU of *Y. enterocolitica* WA(pYV). 2 h after infection, peritoneal lavage was performed and PECs were centrifuged at 300 x g, 4°C for 5 min. PECs were then counted and same cell numbers were used from each mouse to determine the CFU of *Yersinia* that were being phagocytized and survived intracellularly. The cells were first resuspended in PBS containing 200 µg/ml gentamicin and incubated at 37°C for 90 min to kill the extracellular bacteria. Thereafter cells were permeabilized with 0.1% Triton X-100/PBS at 4°C for 5 min, and serial dilutions were plated on LB-agar plates. The number of the phagocytized *Yersinia* could then be counted after ca. 40 h incubation at 27°C as CFU.

2.2.3.7 Respiratory Oxidative Burst

2.2.3.7.1 Peritoneal cells for APF respiratory oxidative burst assay

Mice were injected i.p. with 3 ml 3% Proteose Peptone/D-PBS (0.22 µm/ filter-sterilized, freshly prepared) for 3 h. 3 h later, PECs were carefully prepared as mentioned in chapter 2.2.3.3. The PECs were incubated with 2 ml erythrocytes lysis buffer at RT for 5 min, centrifuged at 4° C x 300 g x 5 min. PECs were then resuspended in 1 ml RPMI1640 (without phenol red, Invitrogen Cat. No. 11835), containing 2.5% FCS, and the cell concentration were adjusted to 8×10^5 /180 µl. PECs were incubated on ice for at least 30 min in order to down regulate any preparation-resulted activation of the PECs. A small part of the cells was used for cell surface staining (see chapter 2.2.3.13) and FACS analysis in order to determine the fraction (%) of the different immune cells within the PECs of each mouse. Only PECs from the mice which had similar fractions of neutrophils (CD45+Ly6G+) and macrophages (CD45+F4/80+) were applied for the assay.

8×10^5 PECs in 180 µl medium were seeded per well in 24-well plate. 20 µl APF, dissolved in RPMI 1640 medium (without phenol red) containing 2.5% FBS were added to each well. This corresponds to a final working concentration of 10 µM (1:500 dilution from a 5 mM stock solution). Cells were incubated at 37°C for 30 min as described previously et.al (Setsukinai et al., 2003). The plates were protected from light during the entire assay period.

30 µl of bacteria suspension (resuspended in RPMI1640 containing 2.5% FCS) were added to the APF-loaded cells at MOI = 10 and incubated for 15 min, 30 min, 60 min, 90 min or 2 h. The actual infection doses were determined (CFU) by plating aliquotes on the LB-agar plates. Prior to infection, bacterial infection doses were incubated at 37°C for 5 min. Noninfected cells were used as control. After infection, the cells were collected in cold FACS-buffer, subjected to cell surface staining (see chapter 2.2.3.13) and analysed by FACS.

2.2.3.7.2 Splenocytes for luminol respiratory oxidative burst assay

Splenocytes were seeded on the white Grainer F bottom 96 well plate at a density of 1×10^5 cells per well in 100 µl RPMI 1640 medium containing 5% FBS, and incubated at 37°C for ca. 30 min to 1 h. Stock solution of luminol reagent (100 µg/ml) was diluted at 1: 100 in D-PBS. 10 µl of the diluted luminol were added to each well and incubated at 37°C for 30 min. Cells were then infected with bacteria at MOI of 2-50. Noninfected cells were used as control. The plate was centrifuged at 300 x g/4°C for 2 min and the measurement of luminescence was started immediately using luminescence plate reader (FLUOstar OPTIMA, BMG LABTECH). The white Grainer F bottom plate can be washed with 70% ethanol followed by immersing in the 70% ethanol overnight, and then next day washed again with 70% ethanol and allowed to dry under the flow, and then it can be reused for new assays.

2.2.3.8 NF-κB transcription factor assay

Splenocytes were resuspended in RPMI 1640, containing 5% FCS, and seeded in 6-well plate at a concentration of ca. 8×10^6 cells/800 µl/well. The plates were incubated at 37°C for 1 h and then infected with bacteria at MOI 10-80 for 30 min, 60 min, or 90 min. Nonstimulated cells were used as control. The actual infection dose (CFU) was determined by plating aliquote of the infection dose on LB-agar plates. The nuclear extracts were prepared using the nuclear extraction kit, according to the manufacturers' protocols (Active Motif). The nuclear extraction samples were stored at -80°C for future use.

NF-κB activation was measured and quantified using TransAM NF-κB family kit (Active Motif). This enzyme-linked immunosorbent assay (ELISA) is based on quantitative determination of p50-, p65-, c-Rel-, p52-, and RelB-binding to specific consensus DNA sequences that are immobilized on 96-well plate. The assay was performed according to the manufacturer's instructions. In some cases also whole cell lysates can be used (see manufacturer's instructions). Whole cell lysates or nuclear extracts were prepared after stimulation for the indicated time. 20 µl of whole cell lysates or nuclear extract were added

per ELISA well, incubated for 1 h at RT, washed 3 times, and then incubated with anti-p50, anti-p65, anti-c-Rel, anti-p52 or anti-RelB primary antibodies for 1 h. Thereafter, the wells were washed 3 times, and then incubated with the secondary peroxidase-conjugated antibody for 1 h at RT. After three times washing, the developing solution was added, incubated for 8-10 min, and then the reaction was stopped by adding 100 µl stop solution. The absorbance was then immediately read at 450 nm with reference wavelength of 655 nm using Sunrise™ microplate absorbance reader (Tecan, Germany).

Phosphatase inhibitors/PBS (20 ml): 10 x PBS 2 ml; H_2O (Amupuwa) 17 ml; phosphatase inhibitors 1 ml (supplied by Active Motif, part of the TransAM™ NFκB Family Kits).

2.2.3.9 Cell signalling assay

BMDCs were seeded at $2x10^6$ cells/well in 12-well plates in RPMI 1640 medium, containing 10% FCS, and incubated for 2-4 h at 37°C to enable cell adherence. Medium was discarded and 500 µl RPMI without FCS were added and incubated for 3-4 hours to perform cell starving. The reason for serum deprivation is that cell culture medium contains FCS which in turn contains many growth factors. Because of these factors and due to autocrine factors released by the cells under culture, cells will be in a state of continuous stimulation. This results in the activation of secondary messenger molecules (such as diacylglycerol, phosphatidylinositols, cAMP, Ca^{2+}, nitric oxide (NO) and carbon monoxide (CO)) in pulses which would interrupt the signalling pathways that should be tracked and mask the effects (Herschman et al., 1991; Ran et al., 1986). Therefore, it is necessary to prevent these signals by serum deprivation. By doing so, cells will enter quiescent state (G0 state) where they rest and there is no or minimum activity going inside the cell (Stice et al., 1999). But they could respond as soon as a stimulant is added.

After cell starving, cells were infected with 100 µl bacteria in RPMI 1640 medium at MOI 15. The plate was centrifuged for 2 min at 300 x g/4°C and then incubated at 37°C for different time points. Thereafter, the plate was incubated on ice, the supernatants were discarded and cells were resuspended in 110 µl denature buffer (CBA Cell Signaling master buffer kit; Cat. No. 560005 BD Biosciences) and transferred to 1.5 ml tube. Samples were incubated at 100°C for 5 min and then put on ice immediately before storing at -80°C for later use.

Phosphorylation states of p38 (T180/Y182), JNK1/2 (T183/Y185) and Erk1/2 (T202/Y204) were analyzed by using CBA Cell Signaling Flex Sets (BD Biosciences). The rate of phosphorylated kinases was determined by calculating the ratio of phosphorylated to the total kinase. Total JNK(1/2) and total p38α were determined using the corresponding multiplex

Flex Set Cytometric Bead Array (BD Biosciences). Before use, cell lysates samples were centrifuged at ca. 15000 x g/4°C for 3 min to pellet debris and samples were diluted at 1:8 with the appropriate volume of assay diluent to reduce the percentage of SDS. The assay was performed according to the manufacturer's instructions. Quantification of non-phosphorylated proteins and phospho-proteins (units/ml) was based on a calibration curve, which was established for each Flex Set using corresponding recombinant (phospho) proteins. FACS data were acquired on FACS CantoII (BD Biosciences) and analysed using the FCAP Array Software. The percent of phosphorylated proteins was determined by normalising the amount (units) of phosphorylated proteins to the corresponding total protein amount.

Denature buffer:

5 x denature buffer 800 µl; H_2O (Ampuwa) 3 ml; 1M DTT 4 µl; protease inhibitors cocktail 40 µl; phosphatase inhibitors 200 µl. Prepare freshly!

2.2.3.10 STAT4 cell signaling assay

Splenocytes and BMDCs were prepared as mentioned in chapter 2.2.4.2 and 2.2.4.3, respectively. $2x10^5$ BMDCs, $5x10^5$ splenocytes, or a mix of $2x10^4$ BMDCs and $4.5x10^5$ splenocytes (ca. 1:22) were seeded in poly-L-lysine-coated wells of 96-well clear-bottom white plate in RPMI 1640 medium, supplemented with 5% FCS, and incubated at 37°C for ca.2 h to let the cells attach to the bottom. Cells were then treated as follows:

Cells were infected with *Y. enterocolitica* WA314, *S. typhimurium*, or *L. monocytogenes* for 1 h at MOI of 5-50. After 1 h, medium was replaced by RMPI1640 medium containing 5%FCS and 6 µg/ml gentamycin, and incubated for further 4 h. Some wells were stimulated with 1 µg/ml LPS for 4 h, or 100 ng/ml recombinant IL12 for 30 min. Experiments were done in triplicate and the actual infection dose (CFU) was determined by plating aliquots of the bacteria on LB-agar plates.

The phosphorylated and/or total STAT4 was measured using FACE™ STAT4 Chemi Kit (Cat. No.48420 Active Motif), according to the manufacturer's instructions. In general, following stimulation, the cells were rapidly fixed to preserve activation-specific protein modifications. Each well was then incubated with the primary antibody that recognizes either phosphorylated STAT4 or total STAT4. Subsequent incubation with secondary HRP-conjugated antibody and developing solution provides an easily quantified chemiluminescent readout. The relative number of cells in each well is then determined using the provided Crystal Violet solution.

2.2.3.11 *In vitro* stimulation of cells for cytokine production

For preparing the cell culture supernatants, $2x10^5$ BMDCs/well or $5x10^5$ splenocytes/well were seeded in 96-well plate in RPMI 1640 medium containing 5% FCS, and incubated for 2-4 h to enable the cells to adhere. Supernatants were removed and new 100 μl RPMI 1640 medium (containing 5% FCS) and supplemented with different Toll-like receptor (TLR) agonists (see table 9) or bacteria at desired MOI (usually MOI=15) were given to the cells. Alternatively, bacteria were heat killed by exposure to 60°C for 1 h (*Yersinia*) (Kampik et al., 2000), 80°C for 45 min (*Listeria*) (Genovese et al., 1999), or 75°C for 1 h (Salmonella) (Sakharov et al., 1961). To control the viability of heat-killed bacteria, an aliquot of the heated suspensions was plated on the appropriate agar plates and incubated for 40 h. Cells were then incubated at 37°C for different time points. In some cases living bacteria were killed 1 h after starting infection by exchanging cell culture medium with another one containing 5 μg/ml gentamicin. Experiments were done in duplicate or triplicate.

After infection/stimulation for the desired time, the plates were incubated on ice, and the supernatants were collected and stored at -80°C for later use.

Prior to use, samples were mixed by vortexing and centrifuged at ca. 15.000 x g /4°C for 3 min to pellet debris. 50 μl of each cell culture supernatant was applied for quantifying cytokine concentrations according to the manufacturer's instructions (BD, Cat. No. 558266).

Table 9- TLRs agonists applied in this study. Table was modified from InvivoGen. All TLR agonists were purchased from InvivoGen/Cayla SAS (Catalog # tlrl-kit1m)

Agonist	TLR	Working con.	Stock solution con.	Volume of solvent
Pam3CSK4	TLR1/2	0.1-1 μg/ml	100 μg/ml	100 μl H$_2$O
HKLM	TLR2	10^8cells/ml	10^{10} cells/ml	100 μl H$_2$O
Poly(I:C)	TLR3	10ng-10 μg/ml	1 mg/ml	500 μl H$_2$O
Poly(I:C) LMW	TLR3	10ng-10 μg/ml	1 mg/ml	500 μl H$_2$O
LPS-EK	TLR4	10ng-10 μg/ml	100 μg/ml	1 ml H$_2$O
ST-FLA	TLR5	10ng-10 μg/ml	100 μg/ml	100 μl H$_2$O
FSL1	TLR6/2	1 ng-1 μg/ml	100 μg/ml	100 μl H$_2$O
ssRNA40	TLR6/7	0.25-10 μg/ml	100 μg/ml	250 μl H$_2$O
ODN1826	TLR9	5 μM	500 μM	31 μl H$_2$O

2.2.3.12 Cytokines measurement using cytometric bead array kit (CBA)

Analysis of cytokines from cell culture supernatants, collected mouse serum or homogenized organs was performed by using a cytometric bead array kit (CBA) (BD, Biosciences) and FACS data were acquired on FACS CantoII (BD Biosciences) and analysed using the FCAP Array Software (Fig.10). Standard curves were determined for each cytokine from a range of 10-5000 pg/ml.

This assay is based on beads coated with antibodies against the respective cytokines of interest which allow the capture of cytokines in a small sample volume. Furthermore, the beads for each cytokine have specific colour allowing the contribution of each beads population to one kind of cytokine and thus make it possible to measure all cytokines of interest within one sample. Captured cytokines can be then detected by incubating the beads with PE-conjugated detection antibodies against the cytokines and the concentration can be quantified by comparing the PE fluorescence intensities with those of the standards for each cytokine. In this assay, only two times of incubation are needed and one hour for each.

The beads for the cytokines of interest were pre-mixed and then incubated with cell culture supernatants (50 µl) or serum (5-25 µl) in a FACS tube at RT. After 1 h, PE-conjugated antibodies against for each cytokines were pre-mixed in a separate tube, added to the samples and incubated for another 1h. Thereafter 1 ml wash-buffer was added; the beads were centrifuged at 200 x g for 10 min and then resuspended in about 200 ul wash-buffer. The samples were then measured by FACS CantoII (BD Biosciences). FACS data were analysed using the FCAP Array Software. Standard curves were determined for each cytokine from a range of 10-5000 pg/ml.

2.2.3.13 Immune cells recruitment assay

Cyld^{+/-} and *Cyld*^{-/-} mice were infected i.p. with 2.5 x 10^{5} *Y. enterocolitica* WA314 for 20 h or 3 days, respectively. Peritoneal lavage and spleens were then harvested; splenocytes and PECs were subjected to cell staining with cell type-specific markers (see table 5 and table 6) and then subjected to FACS Canto II analysis. Data were collected and analyzed with FlowJo-8.8.4. Software (Tree Star Inc, USA). Only the results from mice groups that had similar bacteria loads in their spleen were considered.

2.2.3.13.1 Staining with cell type-specific markers

Antibodies (Abs) against cell type-specific markers were combined in 3 different groups for
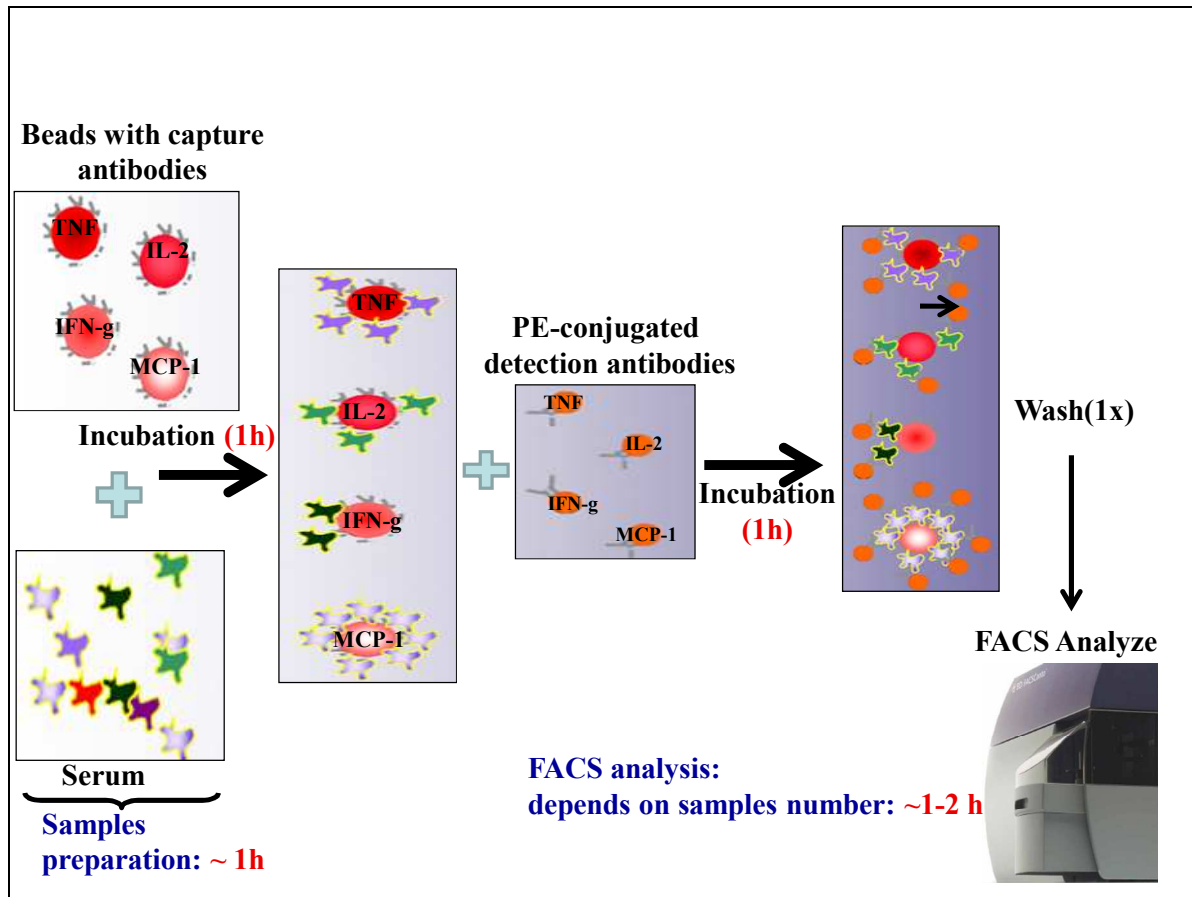
Fig. 10. Work flow of CBA procedure.

splenocytes (table 10) or in 1 group for peritoneal cells (table 11). About $1\text{-}2x10^6$ splenocytes or PECs were taken for each staining group. The appropriate cell number of splenocytes or PECs were centrifuged at 300 x g /4°C for 10 min, resuspended in 100 µl, 220 µl or 320 µl FACS buffer (depending on number of cells and antibody set of interest , containing Fc-Block (Anti-CD16/32, 5 µg Fc Block for ca.1x 10^7 cells), and incubate at 4°C for ca. 20 min. Cell samples were then split where appropriate (into 2 or 3 pre-labelled tubes, ca.100 µl in each tube). 10 µl of the corresponding antibody-set were added to each tube, mixed by pipetting up and down 3-4 times and incubated at 4°C for 30 min. 1000 µl FACS buffer were then added and centrifuged at 300 x g/4°C for 10 min. Cell pellets were resuspended in ca. 300 µl FACS buffer and analyzed by FACS. Alternatively, cell pellets were resuspended in 100 µl 3.7% formaldehyde, incubated at 4°C for 10-30 min. 1 ml FACS Buffer were then added and centrifuged at 300 x g/4°C for 10 min. This wash step was repeated once again to remove completely formaldehyde that can affect especially the tandem fluorophores. Cells were then resuspended in ca. 300 µl FACS Buffer and stored at 4°C, protected from light, for later analysis by FACS.

10^5 cells were acquired on FACS Canto II. Data were collected and analyzed with FlowJo-8.8.4. software (Tree Star Inc, USA). Absolute numbers of splenocytes subpopulations were calculated based on their percentage and the total number of leukocytes.

Table 10- Staining markers for splenocytes

Group	Antibodies	Dilutions (for 10^6 cells in 100 µl)	Cell type
1	CD45-PE-Cy7	1:3	Leukocytes
	B220/CD45R-PE	1:3	B cells
	CD11c-APC-Alexa750	1:5	DCs
	F4/80-PE-Cy7	1:5	Macrophages
2	CD45-PECy7	1:3	Leukocytes
	CD49b-APC	1:3	Natural Killer cells
	CD8-PerCP	1:3	CD8 T cells
3	Ly6G-PE	1:5	Neutrophils
	CD45-PE-Cy7	1:3	Leukocytes
	CD4-PE	1:3	CD4 T cells

Table 11- Staining markers for peritoneal cells

Group	Antibodies	Dilutions (for 10^6 cells in 100µl)	Cell type
1	CD45-PE-Cy7	1:3	Leukocytes
	F4/80-PE-Cy7	1:3	Macrophages
	CD11b-APC	1:5	Monocyte/macrophages
	Ly6G-PE	1:5	Neutrophils

FACS Buffer (0.22 µm-filter sterilized and stored at 4°C):

D-PBS (without magnesium and calcium), 2% FCS, 2 mM EDTA.

2.2.3.14 Immunohistochemistry (IHC)

Mice were sacrificed, tissues were isolated, rinsed in PBS, and carefully embedded in O.C.T embedding compound (Sakura Finetek / Hartenstein) in plastic mold, by avoiding air bubbles. Tissues were shock-frozen by setting the mold on top of liquid nitrogen until 70-80% of the

block turns white. Then, the block was put on top of dry ice. Frozen blocks were stored at -80°C for long-term storage.

For cryosectioning, frozen blocks were mounted on the cryostat holder (never, at any point, let the tissue warm up to temperatures above -15°C). Frozen blocks were allowed to equilibrate in the cryostat chamber for about 5 min. 6-10 µm sections were then cut using a cryomicrotome (Leica CM 1950) and collected onto pre-labelled SuperFrost Plus slides (Menzel-Gläser / Hartenstein). The best sections are usually obtained when the block temperature is around -18°C to -20°C. The sections were allowed to dry by incubating at RT for at least 1 h and processed for staining or stored at -20 °C.

For staining, slides were first fixed by immersing slides in acetone (-20°C cold) for 10 min on ice, and dried for few minutes at RT. The fixed slides were rehydrated two times in Tris-Buffered Saline with 0.1% Tween-20 (TBST) two times for 5 min, whereby TBST solution was changed in between washes (Note: Once the sections are re-hydrated with Tris-saline, never let the tissue dry out again; this will ruin the tissue architecture). Slides were put in cover plates and transferred into a slide rack (Thermo Fisher Scientific). Blocking was performed by incubating slides with 5% normal goat serum in TBST (150 µl/each slide) at RT for 45-60 min, and then washed three times each with 2 ml TBST. Thereafter slides were incubated for 1 h at RT with 150 µl/each slide TBST/2.5% normal goat serum containing rabbit O:8 antiserum (WA vital) raised against *Y. enterocolitica* O8 (Heesemann and Laufs, 1983) diluted 1:5000 in combination with one of the following antibodies that were diluted 1:200: rat anti-mouse CD45R/B220 or hamster anti-mouse CD11c-DC (BD biosciences). Slides were then washed three times with TBST and incubated for 1 h at RT with 150 µl/each slide TBST/2.5% normal goat serum containing Alex fluor 488-conjugated goat anti-rabbit (Invitrogen/Molecular Probes) applied for detection of rabbit anti-O:8 coated yersiniae, combined, where appropriate, with Alex fluor 555-conjugated goat anti-rat (Invitrogen/Molecular Probes) raised against CD45R/B220 antibody, Cy3-conjugated goat anti-hamster (dianova) raised against anti-mouse CD11c, PE-Texas Red-conjugated rat anti-mouse F4/80, or rat Alexa fluor 647-conjugated anti mouse neutrophils (clone 7/4; AbD Serotec). These antibodies were used at 1:200 dilutions. The combinations of antibodies used for IHC are summarized in table 12. Slides were then washed three times with TBST and incubated for 3 min at RT with 1 µg/ml 4',6-Diamidino-2-phenylindole dihydrochloride (DAPI) in 150 µl TBST. Slides were then washed two times with TBST, and covered with Fluoprep (Biomerieux) and a coverslip. Digital images in the DAPI, FITC, PE-Texas Red, Cy3, and Cy5 channels were collected using an Olympus BX-61 fluorescence microscope

(Olympus, Germany) equipped with cell^P software (Olympus Soft Imaging System). Images were converted to RGB, coloured and overlaid.

Table 12- Antibodies combinations used for IHC. Yersinia (WA-vital) was diluted 1:5,000. The other primary and secondary antibodies were diluted 1:200

Combinations	Primary Antibodies	Secondary Antibodies
A	Rat anti-B220	Alexa 555 conujugated goat anti-Rat
	Rabbit anti-O:8	Alexa 488 conujugated goat anti Rabbit
		DAPI
B	Hamster anti-CD3e	Cy3 conujugated anti-Hamster
	Rabbit anti-Yersinia(WA-vital)	Alexa 488 conujugated goat anti Rabbit
		DAPI
C	Rat anti-Ly-49D	Alexa 555 conujugated goat anti-Rat
	Rabbit anti-Yersinia(WA-vital)	Alexa 488 conujugated goat anti Rabbit
		DAPI
D	Hamster anti-CD11c	Cy3 conujugated anti-Hamster
	Rabbit anti-Yersinia(WA-vital)	Alexa 488 conujugated goat anti Rabbit
		DAPI
E		Alexa 647 conujugated rat anti-neutrophils
	Rabbit anti-Yersinia(WA-vital)	Alexa 488 conujugated goat anti Rabbit
		DAPI
F		PE-Texas Red rat anti-F4/80
	Rabbit anti-Yersinia(WA-vital)	Alexa 488 conujugated goat anti Rabbit
		DAPI

Tris-Buffered Saline Tween-20 (TBST):

Dissolve 8.8 g of NaCl, 0.2 g of KCl, and 3 g of Tris base in 800 ml of distilled H_2O. Add 1000 ul of Tween-20, Adjust the pH to 7.4 with HCl. Add distilled H_2O to 1 L. Sterilize by autoclaving.

2.2.3.15 Translocation assay

Beta-lactamases (β-lactamases) comprise a family of bacterial enzymes that cleave penicillins and cephalosporins. Coumarin cephalosporin fluorescein 4 (CCF4)-AM, a Fluorescence

Resonance Energy Transfer (FRET)-based fluorescent substrate, consists of a cephalosporin core bridging a 7-hydroxycoumarin residue and a fluorescein residue and permits the use of CCF4 as substrate and sensitive reporter gene expression. The lipophilic, esterified form of this substrate CCF4-AM readily enters the cell. Cleavage by endogenous cytoplasmic esterases rapidly converts CCF4-AM into its negatively charged form, CCF4, which is retained in the cytosol. Cleavage of the beta-lactam ring of the cephalosporin of CCF4 results in the separation of the fluorophores, cumarin and fluorescein, and subsequent disruption of FRET(Raz et al., 1998) (Fig.11).

Overnight cultures of Yop-Bla-Reporter *Yersinia* which were generated by Hicham Bouabe (this institute, unpublished data) were incubated in LB-Medium, containing 30 µg/ml chloramphenicol, at 27°C. Next day, bacteria were diluted at 1:40 and incubated for 90 min at 37°C. Bacteria were washed with cold HBSS (without Ca, Mg), resuspended in 1 ml HBSS (without Ca, Mg), and OD_{600} was determined. Infection dose (MOI = 20) in 50 µl was adjusted with RPMI/5% FCS according to the initial OD_{600} value of the bacterial suspension or the CFU (see chapter 2.2.1.4). $5x10^5$ BMDCs or freshly prepared splenocytes, resuspended in 120 µl RPMI/5% FCS without antibiotics, were seeded per well in 48 well-plate. Cells were incubated at 37°C for 1-2 h and then infected with the prepared reporter-strains in 50 µl medium at MOI = 20. Plates were incubated at 37° for 1 h. Cells were collected in cold HBSS (without Ca, Mg) and transferred to 1.5 ml tubes, and centrifuged at 300 x g/10 min at 4°C. Cells were resuspended in 300 µl CCF4-AM staining solution (Invitrogen) supplemented with 2.5 µM probenecid (Sigma, efflux inhibitor) which were prepared according to the manufacturer's instructions (Invitrogen), and incubated at RT for 75 min under agitation (ca. 800 rpm) and shelter from light. 1 ml cold HBSS (without Ca, Mg) was added and cells were centrifuged at 300 x g/10 min at 4°C. Cells were resuspended in 300 µl cold PBS/0.5% FCS/2mMEDTA. 10^5 cells per sample were applied for FACS Canto II analysis. Data were collected and analyzed with FlowJo-8.8.4. Software (Tree Star Inc, USA).
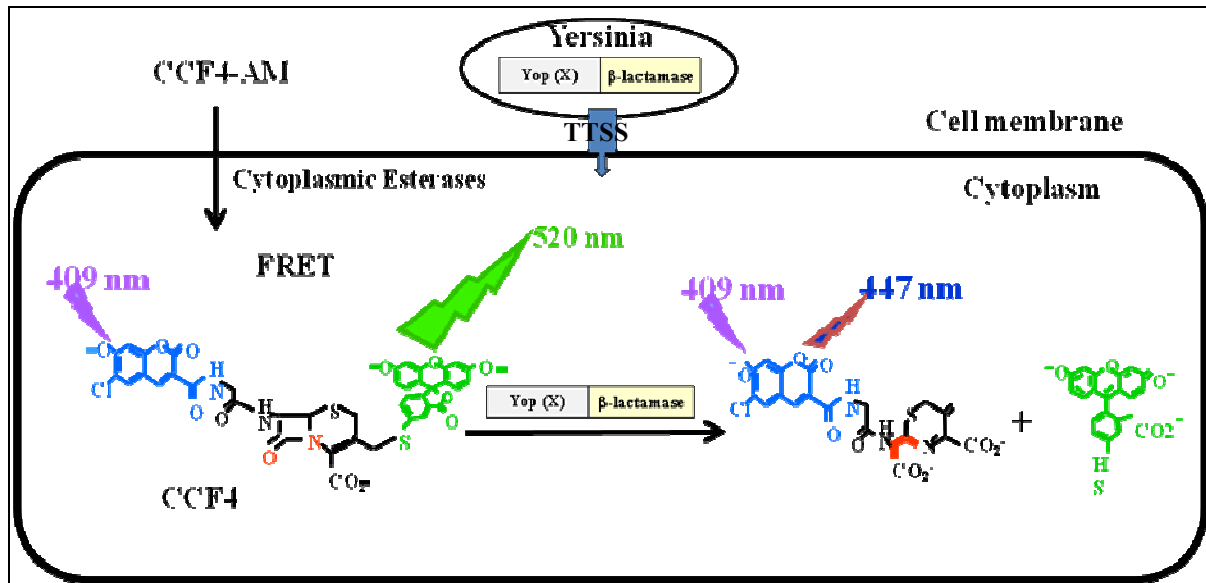
Fig. 11. Scheme of the translocation assay. The lipophilic, esterified form of CCF4-AM readily enters the cell. Cleavage of ester groups by endogenous cytoplasmic esterases rapidly converts this molecule into the negatively-charged substrate CCF4, which is retained in the cytosol. In the absence of β-lactamase activity, excitation of the coumarin (at 409 nm) in the intact molecule, results in FRET to the fluorescein, which emits a green fluorescence signal (at 520 nm). In the presence of β-lactamase (when translocation of Yop-Bla via the TTSS into host cells was occurred), enzymatic cleavage of CCF4 spatially separates the two dyes and disrupts FRET, so that excitation of the coumarin (at 409 nm) now produces a blue fluorescence signal (450 nm).

3. Results

3.1 *Cyld*$^{-/-}$ mice show enhanced resistance to *Yersinia* infection

Yersinia enterocolitica is a Gram-negative, food-borne enteric pathogen causing human self-limiting gastrointestinal diseases such as enteritis, terminal ileitis and mesenteric lymphadenitis, or septicemia with focal abscess formation in the liver and spleen (Bottone, 1997). Similar infection course and diseases can be developed in the mouse infection model, where *Y. enterocolitica*, after e.g. oral infection, replicates in the small intestine, invades Peyer's patches (PPs) of the ileum, and disseminated to the liver and spleen. In the latter organs, yersiniae replicate predominantly extracellularly and form localized lesions consisting of yersiniae microcolony infiltrated preferentially by neutrophile (abscess-like lesions) (Trulzsch et al., 2007).

In order to examine whether CYLD plays a role in the host defense against *Yersinia enterocolitica*, *Cyld*$^{-/-}$ mice and control *Cyld*$^{+/-}$ littermates were infected orally (1 x 10^9 CFU) or intraperitoneally (i.p.) (2 x 10^4 CFU) with *Y. enterocolitica* strain WA-314. Interestingly, whereas there was no significant difference (P = 0.57) in yersiniae load in the Peyer's patches of *Cyld*$^{-/-}$ mice and control mice after oral infection, *Cyld*$^{-/-}$ mice showed decreased yersinia load in the spleen and liver, after both oral and i.p. infection (Fig.12). Moreover, the closely related food-borne enteric pathogen *Yersinia. pseudotuberculosis* (O3; YPIII IB1), which is similar pathogenic and shares many virulence factors with *Y. enterocolitica* (Koornhof et al., 1999; Smego et al., 1999), also showed less infectivity to *Cyld*$^{-/-}$ mice in comparison to *Cyld*$^{+/-}$-mice (Fig.13). Thus, *Cyld*$^{-/-}$ mice show decreased susceptibility to *Yersinia* infection compared with *Cyld*$^{+/-}$-mice.

3.2 Differential susceptibility of *Cyld*$^{-/-}$ mice to enteric pathogen

To investigate whether CYLD possesses specific contribution to the host resistance to yersiniae, we challenged *Cyld*$^{-/-}$ mice and control Cyld$^{+/-}$ mice also with the Gram-negative *S. enterica* Serotype Typhimurium (strain SB300, here denoted as *S.* Typhimurium). In contrary to *Y. enterocolitica* and *Y. pseudotuberculosis*, *S.* Typhimurium is considered as a facultative intracellular pathogen. *S.* Typhimurium is a causative agent of gastrointestinal salmonellosis in humans. Interestingly, the susceptibility of *Cyld*$^{-/-}$ mice to *S.* Typhimurium was comparable (P>0.05) to that of *Cyld*$^{+/-}$ mice, after both oral and *i.p.* infection (Fig.14 A and B).
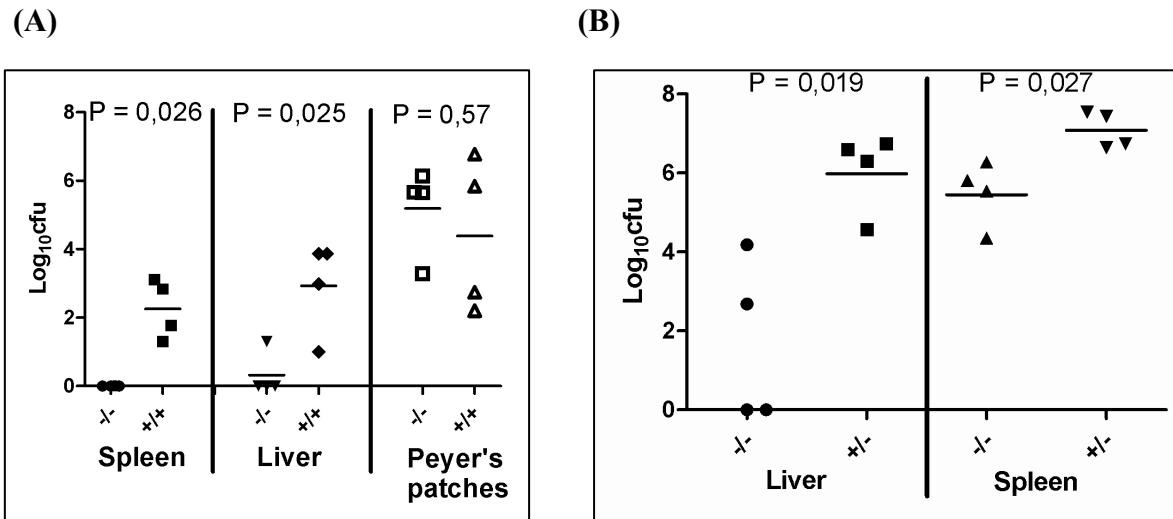
(A)

(B)

Fig. 12. CYLD-deficient mice displayed an enhanced host resistance to infection with *Y. enterocolitica* WA-314. A: Cyld mice were infected with *Y. enterocolitica* WA-314 at 1 x 10^9 orally **B:** *Cyld$^{-/-}$* and *Cyld$^{+/-}$* mice were i.p. 2 x 10^4 CFU infected for 5 hours or 2 x 10^4 *i.p.* for 5 days, respectively. *Cyld$^{-/-}$* and *Cyld$^{+/-}$* mice spleens, livers and Peyer's patches were then surgically removed from the mice, homogenized and plated on LB agar plates to detect the bacteria loads in these organs. Differences were considered statistically significant at P values < 0.05.
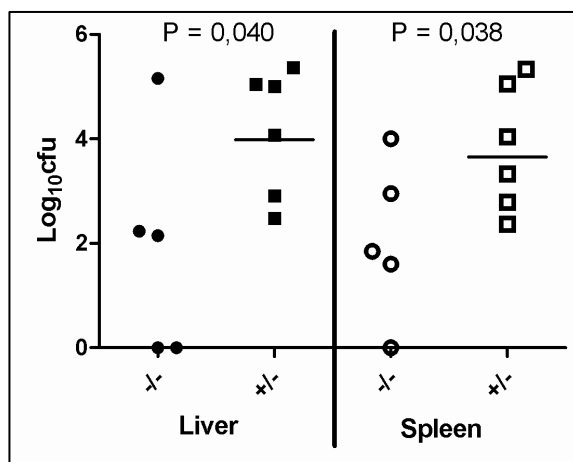
Fig. 13. CYLD-deficient mice displayed an enhanced host resistance to *i.p.* infection with *Y. pseudotuberculosis* (O3; YPIII IB1). 5 *Cyld$^{-/-}$* and 6 $^{+/-}$mice were infected with 1 x 10^5 *Y. pseudotuberculosis i.p.* for 5 days. Spleens and livers were then surgically removed from the mice, homogenized and plated on BHI agar plates to detect the bacteria loads in these two organs. Differences were considered statistically significant at P values < 0.05.

3.3 Similar immune cells influx into the peritoneal cavities and spleens of *Y. enterocolitica* infected *Cyld$^{-/-}$* and *Cyld$^{+/-}$* mice

Recruitment of leukocytes to the site of bacterial infection is integral to immune defense. The recruited leukocytes, such as neutrophilic granulocytes/neutrophils and macrophages, are known to participate in engulfing (phagocytosis), killing (microbicidal activity) and digesting (release several hydrolases such as elastase, catheprin, lysozyme etc.) of bacterial pathogens (Geng, 2001). Thus, we wondered whether the increased resistance of CYLD-deficient mice
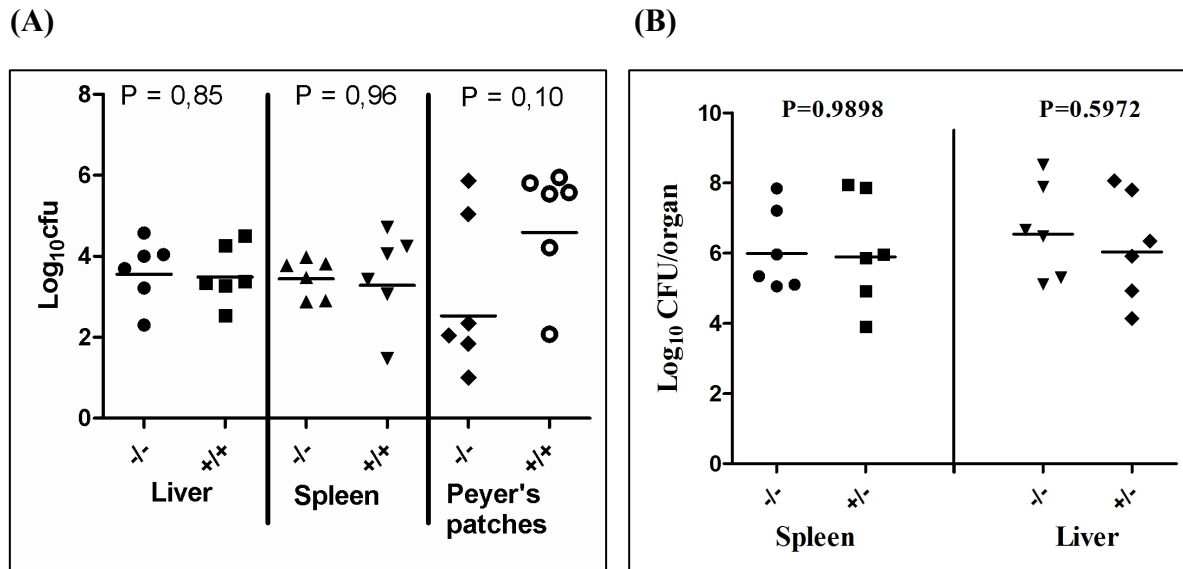
(A)

(B)

Fig. 14. Cyld-deficient and WT mice show similar resistance to *S. typhimurium* WT SB300 infection. Cyld mice were infected with *S. typhimurium* at 1 x 10^7 orally for 5 days **(A)** or 1.9 x 10^4 *i.p.* for 4 days **(B)**, respectively. Spleens and livers were then surgically removed from the mice, homogenized and plated on the LB agar plates to detect the bacteria loads in these organs. Differences were considered statistically significant at P values < 0.05.

to Yersinia infection is due to enhanced leukocyte recruitment to the site of infection leading to improved clearance of yersiniae.

Therefore, we analyzed the leukocytes influx to the peritoneal cavities and spleens of $Cyld^{+/-}$-control micetype and $Cyld^{/-}$ mice after i.p. infection with 2.5x10^5 CFU of *Y. enterocolitica* WA(pYV) for 20 h and 3 days post infection, respectively.

$Cyld^{/-}$ and $Cyld^{+/-}$ mice, which had initially comparable bacteria loads in the peritoneal cavity and spleens, showed similar influx of neutrophils (CD45+Ly6G+) into the peritoneal cavity (Fig.15A). Twenty hours after i.p. *Yersinia* infection, the percentage of neutrophils within CD45-positive peritoneal cell population increased to ca. 57% - 60% for $Cyld^{+/-}$ and $Cyld^{/-}$ mice, respectively and decreased moderately to about 44% - 50% after 3 days. A closer look showed that noninfected mice displayed less than 1% of which ratio increased to 56,7 % and 60,2 % in $Cyld^{+/-}$ and $Cyld^{/-}$ mice, respectively, 20 h after infection. The macrophage (CD45+F4/80+)-ratio, in both $Cyld^{+/-}$ and $Cyld^{/-}$ mice, decreased initially from ca. 22 - 25% to about 9% after 20 h and then increased to about 30 - 39% for $Cyld^{+/-}$ and $Cyld^{/-}$ mice, respectively, after 3 days post i.p. infection. The B cell ratio (CD45+B220+) did not essentially change for both $Cyld^{+/-}$ and $Cyld^{/-}$ mice after 20 h infection (15-20%) but thereafter declined below the value of the non-infected state after 3 days of infection. The CD8-T cells (CD45+CD8+) fraction increased 4-fold (4.3% - 4.9% compared with the nonstimulated ca. 1.1% – 1,5%) for both $Cyld^{+/-}$ and $Cyld^{/-}$ mice after 20 h and 3 days i.p. infection, respectively.

Compared to the peritoneal cavity the influx of immune cells into the spleen upon i.p. Yersinia infection was quite different (Fig.15B). For example, the ratio of the neutrophils increased continuously during the course of infection by 25% in both $Cyld^{+/-}$ and $Cyld^{/-}$ mice. The ratio of macrophages did not change after 20 h i.p. Yersinia infection (ca. 5%). However, after 3 days i.p. *Yersinia* infection the ratio of macrophages decreased to ca. 3%. For B and CD8-T lymphocytes, the percentages did not vary during the whole analyzed infection time and showed similar values like in noninfected mice.

3.4 Growth-inhibition and/or "disruption" of *Yersinia* microcolonies in the spleen of CYLD-deficient mice

The spleen is an important organ for antimicrobial immune reactivity, in particular for the *Yersinia* mouse infection model. To acquire a general view of the Yersinia infection in the spleen of $Cyld^{/-}$ and $Cyld^{+/+}$ mice, 6 to 8 weeks old mice were *i.p.* infected with *Y. enterocolitica* with a dose of 9 x 10^4 CFU and were sacrificed at day 1 (24 h) post infection (p.i.) or challenged with 2 x 10^4 yersiniae and then sacrificed 5 days later. Subsequently, 10-μm cryosections of spleens (part of the spleens were homogenized to check the bacteria loads) were prepared, immunostained with antibodies against neutrophils (Ly6G-Alexa 647), macrophages (F4/80-Texas Red), *Y. enterocolitica* (rabbit anti-*Yersinia* serum: WA-vital) and its corresponding secondary antibody conjugates (FITC-conjugated goat anti-rabbit antibody). This immunostaining was combined with cell nucleus staining using DAPI. The samples were then examined under fluorescence microscope.

Results indicated that at day 1 p.i., microcolonies (a clustered community of bacteria growing in tissue shown as small green spots in Fig. 16A and B) in spleens were tiny and interspersed all over the spleen, especially in the $Cyld^{/-}$ spleen (Fig. 16A). At this time point of infection, we could not see significant recruitment of macrophages or neutrophils into the microcolonies area.

Over the course of 5 days, microcolonies in the spleen of $Cyld^{/-}$ mice increased in size and spread over the entire spleen (Fig.17A and C) being interspersed mainly with neutrophils (Fig.17C). In the spleen of $Cyld^{+/-}$ mice, microabscesses of *Yersinia* instead of microcolonies were distributed homogeneously throughout the organs seemingly without a preferential anatomical location (Fig.17B and D), and being surrounded mainly by neutrophil granulocytes (Fig.17D), indicating the key role of the latter in fighting against *Yersinia*.
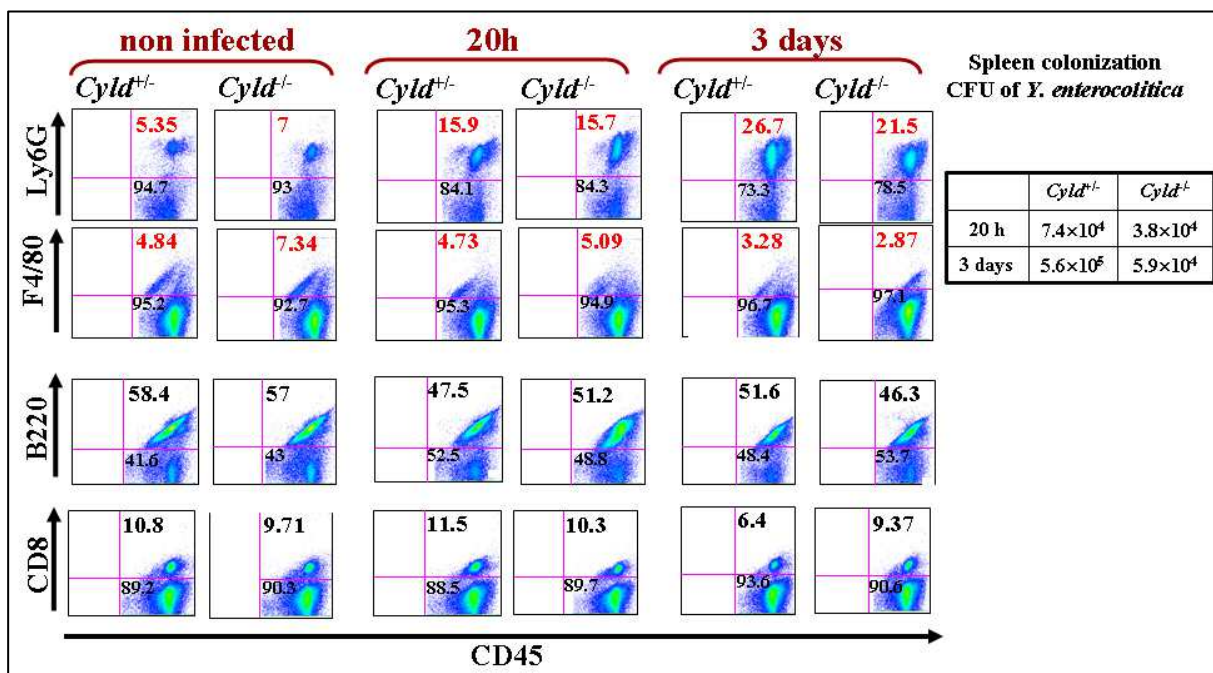
(A) Peritoneal cavity
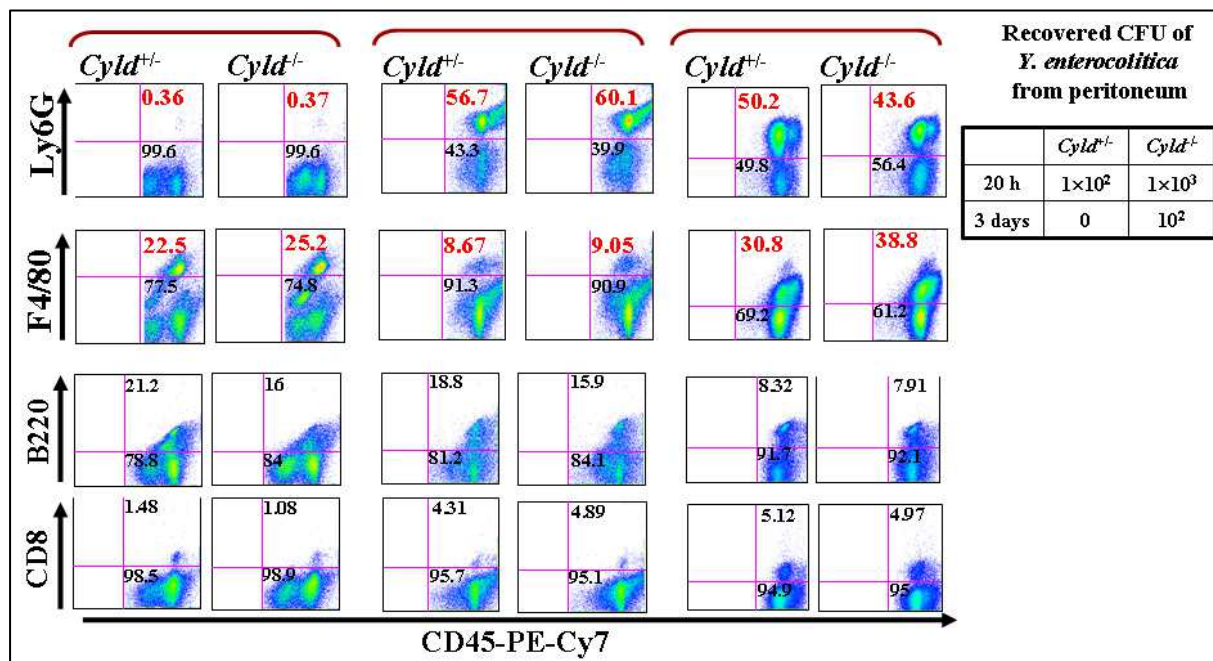
(B) Spleen

Fig. 15. Similar immune cells influx into the peritoneal cavities and spleens of *Yersinia* infected *Cyld^{-/-}* and *Cyld^{+/-}* mice. Mice were infected i.p. with 2.5x10^5 CFU of *Y. enterocolitica*. Peritoneal cells **(A)** and splenocytes **(B)** were stained with antibodies against the indicated cell type specific surface markers and analyzed by flow cytometry. Cells were gated on CD45 and CD45$^+$ leukocytes were analysed for the expression of the indicated cell type markers (F4/80, Ly6G, CD8 and B220). The bacteria burden in the peritoneal cavityperitonea and spleens are indicated in the tables (upper right). Data represent values of two independent experiments using groups of three mice (The indicated numbers are given as % of total CD45-positive cells.).
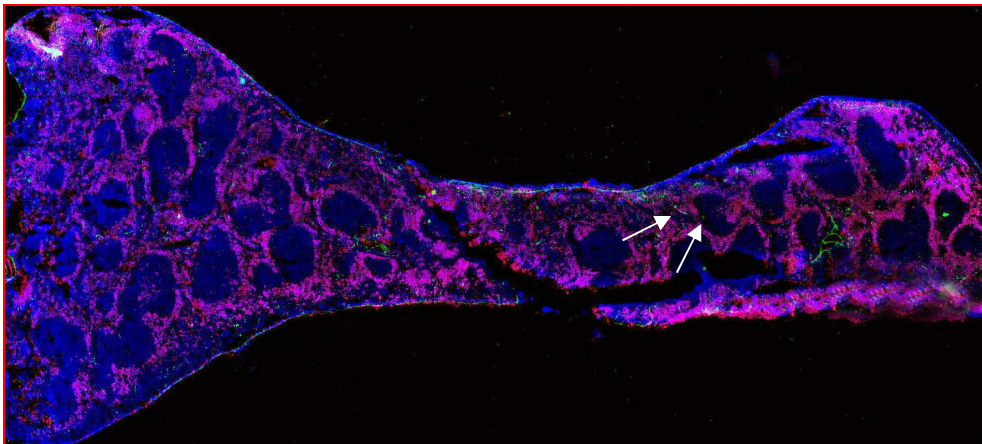
(A)
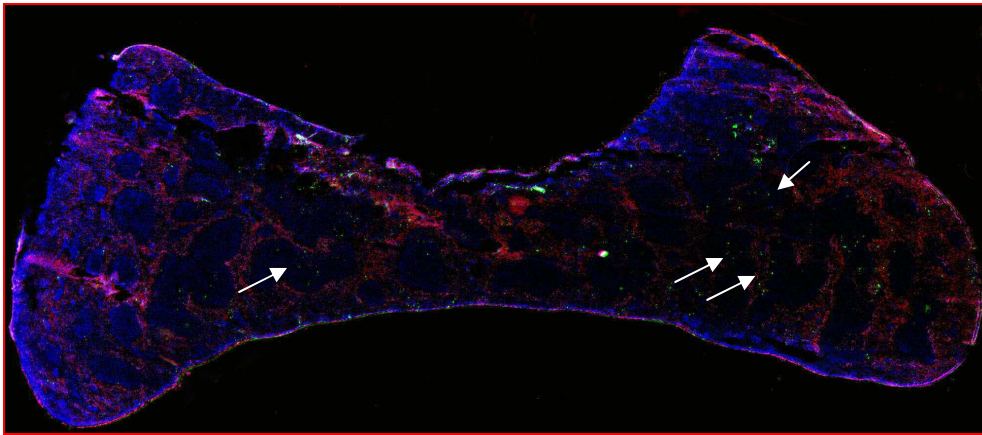
(B)

Fig. 16. Cryosection and immunostaining of the spleen from *Cyld*^{+/-} and *Cyld*^{-/-} mice. Mice were infected *i.p.* with 9 x 10^4 CFU of *Y. enterocolitica* for 24 h. Spleens were removed, placed directly in O.C.T embedding compound, frozen in liquid nitrogen and stored at -80 °C. Frozen tissues were cut at 10 µm thickness using a cryomicrotome. and sections were collected onto SuperFrost Plus slides (Menzel-Gläser / Hartenstein). Tissue sections were stained with a rabbit anti yersiniae serum antibody and a FITC-labeled secondary antibody, neutrophils were stained with Ly6G-Alexa 647, macrophages were stained with F4/80-Texas Red and nuclei were stained with DAPI. In the early infection stage (24 h p.i.), microcolonies (indicated by white arrows) in spleen of *Cyld*^{-/-} mouse were tiny and interspersed all over the spleen **(A)**. In the spleen of *Cyld*^{+/-} mouse, microcolonies were tiny and less than that of *Cyld*^{-/-} mouse **(B)**.

3.5 *Cyld*^{-/-} cells show higher phagocytic and intracellular killing capability for *Y. enterocolitica*

It is well known that the inhibition of phagocytes is a major virulence mechanism of *Y. enterocolitica* which supports extracellular survival and growth of this pathogen (Grosdent et al., 2002). In order to elucidate whether higher phagocytosis rates are involved in the improved resistance of *Cyld*^{-/-} mice in comparison to *Cyld*^{+/-}-mice to *Yersinia* infection, 10% proteose peptone elicited peritoneal cells (PECs) from *Cyld*^{+/-} and *Cyld*^{-/-} mice were used for the phagocytosis assay (see chapter 2.2.3.5). Our pilot experiments revealed that significant
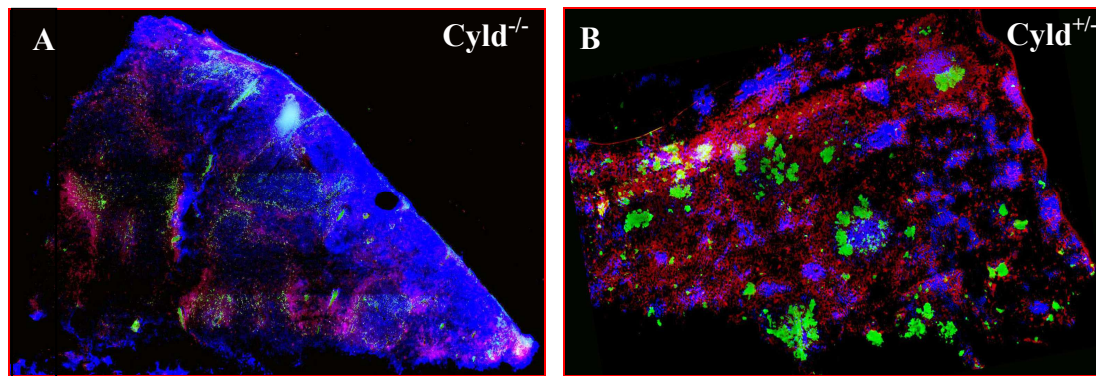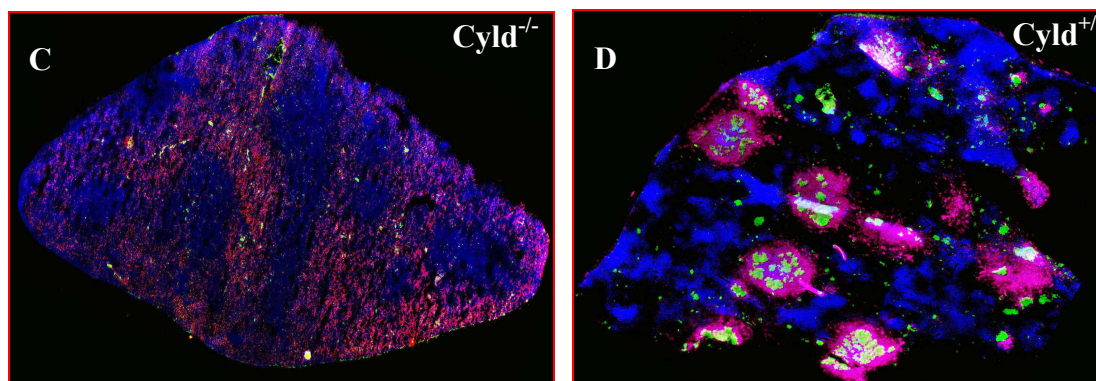
F4/80-PE-TexasRed/*Y.enterocolitica*-**FITC**/**DAPI**

Ly6G-Alexa647/*Y.enterocolitica*-**FITC**/**DAPI**

Fig. 17. Immunostained cryosection of the spleen from *Cyld*^{+/-} and *Cyld*^{-/-} mice. Mice were infected i.p. with 2×10^4 CFU of *Y. enterocolitica*. 5 days later spleens were cryo-cut and the obtaines sections were stained with an anti-*Yersinia* antibody and a FITC-labeled secondary antibody (green), neutrophils were stained with Ly6G-Alexa 647 (pink), macrophages were stained with F4/80-Texas Red (red) and nuclei were stained with DAPI (blue). Microcolonies in the spleen of *Cyld*^{-/-} mice increased in size (compared to their form 24h p.i.; see Fig.16) and spread over the entire spleen being interspersed with the macrophages **(A)** and neutrophils **(C)**. In the spleen of *Cyld*-competent mice, microabscesses instead of microcolonies were distributed homogeneously throughout the organs being surrounded by macrophages (red) **(B)** and neutrophils (pink) **(D)**.

phagocytosis differences between *Cyld*^{-/-} and *Cyld*^{+/-} PECs were obtained at multiplicity of infection (MOI) of 5-10 yersiniae. This MOI allowed direct comparisons between these *Cyld*^{+/-} and *Cyld*^{-/-} cells and reduced potentially confounding effects associated with higher MOI (e.g. endotoxin effects, cell damage).

We first monitored the behavior of *Y. enterocolitica* in contact with PECs at an MOI = 10 (results from plating of infection dose) and after 30 min of infection at 37°C (adherence and uptake phase), gentamicin (100 µg/ml) was added and cells were incubated for further 90 min to kill the extracellular bacteria. Then we determined the bacterial number that were phagocytosed and survival intracellularly by plating the cell lysates and counted the number of recovered *Yersinia* colonies (CFU). Results showed that more bacteria (about three times more) survived in *Cyld*^{-/-} PECs compared to *Cyld*^{+/-} PECs (Fig. 18A). It is of note that this

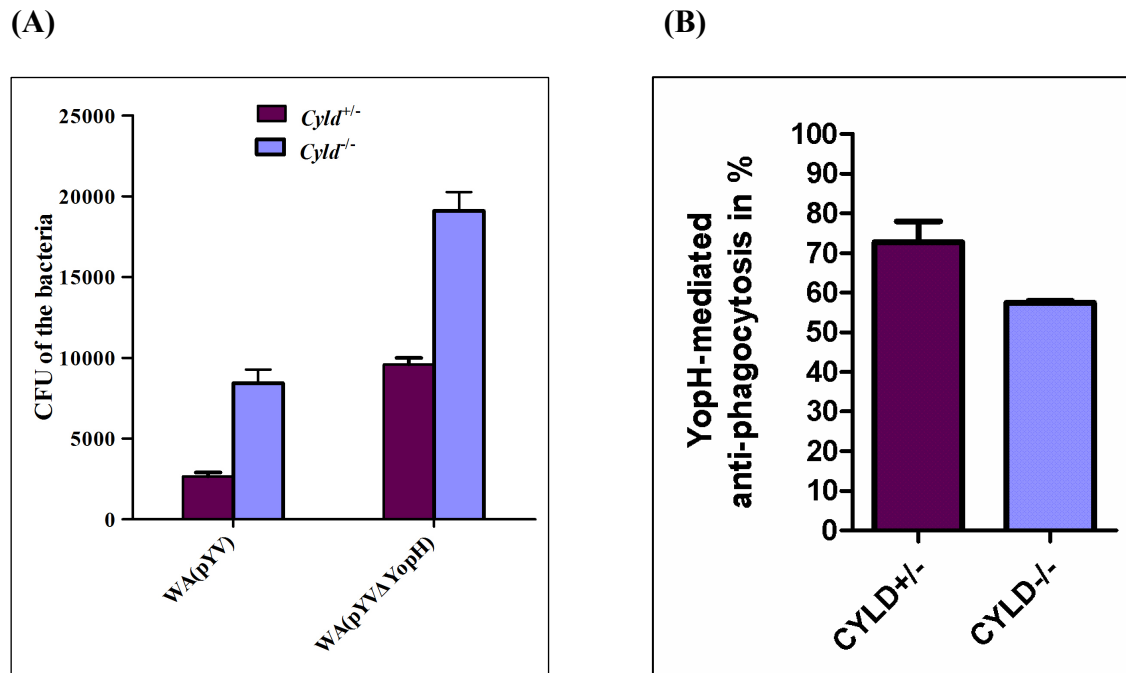gentamicin protection assay does not differentiate between different uptake rates and survival rates.

(A)   **(B)**

Fig. 18. *Cyld^{-/-}* PECs show higher numbers of internalized *Y. enterocolitica in vitro*. PECs were infected (MOI = 10) with *Y. enterocolitica* strain WA(pYV) and mutant WA(pYVΔYopH) (MOI = 10) for 30 min, gentamicin (100 µg/ml) was then added and cells were incubated for further 90 min. Cells were then specifically lysed with 0.1% Triton X-100 and serial dilutions were plated on the appropriate plates. **(A)** Number of CFU recovered from cell's interior. **(B)** The YopH-mediated anti-phagocytosis effect was calculated as follow: CFU of WA(pYV) x 100/ CFU of WA(pYVΔYopH).

Several studies by other investigators demonstrated that YopH is an important effector that allows yersinia to resist phagocytosis by cells (Fallman et al., 1995; Grosdent et al., 2002; Rosqvist et al., 1988). To explore the impact of YopH on the host phagocytosis of *Y. enterocolitica* in our study, YopH mutant (WApYVΔYopH) was applied to the assay under the same conditions described above for strain WA(pYV). Our results are also in accordance with the other reports that there were more WA(pYVΔYopH) being phagocytosed (Fig.18A) by both the *Cyld^{-/-}* PECs and *Cyld^{+/-}* PECs compared with the strain WA(pYV), confirming the involvement of YopH in anti-phagocytosis effect of *Yersinia*. Meanwhile, our results also demonstrated that there were still more WA(pYVΔYopH) being phagocytosed by *Cyld^{-/-}* PECs compared to *Cyld^{+/-}* PECs. However, this time *Cyld^{-/-}* PECs phagocytosed only two times more WA(pYVΔYopH) compared to *Cyld^{+/-}* PECs. Thus, the anti-phagocytosis efficiency mediated by YopH seemed a little higher (Fig.18B) in *Cyld^{+/-}* PECs (ca.73%) compared with *Cyld^{-/-}* PECs (ca.58%) which indicates that YopH is more effective under the presence of CYLD. Furtheremore, although the improvement of *Yersinia* phagocytosis by *Cyld^{-/-}* cells seems to be due to attenuated function of YopH in these cells, also the

impairment of the anti-phagocytosis effect of other *Yersinia* effectors (e.g. YopE, YopO, YopT) in the absence of CYLD seems to contribute to this phagocytosis phenotype.

To exclude the possibility that *Cyld*^{-/-} cells exhibit an intrinsic stronger phagocytic capability that is not specifically restricted to *Y. enterocolitica*, we applied PECs from *Cyld*^{+/-} and *Cyld*^{-/-} mice for the phagocytosis assay to the non-pathogenic bacteria such as *E. coli* JM109 infection. The results showed similar phagocytosis and intracellular growth of *E. coli* by both the *Cyld*^{-/-} and *Cyld*^{+/-} PECs after 1.5 h and 13 h p.i., respectively (Fig.19).
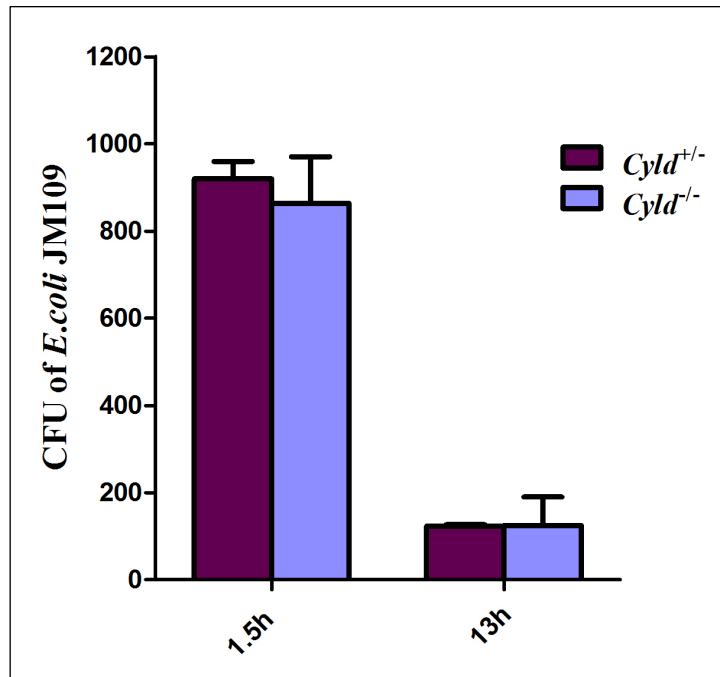

Fig. 19. Non-pathogenic *E. coli* JM109 is similarly phagocytosed by *Cyld*^{+/-} and *Cyld*^{-/-} cells. PECs were infected with *E. coli* JM109 (MOI 30) for 60 min, Gentamicin (10 µg/ml) was then added and cells were incubated for further 1.5 h or 13 h, respectively.

The increased *Yersinia* phagocytosis by *Cyld*^{-/-} PECs could be responsible for the increased resistance of *Cyld*^{-/-} mice to *Yersinia* infection. To substantiate this suggestion we checked the survival of *Y. enterocolitica* within PECs at different time points, under sustained presence of gentamicin (at a lower concentration, 6 µg/ml) to kill only the extracellular bacteria. As shown in Fig.18, the CFU of intracellular *Y. enterocolitica* rapidly dropped for both the *Cyld*^{+/-} PECs and *Cyld*^{-/-} PECs during the period of 2 h to 6 h p.i. However, in *Cyld*^{-/-} PECs the number of intracellular bacteria decreased more rapidly (from 4.5×10^5 at 2 h p.i. to less than 5×10^3 at 6 h p.i.) compared with *Cyld*^{+/-} PECs (from 3.2×10^5 at 2 h p.i. to less than 1×10^4 at 6 h p.i.). And after 12 h the majority of intracellular yersiniae in both cell types dropped below 10^3.
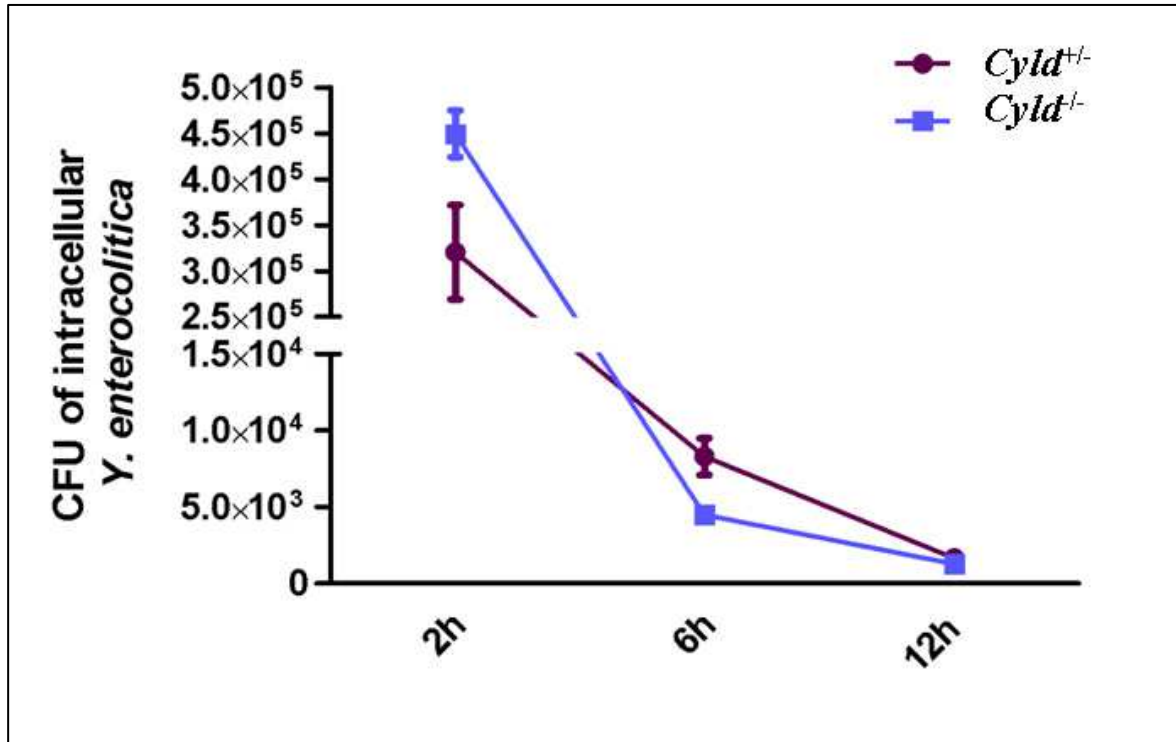
Fig. 20. *Cyld*^{-/-} **PECs display more efficient intracellular killing of internalized *Y. enterocolitica* than *Cyld*^{+/-} cells.** PECs were infected with strain WA(pYV) (MOI = 5) for 60 min. Gentamicin (100 μg/ml) was added and cells were incubated for further 90min to kill rapidly extracellular yersiniae. For longer infection time, medium was exchanged with fresh medium containing only 6 μg/ml gentamicin. Cells were then lysed with 0.1% Triton X-100 and serial dilutions were plated on appropriate plates.

To validate the phagocytosis data under *in vivo* conditions, we performed phagocytosis assay *in vivo* (see chapter 2.2.3.6 in the method part).

Mice were injected i.p. with 1 ml 10% proteose peptone in order to recruit phagocytic cells in the peritoneal cavity. Ca. 40 h later, mice were infected i.p. with *Y. enterocolitica* WA(pYV). After 2 h, peritoneal lavage was performed and PECs were treated with gentamicin for 90 min to kill the extracellular bacteria. Then we determined the CFU by plating PECs. Results of CFU showed that there were almost twofold more bacteria being phagocytosed by *Cyld*^{-/-} PECs *in vivo* compared with *Cyld*^{+/-} PECs (Fig.21), and thus confirming the *in vitro* phagocytosis data.

3.6 *Cyld*^{-/-} PECs cells show higher respiratory oxidative burst response specifically to *Y. enterocolitica* WA(pYV)

It is well established that during phagocytosis of microorganisms or upon cell stimulation with soluble agents, such as the peptide formyl-methionyl-leucyl-phenylalanine (fMLP) derived from bacteria, phagocytes produce superoxide via catalysis of one-electron reduction
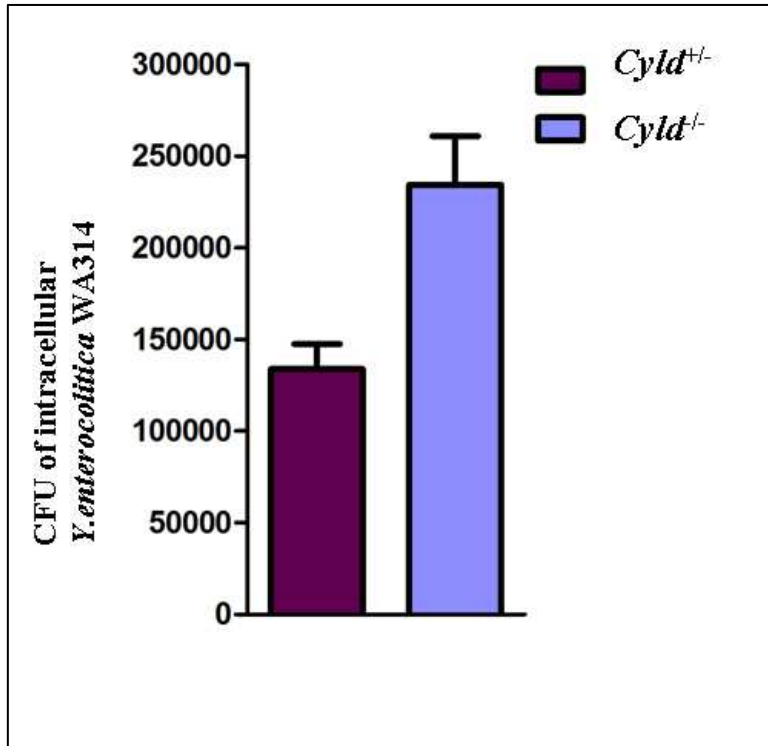
Fig.21. *Cyld*[/-] **PECs show higher numbers of intracellular** *Y. enterocolitica.* CYLD mice were injected *i.p.* with 1 ml 10% proteose peptone for ca. 40h and then the mice were infected i.p. with 5×10^7 CFU of WA(pYV). 2 h later, PECs were prepared by lavage and same cell numbers were used from each mouse to determine the number of the being phagocytosed *yersinia* by performing permeabilization with 0.1% Triton X-100 for 5 min, at 4°C. Serial dilutions were plated on the appropriate agar plates. The number of phagocytosed *Yersinia* could then be counted after ca. 40 h incubation at 27°C.

of oxygen to superoxide by activated phagocyte NADPH oxidase, (Akasaki et al., 1999; Stuart and Ezekowitz, 2005; Takeshige et al., 1996). The reactive oxygen species (ROS) subsequently derived from superoxide, a precursor of microbicidal oxidants, are essential for microbial killing (Roos et al., 1996). The NADPH oxidase consists of cytochrome b558, a membrane-spanning glycoprotein, and three cytosolic proteins (p47phox, p67phox, p40phox and the small G-protein Rac) (Kikuchi et al., 1994; Koga et al., 1999; Kuribayashi et al., 2002; Sumimoto et al., 1994). Cytochrome b558, located in the plasma membrane of phagocytes, is a heterodimeric protein composed of a 91-kDa glycoprotein (gp91phox) and a 22-kDa protein (p22phox) (Yamauchi et al., 2001; Yu et al., 1997). In resting cells, the NADPH oxidase is non-functional ("dormant") because important components have to be activated to translocate from the cytoplasma to the cytoplasma membrane. After cells are stimulated, signaling cascades trigger the exchange of Rac-bound GTP by GTP, in Rac, and the phosphorylation of the cytosolic phox proteins (p47phox, p67phox, p40phox) by kinases. The activated cytosolic components of the NADPH oxidase translocate to the membrane and form a complex together with cytochrome b558 where they catalyze the production of superoxide (Ago et al., 1999; Nakanishi et al., 1992; Sumimoto et al., 1994).

The oxidative burst, as a rapid, transient way to produce huge amounts of ROS, represents one of the earliest powerful anti-microbial defense strategy, but on the other hand, generated ROS released in excess into media can damage host tissue. Various techniques have been described to determine ROS production including chemiluminescence (Briheim et al., 1989), fluorescence (Rest, 1994) and cytochrome c reduction (Smith and Weidemann, 1993).

We compared ROS production of $Cyld^{+/-}$ and $Cyld^{-/-}$ cells using two different ROS-sensitive probes. The first one was a chemiluminometric probe, 5-amino-2, 3-dihydro-1, 4-phthalazinedione (luminol) (Allen and Loose, 1976), that reacts with ROS generated by phagocytes to produce an excited aminophtalate anion that emits light when returning to ground state. Light emission could be measured quantitatively by luminescence plate reader. The second one was a fluorimetric probe, Aminophenyl Fluorescein (APF) (Setsukinai et al., 2003). APF is nonfluorescent because the fluorescence of fluorescein is quenched by protection of the phenolic hydroxy group at the 6'-position of fluorescein with an electron-rich aromatic ring (aminophenyl). APF is O-deacylated upon reaction with ROS to yield strongly fluorescent fluorescein. Table13 summarizes the properties of the probes applied in our study.

Table 13- Properties of the APF and Luminol probes applied in the study to measure respiratory oxidative burst activation. (Modified from Freitas et al., 2009).

Probe	APF/HPF	Luminol
Reactive species detected	HO•, ONOO−, HOCl (only APF)	O_2•−, H_2O_2, HO•, HOCl, •NO, ONOO
Intra or extracellular localization	Intracellular	Intracellular, extracellular
Excitation/emission (nm)	500/520	Visible laser
Advantages	It is possible to detect HOCl selectively.	Highly sensitive
Limitations	HPF and APF are not auto oxidized by light irradiation.	Luminol can act as a source of O_2

3.6.1 Oxidative burst analysis by flow cytometry using APF

We analyzed the intracellular ROS production by PECs using the fluorimetric probe, Aminophenyl Fluorescein (APF) (see chapter 2.2.3.7.1.).

PECs from $Cyld^{+/-}$ and $Cyld^{-/-}$ mice were prepared by injecting *i.p.* 3% Proteose peptone. After 3 h neutrophils were prepared by lavages of the peritoneal cavity (Luo and Dorf, 2001).

PECs from mice that showed similar cell influx, especially neutrophils (CD45+Ly6G+) and macrophages (CD45+F4/80+), into the peritoneal cavities (Figure. 22) were applied to the APF assay. As seen in the representative example in Figure.25, the $Cyld^{+/-}$ mice No. 4351 and 4352, showed similar relative portion of neutrophils (CD45+Ly6G+) influx as the $Cyld^{-/-}$ mice No. 4355 and 4353, reaching an recruited portion of about 30% of total cells. The percentages of macrophages (CD45+F4/80+) were 16% and 17.3% in the $Cyld^{+/-}$, and 16.2% and 19.2% in the $Cyld^{-/-}$ mice, respectively (Fig.22).
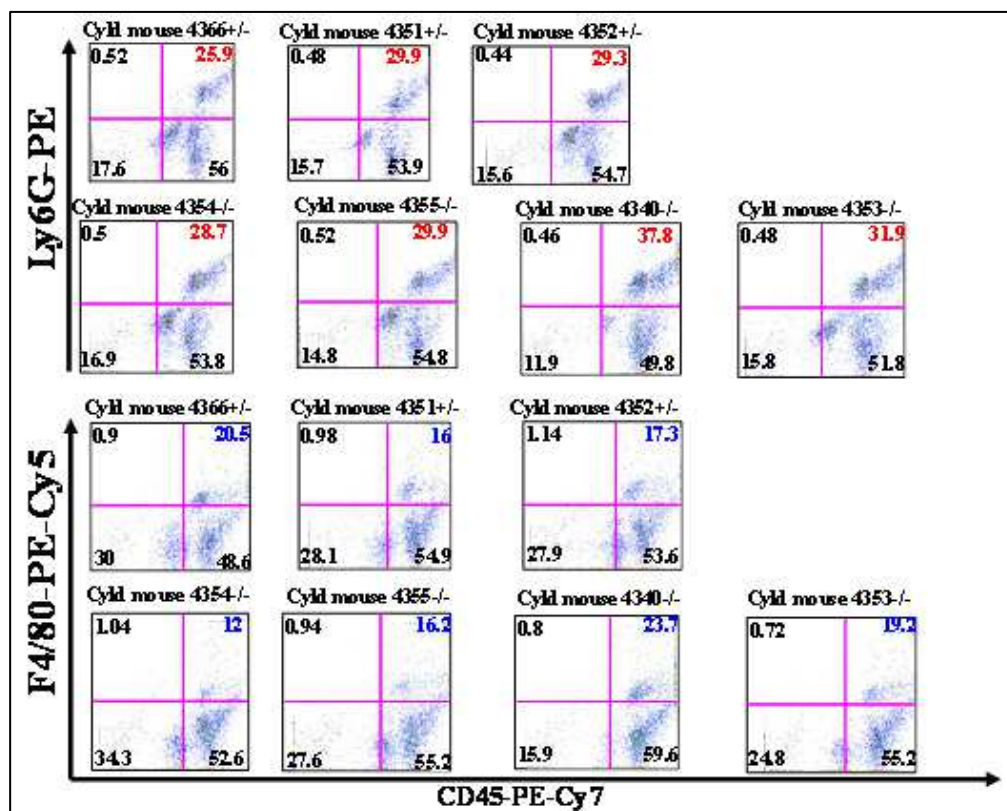

Fig. 22. Analysis of the relative composition (%) of PECs. PECs from $Cyld^{-/-}$ mice were stained with antibodies against cell surface markers CD45, Ly6G and F4/80 and analyzed by FACS, Cells with similar numbers, especially of Ly6G+ and F4/80 + cells were applied to the oxidative burst assay.

The PECs from these mice with similar neutrophil portion (%) were loaded with APF and then infected with *Y. enterocolitica* WA(pYV), *L. monocytogenes* or *S.* Typhimurium. Infection was stopped at different time points, cells were immunostained against cell type specific markers, and analysed by flow cytometer. Neutrophils (CD45+Ly6G+) were gated and then analyzed for the fluorescence of APF-fluorescein (oxidative burst activity) (Fig.23). The level of ROS production was determined by calculating the intensity, the geometric mean of the green fluorescence of APF (Fig.24).
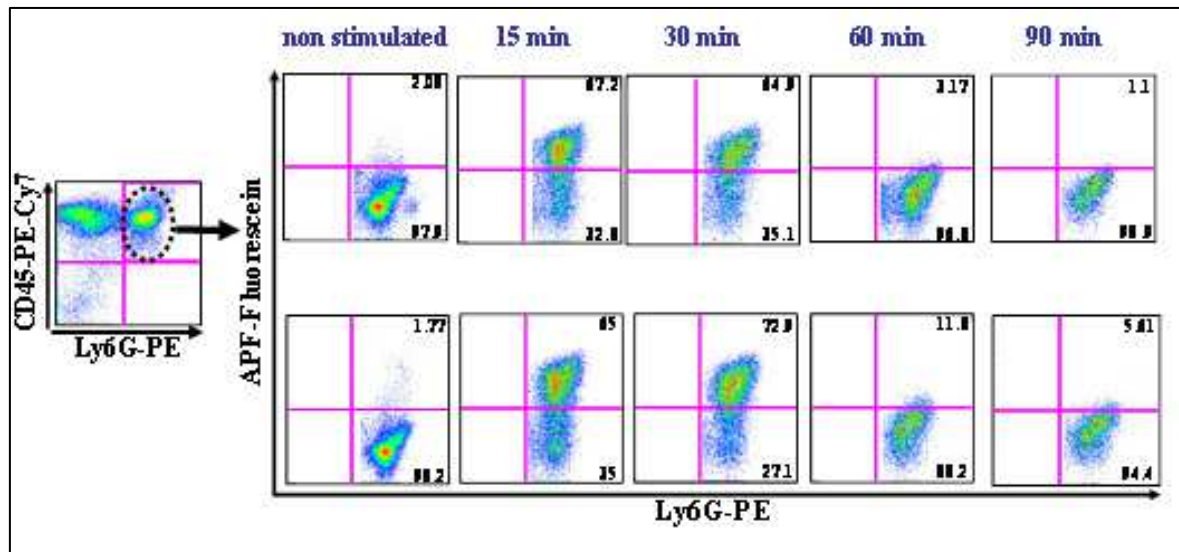
Fig. 23. Oxidative burst analysis by flow cytometry using APF. One representative figure is choosen to show how the oxidative burst was analyzed. CD45+Ly6G+ cells were gated and then analyzed for APF-fluorescein. Data were analyzed by the FlowJo-8.8.4. software.
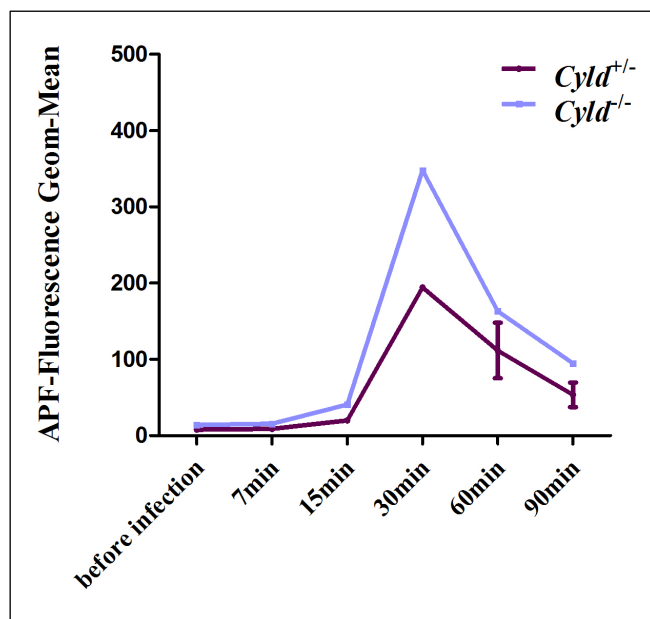

Fig. 24. *Cyld*^{-/-} cells show stronger respiratory burst response to *Y. enterocolitica* infection compared with *Cyld*^{+/-} cells. PECs were infected with strain WA(pYV)at MOI = 10 for different time points and oxidative burst was analyzed by flow cytometry using APF. The geometric means of APF-fluorescence of gated CD45+Ly6G+ PECs was determined at different time points. Data were analyzed by the FlowJo-8.8.4. software. CD45+Ly6G+ cells were gated and then analyzed for APF-fluorescein. Each sample was analyzed in duplicate.

Interestingly, although similar numbers of *Cyld*^{+/-} and *Cyld*^{-/-} PECs showed oxidative burst activity (Fig.23), the quantification of APF fluorescence intensity by calculating the geometric mean of the green fluorescence of APF revealed almost 2-fold higher signals for *Cyld*^{-/-} PECs than for *Cyld*^{+/-} PECs 30 min p.i. with strain WA(pYV) (Fig.24).

Studies with other bacteria strains, such as *L.* monocytogenes (infection at MOI = 24) or *S.* Typhimurium (infection at MOI 9) showed similar level of intracellular respiratory burst response to the respective infections (Fig.25). However, *S.* Typhimurium infected PECs (both *Cyld*^{-/-} and *Cyld*^{+/-} cells) reached the highest oxidative burst activity at 15 min post infection and this high level of APF-fluorescence sustained during the whole analyzed infection time of ca. 90 min, while the *L. monocytogenes* infected PECs showed steadily ascending intensity of fluorescence of APF-fluorescence geometric means during the whole analyzed infection time of ca. 90 min.
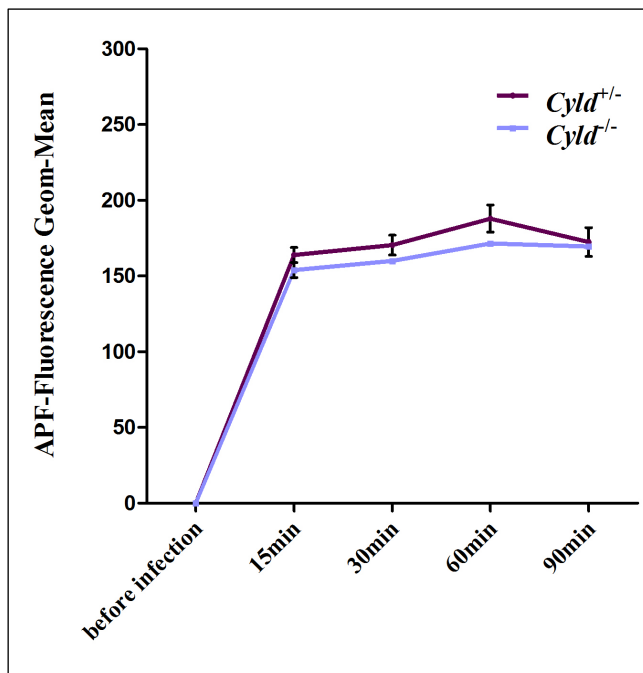

Fig. 25. PECs from *Cyld*^{-/-} and *Cyld*^{+/-} mice showed similar intracellular respiratory burst response to *S.* Typhimurium infection. PECs were infected with *S. typhimurium* (MOI = 9) for different time points. The oxidative burst was analyzed by flow cytometry using APF. The geometric means of APF-fluorescence of gated CD45+Ly6G+ PECs was determined at different time points. Each sample was analyzed in duplicate.

3.6.2 Oxidative burst analysis using luminol

To validate the oxidative burst phenotype of *Cyld*^{+/-} and *Cyld*^{-/-} cells detected by APF-technique, we analyzed the ROS production by PECs using another independent method based on the chemiluminometric probe, luminol.

Our pilot experiments revealed that the most consistent results for luminol-based anylasis of oxidative burst could be generated using splenocytes. The use of PECs for oxidative burst assays was time and mice consuming. Only PECs with similar percentage e.g. of neutrophils and macrophages, after proteose peptone treatment of mice, could be subjected to the oxidative burst assay (see part 3.6.1.). Another problem is that pretreatment of mice with proteose peptone leads to differential priming level of PECs in each mouse, which would

result in non-consistent results in the subsequent oxidative burst assay. In contrast, splenocytes exhibit many advantages compared with PECs. (i) Splenocytes are removed from naïve mice which are not primed and thus should display similar background activities. (ii) Although the main ROS producers such as macrophages and granulocytes, , constitute together only ca. 10% of total splenocytes, this proportion is enough to detect ROS production using luminol, since the quantum yield of the luminol is very high and thus ROS production can be detected by using less than 100 phagocytes (Freitas et al., 2009).

Splenocytes obtained from $Cyld^{+/-}$ and $Cyld^{-/-}$ mice were infected with *Y. enterocolitica* WA(pYV) and real time production of ROS was determined by measuring chemiluminescence of luminol, using luminescence plate reader (see chapter 2.2.3.7.2).

Our results indicated that $Cyld^{-/-}$-deficient splenocytes show higher respiratory oxidative burst response to *Y. enterocolitica* infection as measured by luminol-dependent chemiluminescence (relative light units: about 1,000 at the peak point) compared with that of $Cyld^{+/-}$ splenocytes (with the relative light units of about 500 at the peak point of stimulation) (Fig.26). Both of the $Cyld^{+/-}$ and $Cyld^{-/-}$ cells approached their respiratory oxidative burst peak quickly, around 10 to 15 min p.i. (Fig.26). And then, the relative light units of $Cyld^{+/-}$ splenocytes dropped very quickly to the ground state (with relative light units of about 200) at 25 min while $Cyld^{-/-}$ cells did not approach to the basic level until ca. 45 min post infection (Fig.26).

In agreement with the results using APF, the analysis of ROS production during infection with *L. monocytogenes* and *S.* Typhimurium using luminol-dependent chemiluminescence showed similar level of respiratory burst response by $Cyld^{+/-}$ and $Cyld^{-/-}$ cells (Fig.27). Furthermore, in contrast to infection with *Yersinia*, *Listeria* infected splenocytes (both $Cyld^{-/-}$ and $Cyld^{+/-}$ cells) showed sustained high level of chemiluminescence (with the relative light units of about 1,000) during the whole analyzed infection time of ca. 85 min.

These data suggest that CYLD is involved in the negative regulation of cellular oxidative burst activity during *Yersinia* infection. Thus, we conclude that Yops-mediated inhibition of oxidative burst seems requires CYLD.
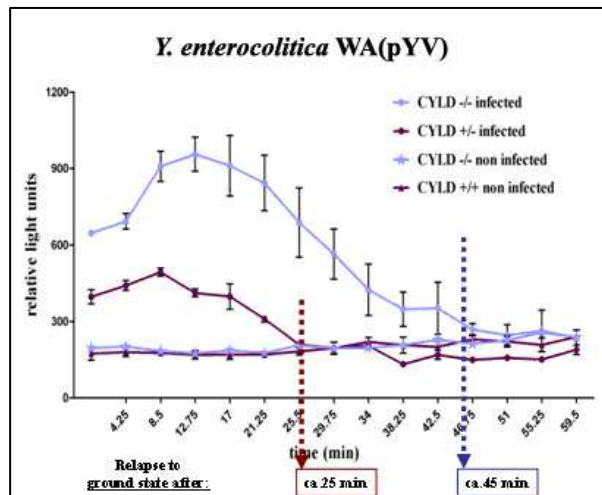
Fig. 26. ROS production by *Cyld*$^{+/-}$ and *Cyld*$^{-/-}$ splenocytes measured by luminol chemiluminescence. 10^5 splenocytes were seeded in 96-well plates in medium complemented with luminol. Cells were then infected with *Y. enterocolitica* WA(pYV) at MOI = 10. Noninfected cells were used as control. The plate was centrifuged at 300 x g / 4°C / 2 min and the monitoring of luminescence was started immediately using luminescence plate reader. Each sample was analyzed in triplicate.
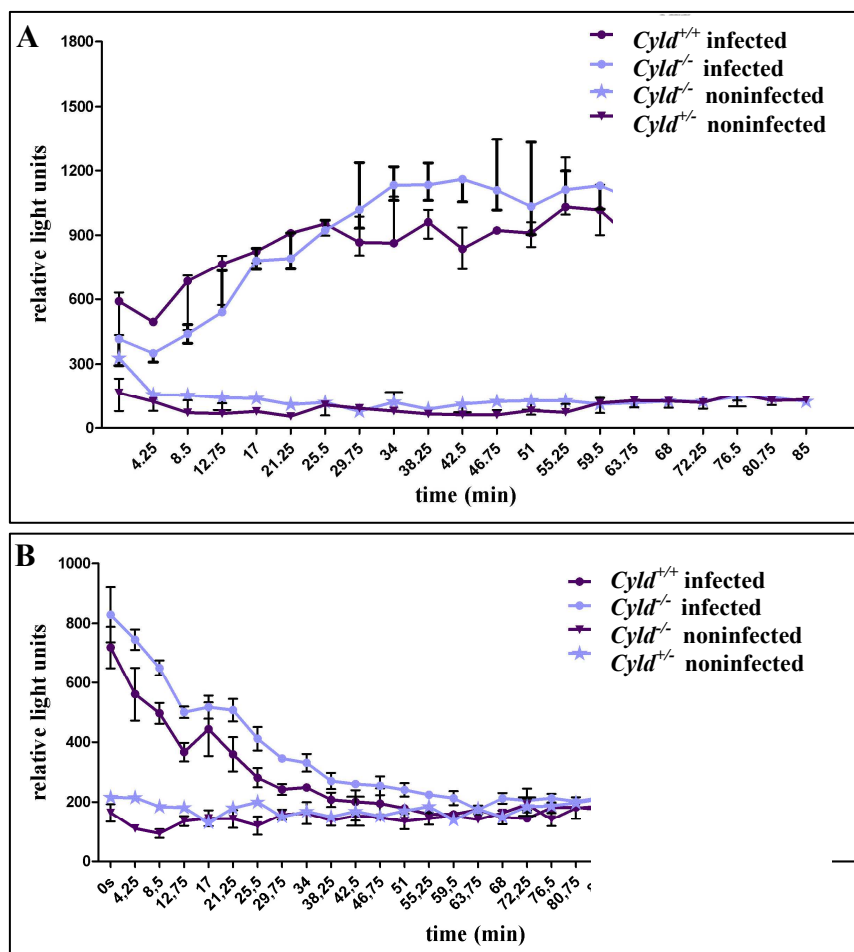

Fig. 27. ROS production by *Cyld*$^{+/-}$ and *Cyld*$^{-/-}$ splenocytes measured by luminol chemiluminescence. 10^5 splenocytes were seeded in 96-well plates in medium complemented with luminol. Cells were then infected with *L. monocytogenes* at MOI = 19 **(A)** or *S.* Typhimurium (SB300 strain) at MOI = 44 **(B)**. Noninfected cells were used as control. The plate was centrifuged at 300 x g / 4°C / 2 min and the monitoring of luminescence was started immediately using luminescence plate reader. Each sample was analyzed in triplicate.

To analyze the direct contribution of CYLD to Yops-mediated inhibition of oxidative burst, we performed oxidative burst studies using different *Y. enterocolitica* mutants that are deficient in the expression of one *yop* gene. If CYLD is involved in Yop-mediated inhibition of oxidative burst, the infection of CYLD-deficient and CYLD-competent cells with strains deficient in this particular Yop should result in comparable oxidative burst responses.

It is known that YopH inhibits oxidative burst (Ruckdeschel et al., 1996). Furthermore, CYLD and YopP show overlapping functions e.g. as negative regulators of MAPK (Reiley et al., 2004; Yoshida et al., 2005; Zhou et al., 2005a). MAPKs are known to be involved in the activation of oxidative burst (Brown et al., 2004; El Benna et al., 1996a; El Benna et al., 1996b; Laroux et al., 2005; Sakamoto et al., 2006; Yamamori et al., 2002) and thus YopP is suggested to be also involved in the inhibition of ROS production by blocking the MAPK pathways (Visser et al., 1999).

Thus, we first concentrated on the analysis of oxidative burst response of $Cyld^{-/-}$ and $Cyld^{+/-}$ splenocytes to infection with WA(pYVΔYopH) and WA(pYVΔYopP).

Data presented in Figure.28 show that both *mutant* WA(pYVΔYopH) (Fig.28A) and WA(pYVΔYopP) (Fig.28B) stimulated ROS production of splenocytes and dropped to ground level of the respiratory oxidative burst much later (more than 50 min post stimulation) than that of infected $Cyld^{+/-}$ splenocytes (Fig.26). Thus, the stronger oxidative burst activity in $Cyld^{-/-}$ cells seems not to be a direct effect of CYLD, but rather due to the inability of YopH or YopP to inhibit oxidative burst in the absence of CYLD.
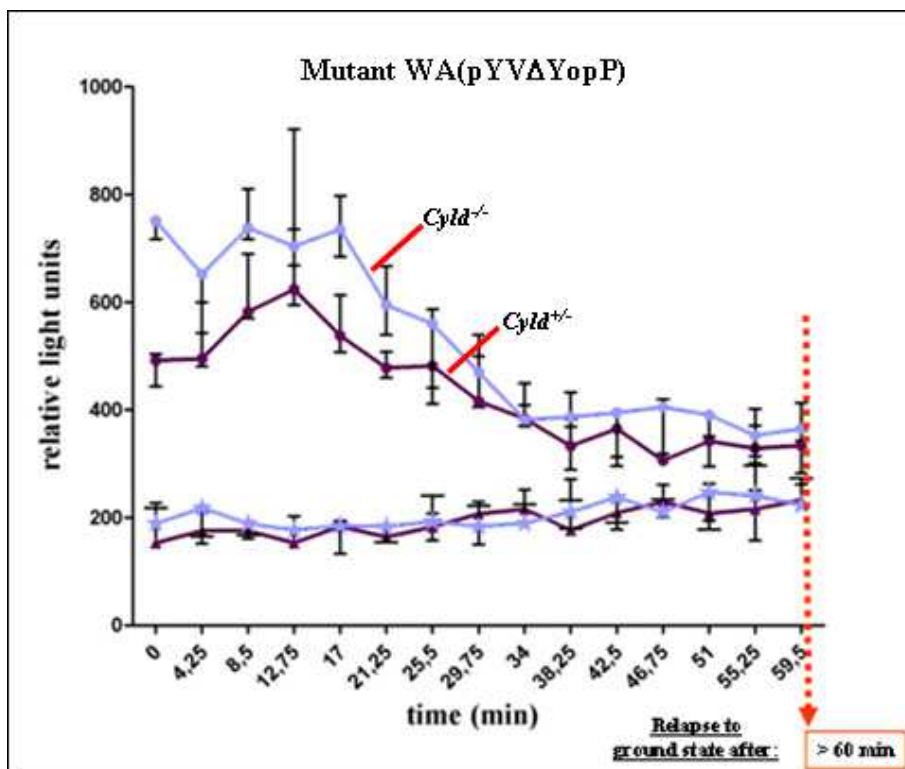
(A)
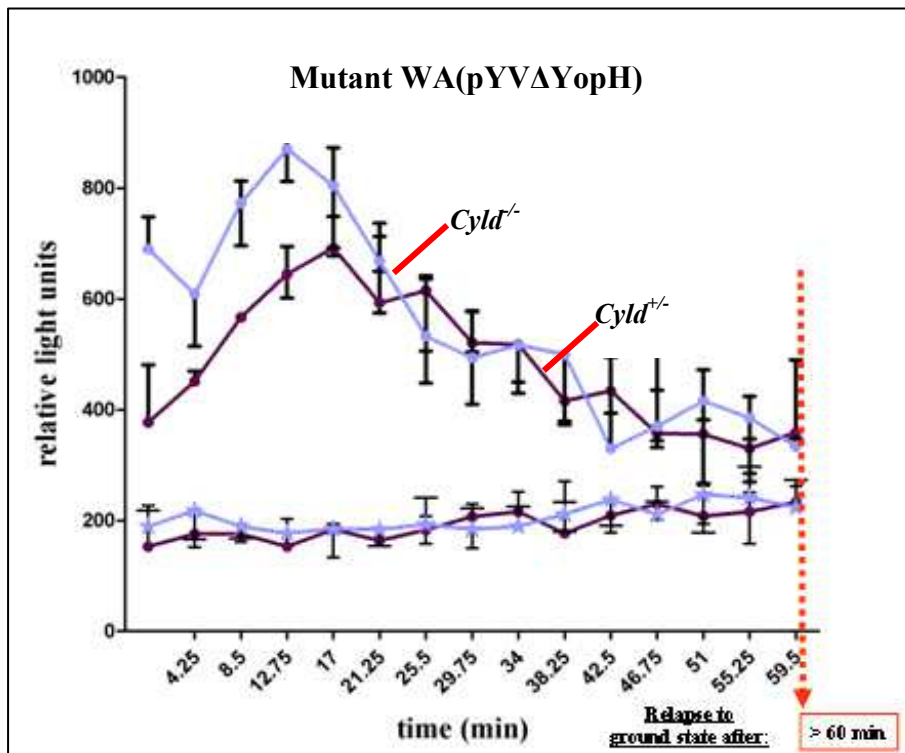
(B)

Fig. 28. ROS production by *Cyld*$^{+/-}$ and *Cyld*$^{-/-}$ splenocytes measured by luminol chemiluminescence. 10^5 splenocytes were seeded in 96-well plates in medium complemented with luminol. Cells were then infected with mutant WA(pYVΔYopH) at MOI = 27 **(A)** or with WA(pYVΔYopP) at MOI = 16 **(B)**. Noninfected cells were used as control. The plate was centrifuged at 300 g / 4°C / 2 min and the measurement of luminescence was started immediately using luminescence plate reader. Each sample was analyzed in triplicate. *Cyld*$^{-/-}$: blue line, *Cyld*$^{+/-}$: purple line.

3.7 Analysis of cytokine production of infected $Cyld^{-/-}$ and $Cyld^{+/-}$ mice (in vivo) and bone marrow derived dendritic cells (BMDCs, in vitro)

A major function of the innate immune cells during microbial infection is the production of inflammatory mediators such as cytokines, chemokines, nitric oxide, and ROS. The production of inflammatory cytokines is known to be critical for the resistance of the host to infections (Netea et al., 2004). The mobilization of the leukocytes to the infection site, the initiation of acute phase response and the adaptive immune response are some of the mechanisms triggered by proinflammatory cytokines and chemokines.

It has been shown that CYLD deficiency results in enhanced induction of e.g. IL-1β, IL-6, IL-8, IFN-α and IFN-β upon stimulation by agonists and/or infection (Yoshida et al., 2005; Zhang et al., 2006). Furthermore, *Y. enterocolitica* is known to inhibit cytokine production by immune cells (Brubaker, 2003; Monnazzi et al., 2004). Therefore, we wondered whether the improved resistance of $Cyld^{-/-}$ mice to *Y. enterocolitica* infection can be assigned to the enhanced cytokine response.

3.7.1 Similar cytokine production level of cytokines in $Cyld^{-/-}$ and $Cyld^{+/-}$ mice

We first analyzed the cytokines production in serums of $Cyld^{+/-}$ mice and the control littermates on day1 post infection with *Y. enterocolitica*. There was no significant difference in the induction of cytokines being checked in this study, such as TNF-α, IL6, IL10, MCP-1, KC and IFN-γ (Fig.29A). Furthermore, we determined cytokine production also on day 5 post infection in serum and liver homogenates of the same mice. Interestingly, there was higher production of these cytokines and chemokines except for IL 10 in the $Cyld^{+/-}$ mice compared with $Cyld^{-/-}$ mice (Fig. 29A and B).

However, this enhanced cytokine production in the control littermate mice 5 days post infection, correlates with their higher bacteria burden compared to the $Cyld^{-/-}$ mice (Fig. 12B). Thus, under the chosen experimental conditions (time point of infection and analysed samples –serum and liver-), we suggest that $Cyld^{-/-}$ mice display a normal (as $Cyld^{+/-}$-mice) cytokine response to infection.
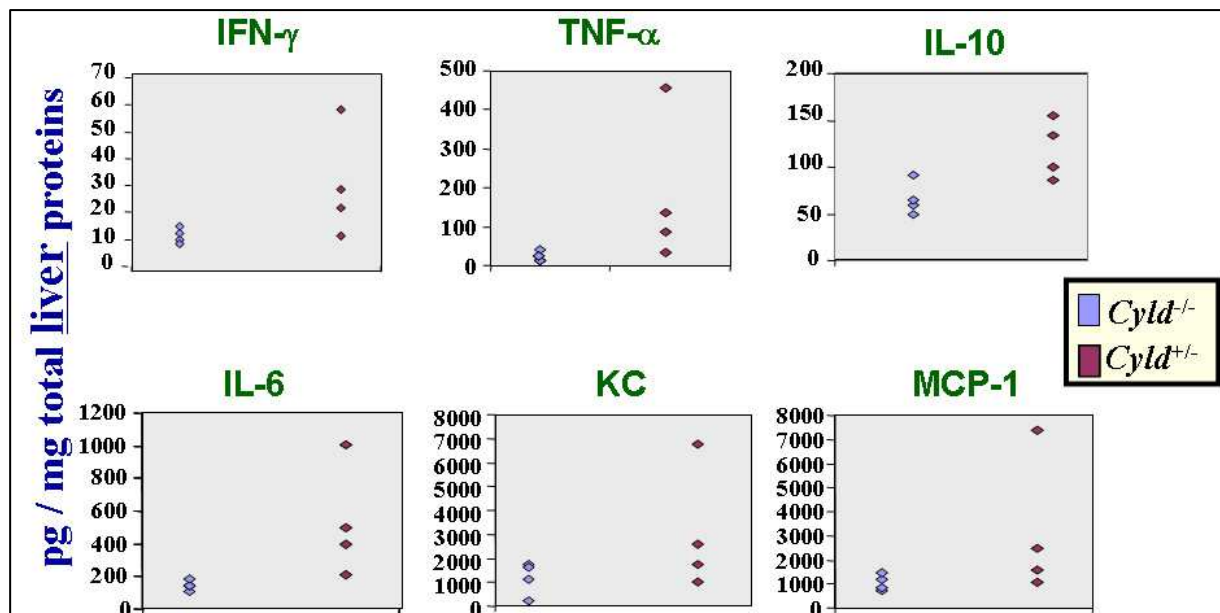
(A)
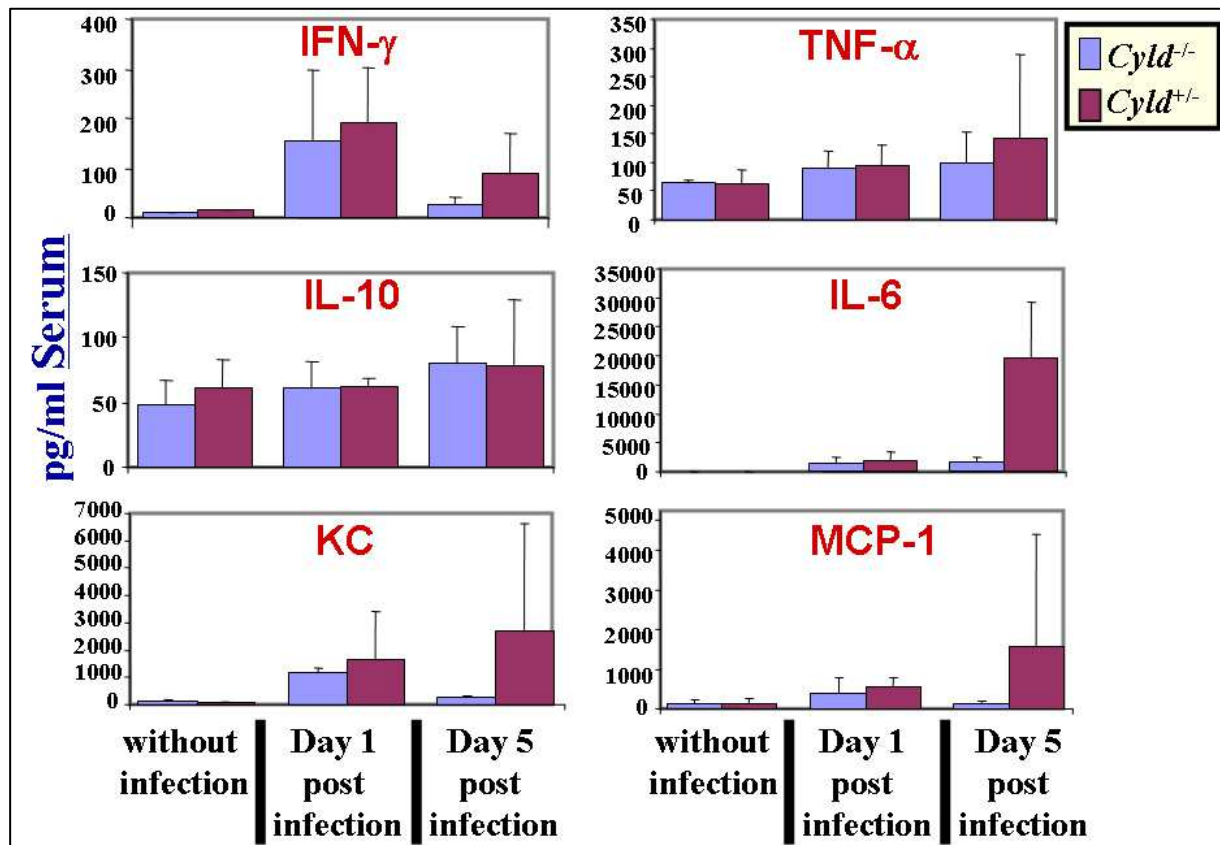
(B)

Fig. 29. Cytokine production profiles *in vivo*. *Cyld*^{-/-} (n = 4) and *Cyld*^{+/-} (n = 4) mice were i.p. infected with 2x10^{4} CFU of *Y. enterocolitica*. (A) After 1 day and 5 days post infection, blood was collected; serum was prepared and subjected for cytokines measurement. **(B)** After 5 days post infection, the mice were scarified, liver were removed and homogenized. Equally amount of total liver proteins were subjected to cytokines/chemokines measurement. (Spleens were homogenized and plated to determine the bacteria loads in the corresponding mice).

3.7.2 Differential expression profile of MCP-1, IL-10 and TNF-α by *Cyld*[/-] and *Cyld*^{+/-} cells *in vitro*

Given the fact that the cytokines measured in serum and liver of infected mice would reflect the concentration of systemically diffused cytokines, which might differ from their microenvironmental concentration at the infection site, we decided to examine *in vitro* cytokine response of stimulated BMDCs and splenocytes in order to gain a more accurate picture of the cytokine expression profile in *Cyld*[/-] and *Cyld*^{+/-} mice.

Thus, we analyzed *in vitro* the cytokine response of BMDCs upon infection with *Y. enterocolitica*. As control for pathogen specificity, we also analyzed cytokine response to infection with *L. monocytogenes* and *Salmonella* Typhimurium.

The levels (pg/ml cell supernatant) of TNF-α, MCP-1 and IL10 in the culture supernatants of the non-infected and infected BMDCs were measured, respectively. Results indicated that *Cyld*^{+/-} and *Cyld*[/-] cells show similar TNF-α production upon infection with the respective pathogens, irrespective whether the pathogens were alive or heat-killed (HK) (Fig.30A). In the case of MCP-1, *Cyld*[/-] cells show decreased MCP-1 production upon infection with *Y. enterocolitica* and *Salmonella* Typhimurium (both live and heat-killed) (Fig.30B). As for IL-10, *Cyld*^{+/-}- and *Cyld*[/-] cells show similar IL-10 production upon infection with *Y. enterocolitica* and *Salmonella* Typhimurium, respectively (Fig.30C). However, surprisingly *Cyld*[/-] cells show higher IL-10 production to live *L. monocytogenes* infection on one hand, but decreased IL-10 production to heat-killed *L. monocytogenes* on the other hand (Fig.30C). Considerably, *Cyld*^{+/-} cells show similar IL-10 production to both live and heat-killed *L. monocytogenes* infection (Fig.30C).

3.7.3 *Cyld*[/-] cells show enhanced production of IL-12 and IFN-γ upon infection with *Yersinia* and *Listeria*

The IL-12 family is a central immunoregulatory cytokine that promotes cell-mediated immune responses and the differentiation of naïve CD4^{+} cells into Th1 cells (Guler et al., 1996). Three members constitute the IL-12 family, IL-12p70 (IL-12p40/IL-12p35), IL-23 (IL12-p40/IL-23p19) and IL-27 (EBI3 and p28). IL-12 is produced mainly by macrophages and dendritic cells when induced e.g. by pathogenic organisms, including bacteria, parasites, fungi, and viruses (Watford et al., 2004).

IFN-γ is a pleiotropic cytokine that plays an essential role in the innate and adaptive immunity. It is a major activator of macrophage functions including the release of reactive nitrogen and oxygen intermediates and the production of IFN-γ can be induced by diverse intracellular
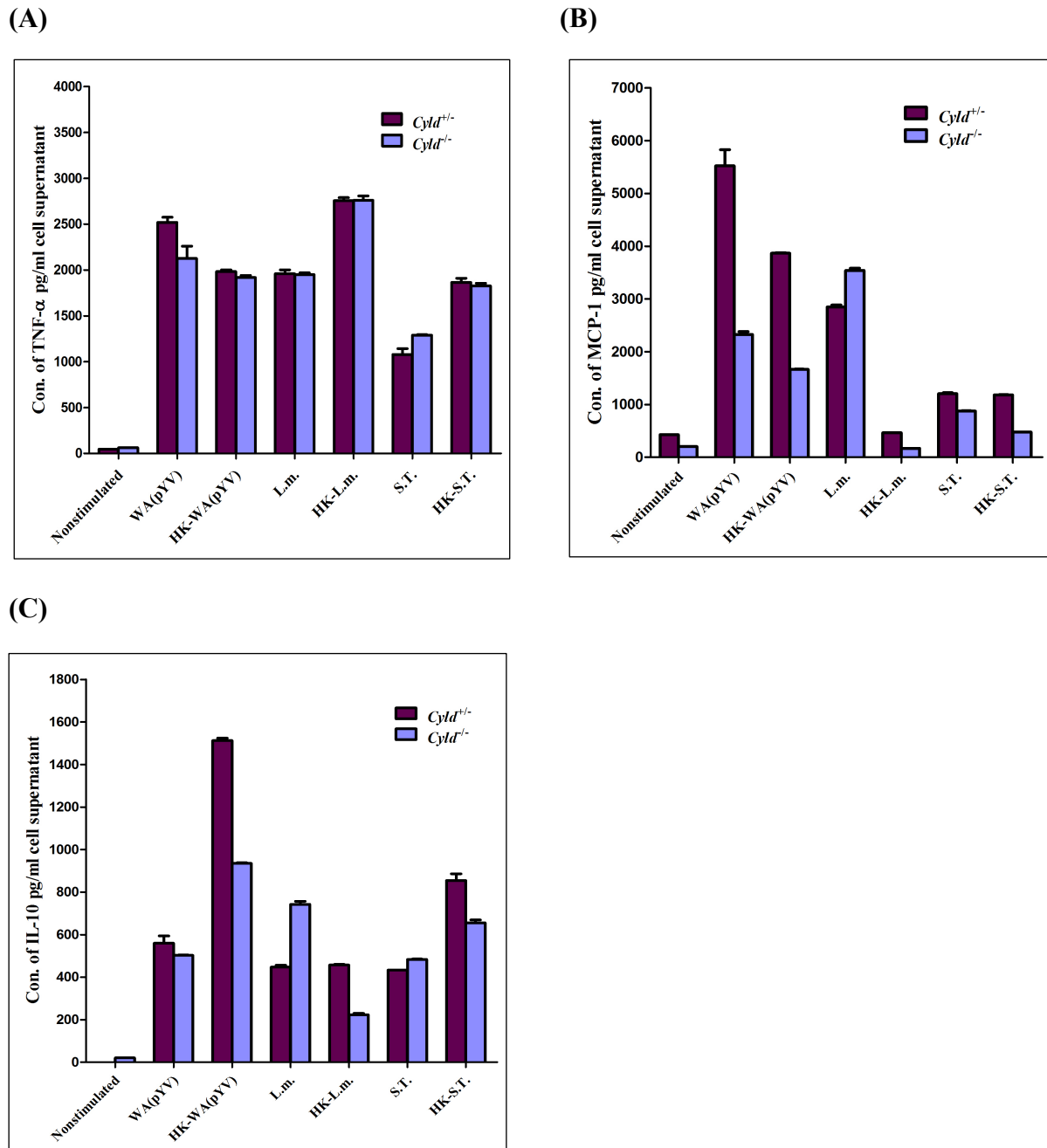
(A)

(B)

(C)

Fig. 30. Differential expression profile of TNF-α (A), MCP-1 (B), and IL-10 (C) by *Cyld*[/-] and *Cyld*^{+/-} BMDCs upon *in vitro* challenge. BMDCs from *Cyld*[/-] and *Cyld*^{+/-} mice were seeded at 2×10^5/well in RPMI 1640 medium containing 5% FBS for 2-4 h. Cells were then infected with live or heat-killed (HK) *Y. enterocolitica* (WA(pYV), MOI = 10)*, L. monocytogenes* (L.m., MOI = 24)*,* and *Salmonella* Typhimurium (S.T., MOI = 17). As for BMDCs infected with live bacteria, medium was exchanged 1 h post infection for 5 µg/ml gentamicin-containing medium. Supernatants were collected after 24 h and subjected to CBA cytokine assay.

pathogens, such as *L. monocytogenes* and *Salmonella* Typhimurium early during primary infection (Bao et al., 2000; Buchmeier et al., 1985).

IFN-γ production by the activated natural killer (NK) cells and T cells is described as part of a positive feedback loop of innate immune response (Tripp et al., 1993; Tripp et al., 1994; Unanue, 1997; Warschkau et al., 1998): microbes stimulate macrophages and DCs to produce cytokines such as IL-12, which activate NK cells and T cells to release IFN-γ. IFN-γ, in turn,

stimulates macrophages and DCs for further IL-12 production (Ma et al., 1996). The IFNγ-activated macrophages show increased ability to kill phagocytosed bacteria, e.g. by producing toxic metabolites, which may limit multiplication and survival of pathogens (MacMicking et al., 1997).

IL-12 and IFN-γ has been shown to play an important role in controlling *Yersinia* infection (Bohn and Autenrieth, 1996; Bohn et al., 1998; Hein et al., 2001).

Thus, due to the importance of the IL-12/IFN-γ axis in immune response to infection, we measured the production of IL-12 and IFN-γ upon infection of *Cyld*^{-/-} and *Cyld*^{+/-} BMDCs. Our results indicated that *Cyld*^{-/-} BMDCs show increased (about 2.5 times more) IL12/IL23p40 production upon infection with live *Y. enterocolitica* WA(pYV) while the difference was not significant when *Cyld*^{-/-} and *Cyld*^{+/-} cells were stimulated with heat-killed WA(pYV) (Fig.31A). The release tendency of IL12/IL23p40 upon *L. monocytogenes* or *Salmonella* Typhimurium infection just resembles that upon infection with *Y. enterocolitica* with the exception that the concentration of IL12/IL23p40 in the infection of live *L. monocytogenes* (BMDCs of *Cyld*^{+/-} *vs* BMDCs of *Cyld*^{-/-}: 140 pg/ml vs 460 pg/ml) or live *S. typhimurium* (BMDCs of *Cyld*^{+/-} *vs* BMDCs of *Cyld*^{-/-}: 96 pg/ml vs 206 pg/ml) is much lower than that of live *Y. enterocolitica* (BMDCs of *Cyld*^{+/-} *vs* BMDCs of *Cyld*^{-/-}: 3,400 pg/ml vs 10,000 pg/ml) (Fig.31A).

Since activated T cells and activated NK cells are the main source of IFN-γ, and because our pilot experiments revealed that splenocytes (that contains e.g. T cells and NK cells) but not BMDCs produce significant amounts of IFNγ upon stimulation, we used splenocytes to study the production of IFN-γ. Splenocytes from *Cyld*^{-/-} and *Cyld*^{+/-} mice were infected with *Y. enterocolitica* (MOI = 10), *L. monocytogenes* (MOI = 14), and *Salmonella* Typhimurium (MOI = 4) for one hour, thereafter medium was changed by ca. 100 µg/ml gentamicin containing medium, in order to kill extracellular bacteria. The supernatants were then collected at 12h, 24 or 36 hours post infection. Our results show that *Cyld*^{-/-} splenocytes showed increased (at least two times more) IFN-γ production upon challenge of these three pathogens compared with *Cyld*^{+/-} splenocytes, whereby *L. monocytogenes* induced higher IFN-γ release than *Y. enterocolitica* (Fig.31B).
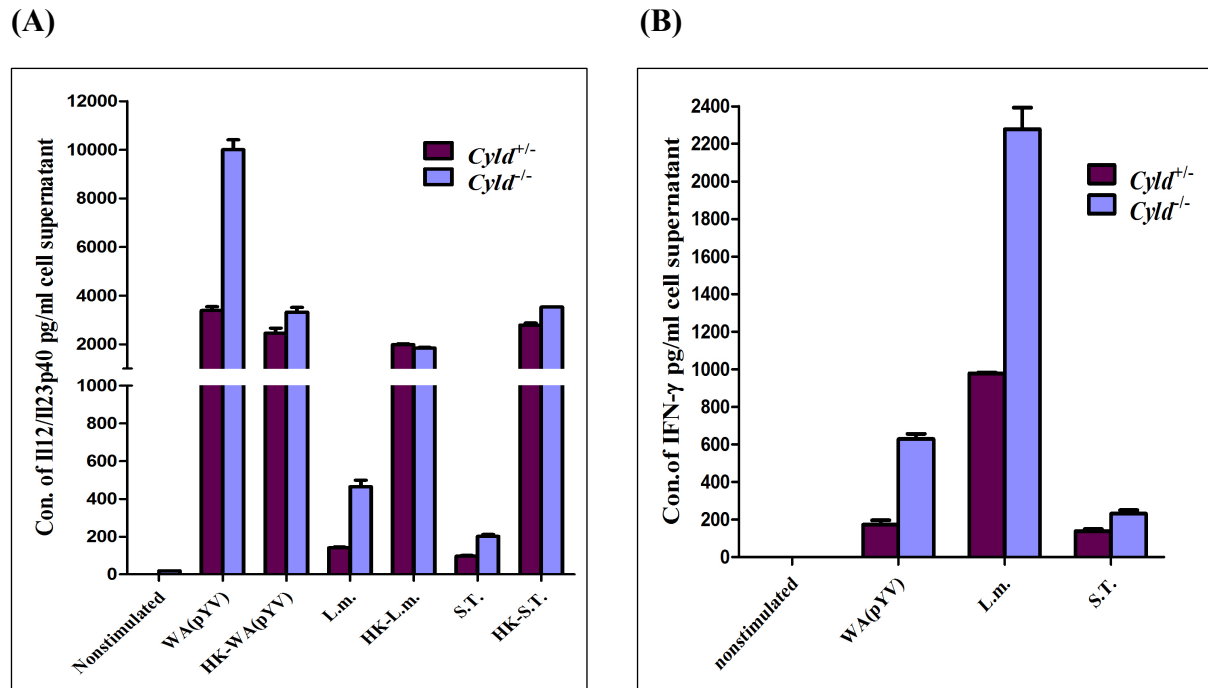
(A)

(B)

Fig. 31. *Cyld*^{-/-} **BMDCs and splenocytes show enhanced production of IL-12 and IFN-γ, respectively, upon bacterial infection *in vitro*. (A)** BMDCs from *Cyld*^{-/-} and *Cyld*^{+/-} mice were seeded at $2x10^5$ cells/well or $5x10^5$ cells/well, respectively, in RPMI 1640 medium containing 5% FBS for 2-4 h. Cells were then infected with living or HK *Y. enterocolitica* (WA(pYV), MOI = 10), *L. monocytogenes* (L.m., MOI = 24), *and Salmonella* Typhimurium (S.T., MOI = 17). As for BMDCs infected with live bacteria, medium was exchanged 1 h post infection by one 100 µg/ml gentamicin containing medium. Supernatants were collected after 24 h and subjected to CBA cytokine assay. **(B)** Splenocytes were infected with *Y. enterocolitica* (MOI 10), *L. monocytogenes* (MOI 14) and *Salmonella* Typhimurium (MOI 4) for 24h. Supernatants were collected after 24 h and subjected to CBA cytokine assay.

3.7.4 Differential cytokine expression profile of *Cyld*^{-/-} and *Cyld*^{+/-} cells upon stimulation with PAMPs *in vitro*

Since TLR2 and the adaptor protein myeloid differentiation primary response gene 88 (Myd88) that conveys many TLR signals, have been shown to be crucial for host defense against many pathogens, such as *L. monocytogenes* (Janot et al., 2008; Torres et al., 2004) and pathogenic *Yersinia* species (Depaolo et al., 2008; Dessein et al., 2009; Sing et al., 2002), and as previous works documented that CYLD acts as a negative regulator on TLR signaling resulting in damped cytokine production (Lim et al., 2008; Lim et al., 2007; Sakai et al., 2007; Yoshida et al., 2005; Zhang et al., 2006), we wondered whether TLRs in *Cyld*^{-/-} and *Cyld*^{+/-} cells would show different activation level upon stimulation with their respective specific PAMPs. The production of proinflammatory cytokines represent a major early host response triggered by pathogen-associated molecular patterns (PAMPs)-mediated stimulation of TLRs and thus represent an accurate readout for TLR activity. Therefore, we analyzed cytokine response of BMDCs upon stimulation for 24 h with FSL-1 (1 ug/ml, a synthetic diacylated lipoprotein recognized by TLR2 and TLR6); with ultrapure LPS (500 ng/ml) TLR4 agonist,

from *E. coli* K12; or a polyinosinic: polycytidylic acid (1 ug/ml Poly (I:C)), a synthetic analog of double-stranded RNA (dsRNA, that stimulates TLR3).

The results indicated that $Cyld^{+/-}$ and $Cyld^{-/-}$ BMDCs show similar TNF-α production upon stimulation with all three tested TLR-agonists (Fig.32A). In the case of MCP-1, $Cyld^{-/-}$ cells show decreased MCP-1 production upon stimulation with LPS and Poly (I: C) (Fig.32B). FSL-1, a PAMP for TLR2/TLR6, did not induce any MCP-1 production by both $Cyld^{+/-}$ and $Cyld^{-/-}$ BMDCs (Fig.32B). As for IL-10, $Cyld^{-/-}$ cells show lower IL-10 production upon stimulation with LPS than for $Cyld^{+/-}$ cells (Fig.32C). FSL-1 and Poly (I:C) induced, IL-10 production near detection limit for both $Cyld^{+/-}$ and $Cyld^{-/-}$ BMDCs (Fig.32C).

The stimulation of BMDCs with LPS showed slightly higher production of IL12/IL23p40 by $Cyld^{-/-}$ cells, compared to $Cyld^{+/-}$ cells (Fig.32D). Furthermore, in comparison to WT BMDCs, $Cyld^{-/-}$ BMDCs showed increased and decreased production of IL12/IL23p40 upon stimulation with FSL-1 and Poly (I: C), respectively (Fig.32D). Considerably, FSL-1 or Poly (I: C) induced, generally, lower amount of IL12/IL23p40 (lower than 500 pg/ml), compared to LPS stimulation (Fig.32D). These results demonstrate that TLR2 and TLR4 agonists show differentially responses which depends on the presence of CYLD.

3.8 STAT4 cell signaling assay

The aforementioned experiments (chapter 3.7.3) have demonstrated that $Cyld^{-/-}$ cells show increased IFN-γ production upon infection with *Y. enterocolitica*. Therefore, we wanted to explore the mechanism underlying the CYLD-dependent modulation of IFN-γ production upon *Yersinia* infection.

A main mechanism involved in IFN-γ induction is that mediated by IL-12 and STAT4. IL-12 binds specifically to two noncovalently linked receptor chains, IL-12R1 and IL-12R2 (Chua et al., 1994; Presky et al., 1996; Szabo et al., 1997), which are e.g. expressed on NK cells and activated T and B cells. The IL-12R1-chain interacts with Non-receptor tyrosine-protein kinase TYK2 (Chua et al., 1994; Zou et al., 1997) while the IL-12R2-chain interacts with JAK2 (Presky et al., 1996; Zou et al., 1997). The binding of IL-12 to its receptors leads to activation of JAK2 and TYK2, which in turn phosphorylate IL-12R, providing docking sitesfor the SH2 domain of STAT4 (Bacon et al., 1995a; Jacobson et al., 1995). STAT4 specifically binds to the IL-12R2 peptide sequence pYLPSNID (where pY represents phosphotyrosine) (Naeger et al., 1999) and the receptor-bound STAT4 is phosphorylated on
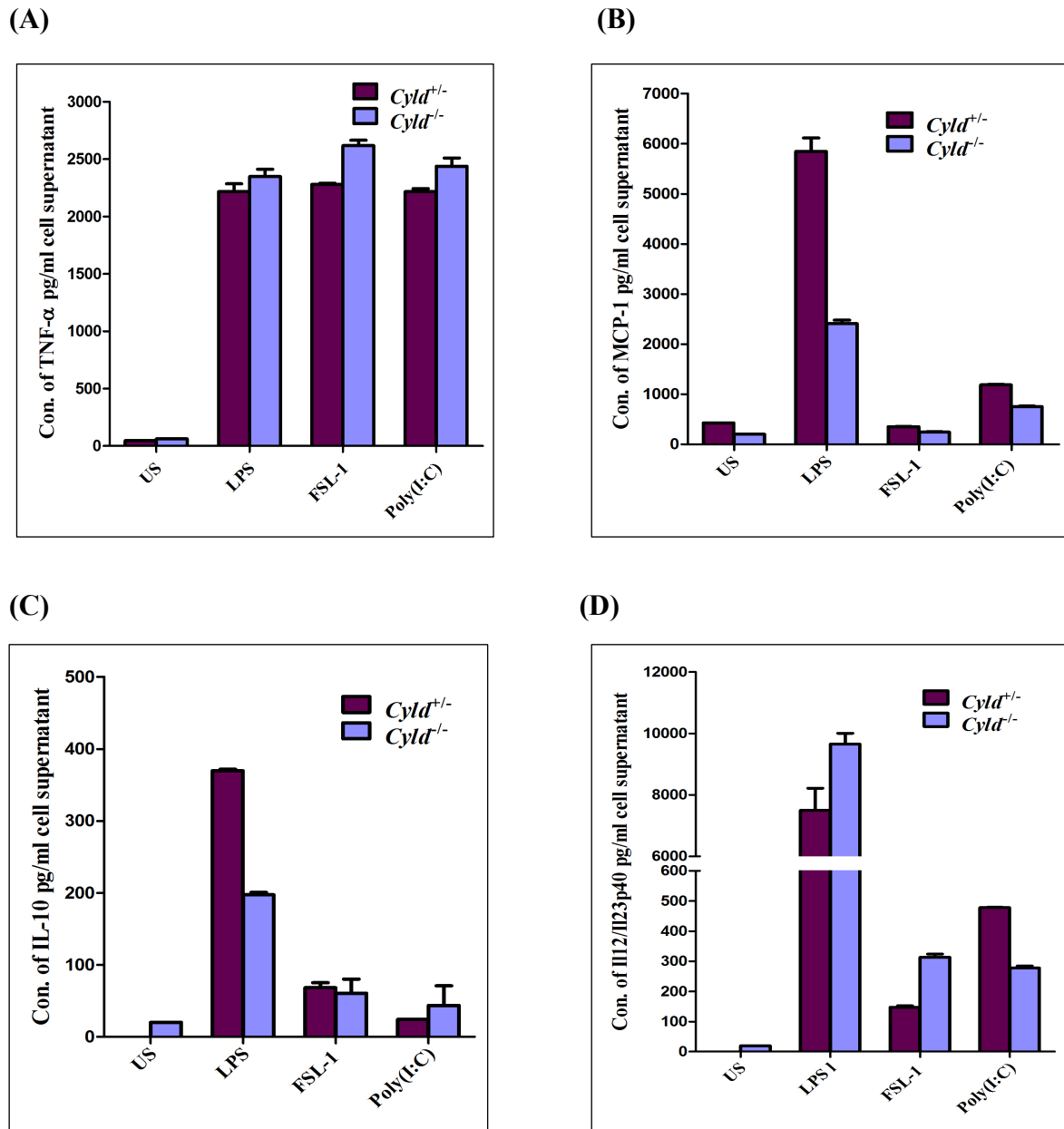
(A)

(B)

(C)

(D)

Fig. 32. Differential cytokine expression profile of *Cyld^{-/-}* and *Cyld^{+/-}* BMDCs upon stimulation with different PAMPs *in vitro*. BMDCs from *Cyld^{-/-}* and *Cyld^{+/-}* mice were seeded at $2x10^5$/well in RPMI 1640 medium containing 5% FBS for 2-4 h. Cells remained unstimulated (US) or were then stimulated with LPS (500 ng/ml TLR4), FSL-1(1 ug/ml, TLR6/TLR2) or Poly(I:C) (10 ug/ml TLR3) for 24 h. Culture supernatants were collected after 24 h and subjected to CBA cytokine assay to analyse the production of TNF-a **(A)**; MCP-1 **(B)**; IL-10 **(C)** and IL-12/IL-23p40 **(D)**.

tyrosine 693 by the JAKs, promoting STAT dimerization, translocation to the nucleus, and regulation of IFN-γ gene expression (Bacon et al., 1995b; Cho et al., 1996).

Besides the Jak-STAT pathway mentioned above, MKK6/p38α/STAT4 pathway as an important mediator of IL-12 actions has also been established (Visconti et al., 2000; Zhang and Kaplan, 2000). In this pathway, p38α and its upstream activator, MKK6, phosphorylate STAT4 on serine 721, and are required for STAT4 full transcriptional activity induced by IL-12.

Since STAT4 is of particular importance in IFN-γ production, we checked the STAT4 activation state in $Cyld^{-/-}$ and $Cyld^{+/-}$ cells upon different kinds of stimulation.

An established method to study IL-12-dependent activation of STAT4 and IFN-γ is as follows: pre-treated (e.g. *Yersinia*-infected) or non-treated cells, such as NK cells or T cells (which are major sources for IFN-γ), are first stimulated with recombinant IL-12 and IL-18 that cooperate in the induction of IFN-γ. Subsequently, the production of IFN-γ and activation level of STAT4 are measured. However, this system is highly artificial and does not consider the physiological cell-cell interactions. Thus, we used another experimental procedure that doesn't need the addition of exogenous stimulation factors (like IL-12 and IL-18).

Our pilot experiments revealed that LPS-stimulated BMDCs produce high level of IL-12 but no significant amount of IFN-γ, whereas splenocytes (containing NK cells and T cells) produce strongly IFN-γ but no significant amount of IL-12. Thus, none of these cell types alone were appropriate to study the IL-12/STAT4/IFN-γ axis. Therefore, we decided to combine BMDCs and splenocytes in order to establish an experimental system enabling to study the IL-12/STAT4/IFN-γ axis. We supposed that BMDCs supply IL-12 which is important for the induction of IFN-γ production by e.g. NK cells and T cells of splenocytes. Therefore, splenocytes and BMDCs were prepared as mentioned in the materials and methods section (chapter 2.2.3.2 and chapter 2.2.3.3). 2×10^4 BMDCs were mixed with 4.5×10^5 splenocytes (ca. 1:22) in RPMI 1640 medium containing 5% FCS, seeded on poly-L-Lysine-coated wells of 96-well clear-bottom white plate and incubated at 37°C for ca. 2 h to let the cells attach to the bottom. Cells were then infected with *Y. enterocolitica* WA(pYV) (MOI = 7) or *S.* Typhimurium (MOI = 19), or stimulated with 1 μg/ml LPS. Unstimulated cells were applied as control. 1 h post infection, media were replaced by RMPI1640 medium containing 5%FCS and 6 μg/ml gentamicin. Cells were incubated for further 4 h and then analysed for STAT4 activity (phosphorylation of tyrosine 693) using FACE™ STAT4 Chemi Kit (Active Motif) (see chapter 2.2.3.10).

The results indicated that $Cyld^{-/-}$-cells show higher STAT4 activation upon *Y. enterocolitica* infection but slightly less STAT4 activation upon LPS stimulation, compared to $Cyld^{+/-}$-cells (Fig.33), and thus reflect the corresponding production level of IL-12 and IFNγ upon *Yersinia* infection (Fig. 31) and LPS stimulation (Fig. 32). Furthermore, upon *S.*Typhimurium infection, both $Cyld^{-/-}$ and $Cyld^{+/-}$ cells don't show a STAT4 activation level higher than that of unstimulated cells (Fig.33). This is in line with our previous finding that *Salmonella* Typhimurium infected-BMDCs or splenocytes don't produce significant amout of IL-12 or IFN-γ, respectively (Fig. 31).
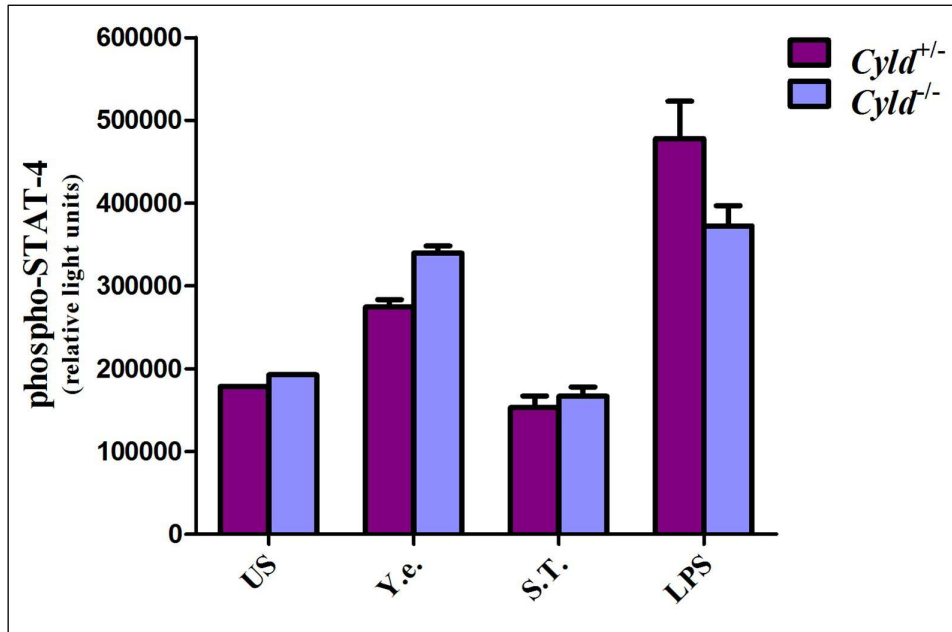
Fig. 33. STAT-4 phosphorylation (Y693-P) of mixed cells after infection or LPS treatment. 2×10^4 BMDCs were mixed with 4.5×10^5 splenocytes (ca. 1:22) and infected with *Y. enterocolitica* (MOI = 7) or *S. typhimurium* (MOI = 19), or stimulated with 1 µg/ml LPS for 4 h (unstimulated/US control). STAT4 Y693-phosphorylation activity was determined using FACE™ STAT4 Chemi Kit. US: unstimulated

3.9 Cell signalling assay

The results presented above indicate that the suppression of phagocytosis and oxidative burst by *Yersinia* effector proteins (e.g. YopH and YopP) is reduced in CYLD-deficient cells resulting in improved phagocytosis and killing of *Y. enterocolitica*. Furthermore, we could show that cytokine production (IFN-γ and IL-12) and STAT4-phosphorylation of Y693 are enhanced in *Yersinia*-infected *Cyld*$^{-/-}$ cells compared to *Cyld*$^{+/-}$ cells (Fig. 31 – 33).

Several studies reported that mitogen-activated protein kinases (MAPKs), such as p38, are involved in the activation of signaling cascades coupling receptor stimulation with several cellular responses, such as phosphorylation of NADPH oxidase and STAT4, and the induction/activation of transcription factors, such as Elk-1, ATF-2 and AP1, that regulate e.g. the production of cytokines (Cui et al., 2000; El Benna et al., 1996a; Lal et al., 1999; Nick et al., 1997; Yamamori et al., 2000).

p38, together with the extracellular signal-regulated kinase (ERK), c-Jun NH2-terminal kinase (JNK), are the three well-defined MAPK subfamilies (Whitmarsh and Davis, 1996), which are highly conserved serine/threonine protein kinases in eukaryotes (Nishida and Gotoh, 1993). MAPKs play pivotal roles in a variety of cellular processes including proliferation, differentiation, apoptosis, stress response, and host immune defense. Activated MAPKs can phosphorylate a wide array of downstream targets, including protein kinases and other enzymes. p38 was first identified as a phosphorylated protein (Han et al., 1994), which is

activated by phosphorylation of tyrosine and threonine residues in response to a variety of stimuli such as N-formyl-methionyl-leucyl-phenylalanine (fMLP), GM-CSF, LPS, serum-opsonized zymosan (OZ), and TNF-α (Krump et al., 1997; McLeish et al., 1998; Nick et al., 1996; Yamamori et al., 2000).

Researchers have shown that YopP, a virulence factor of *Y. enterocolitica* (YopJ in *Y. pseudotuberculosis* and *Y. pestis*), perturbs a multiplicity of signaling pathways, such as ERK, JNK, and p38 pathways and inhibits nuclear factor kappa B (NF-κB) pathway (Palmer et al., 1998; Ruckdeschel et al., 1998) (see introduction). Furthermore, CYLD was also shown to inhibit the activation of c-Jun kinase (JNK) and p38 (Reiley et al., 2004; Yoshida et al., 2005). Considering this knowledge, we wondered whether the impaired suppression of cytokine production, phagocytosis and oxidative burst by *Yersinia* in *Cyld*^{-/-} cells is a result of its inability to inhibit MAPKs activation. Thus, we analyzed the activation of the MAPKs, *viz.* p38, ERK and JNK, whereby only the results about p38 and JNK will be presented and discussed here.

BMDCs were infected with *Y. enterocolitica* WA(pYV) (MOI = 5)*, Yersinia* mutant WA(pYVΔYopP) (MOI = 16) or *Salmonella* Typhimurium (MOI = 26). Infections were terminated at different time points by lysing cells and cell lysates were then subjected to CBA Cell Signalling assay for phospho-p38 and phospho-JNK (BD, Biosciences; and see chapter 2.2.3.9).

As shown in Fig. 34, Yersinia-infected *Cyld*^{-/-} BMDCs showed higher p38 activation 30 min post infection (with ca. 7% phospho-p38 of total p38) compared to *Cyld*^{+/-} BMDCs (with ca. 3% phospho-p38) (Fig.34). 15 min post infection, both cells types showed similar activation level of p38 (both about 4% phospho-p38) (Fig.34). 60 min post infection, the phosphorylation of p38 returned to the ground level (the unstimulated state) in *Cyld*^{+/-} cells, while *Cyld*^{-/-} cells still show some minor activation (about 2.5% phospho-p38) and did not return to the ground level before 90 min post infection (Fig. 34).

In the case of infection with the mutant WA(pYVΔYopP), as expected, both *Cyld*^{-/-} and *Cyld*^{+/-} BMDCs show higher and sustained p38 activation compared to WA(pYV)-infection. However, WA(pYVΔYopP)-infected *Cyld*^{-/-} cells still displayed increased p38 activation at 30 min and 60 min post infection compared to *Cyld*^{+/-} cells (Fig. 34). At 90 min post infection, the phosphorylation of p38 decreased to reach an equal level in both *Cyld*^{-/-} and *Cyld*^{+/-} cells (Fig. 34). However, the increased phosphorylation level was still highly significant, compared to cells infected with WA(pYV) (Fig.34).

To calculate the efficiency of YopP-mediated blockade of p38 activation, the % values for 30 min were presented and the differences (Δ-values) which are then divided by the 100 % value obtained from WA(pYVΔYopP)/Cyld$^{-/-}$ cells. It is obvious that YopP could block about 77% of p38 phosphorylation of Cyld$^{+/-}$ cells and only 61% of that in Cyld$^{-/-}$ cells (Table.14).
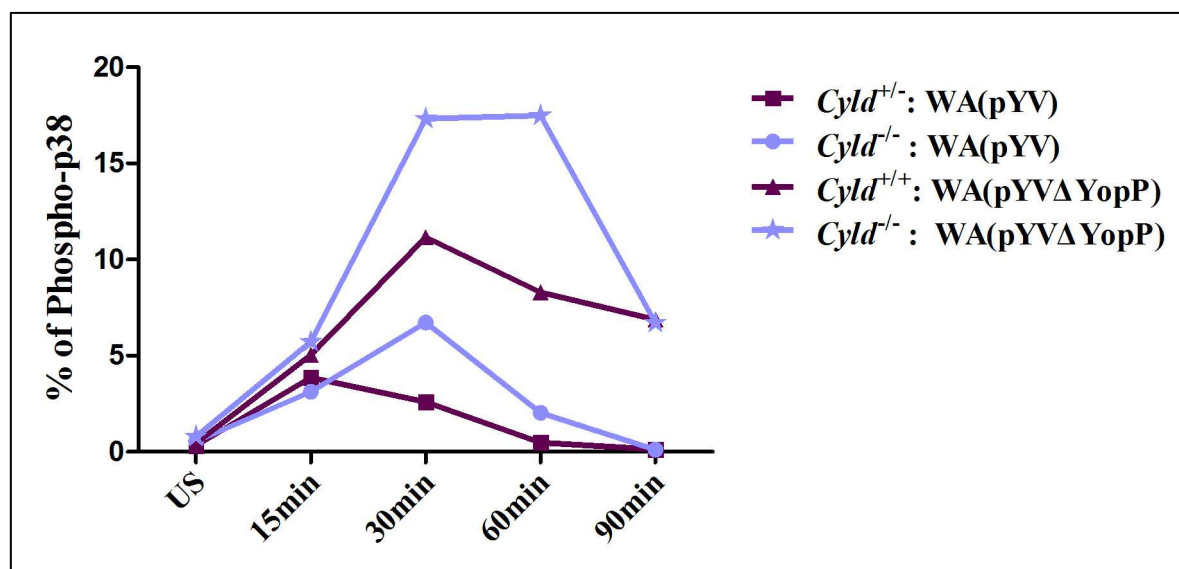

Fig. 34. CYLD and YopP are involved in suppression of p38 after infection. BMDCs (2 x10^6) were infected with strain WA(pYV)314 (MOI = 5) or WA(pYVΔYopP) (MOI = 16). Infections were terminated at different time points by lysing cells and cell lysates were then subjected to CBA Cell Signalling assay for phospho-p38 and Total p38. Cyld$^{-/-}$-cells show higher p38 phosphorylation upon both with WA(pYV) or WA(pYVΔYopP) (US: unstimulated).

Table 14- Comparison of YopP-mediated suppresion of p38 in Cyld$^{+/-}$ and Cyld$^{-/-}$ cells.

30 min	p38 %	Δ	Contribution of YopP or *Cyld*
WA(pYV), *Cyld$^{+/-}$*	2.60	(6.71 –2.60) x 100 : 6.71	= 61.25 % *Cyld* effect
WA(pYV), *Cyld$^{-/-}$*	6.71		
WA(pYVΔYopP),*Cyld$^{+/-}$*	11.15	(17.32 –11.15) x 100 : 17.32	= 35.62 % *Cyld* effect
WA(pYVΔYopP), *Cyld$^{-/-}$*	17.32		

WA(pYV), *Cyld$^{-/-}$*	6.71	(17.32 –6.71) x 100 : 17.32	= 61.26 % YopP effect
WA(pYVΔYopP), *Cyld$^{-/-}$*	17.32		
WA(pYV), *Cyld$^{+/-}$*	2.60	(11.15 –2.60) x 100 : 11.15	= 76.68 % YopP effect
WA(pYVΔYopP), *Cyld$^{+/-}$*	11.15		

To investigate whether CYLD is involved in the modulation of p38 activity in a pathogen specific manner, we infected BMDCs with *Salmonella* Typhimurium (MOI = 26) and analyzed the phosphorylation of p38 at different time points post infection (Fig.35). The results show similar p38 activation between WT- and CYLD-deficient BMDCs.
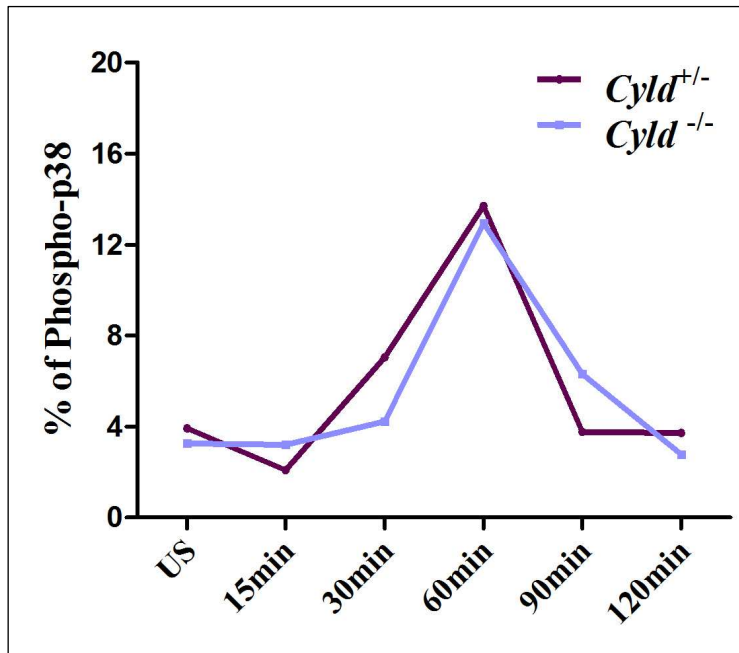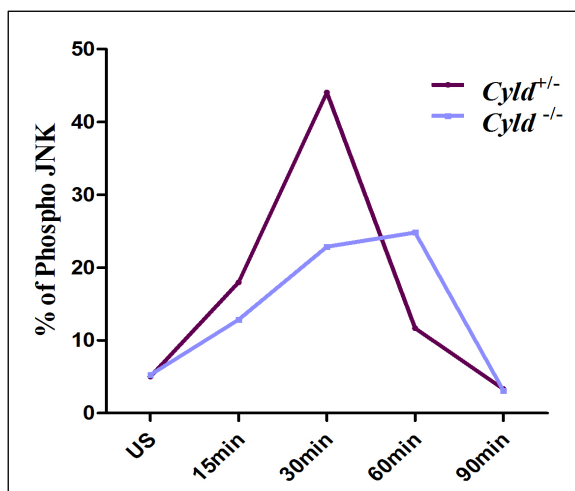
Fig. 35 *Cyld*^{+/-}-and *Cyld*^{-/-}-**BMDCs show similar p38 activation upon *Salmonella* Typhimurium infection.** BMDCs (2 x10^{6}) were infected with ***Salmonella* Typhimurium (MOI = 26)**. Infection was stopped at different time points by lysing cells and cell lysates were then subjected to CBA Cell Signalling assay for phopho-p38 and Total p38. US: unstimulated

(A)
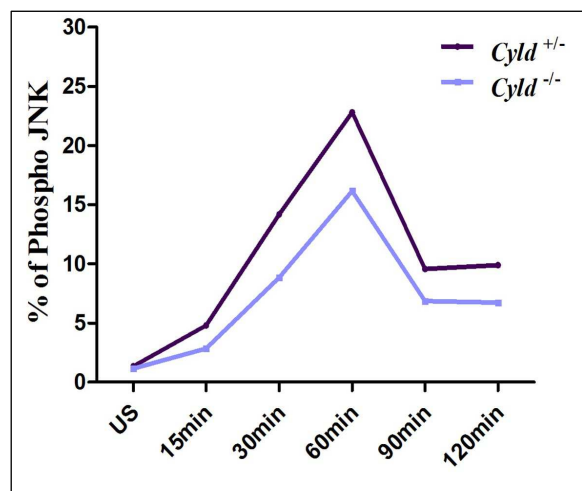
(B)

Fig. 36. Cyld^{-/-}-BMDCs show reduced JNK activation upon *Y. enterocolitica* infection in comparison to Cyld^{+/-}-cells. BMDCs (2 x10^{6}) were infected with WA(pYV) (MOI = 5) **(A)** or WA(pYVΔYopP) (MOI = 12) **(B)**. Infections were terminated at different time points by lysing cells and cell lysates were then subjected to CBA Cell Signalling assay for phopho-JNK and Total JNK. US: unstimulated.

Next, we analysed the activation state of another MAPK member, JNK, using the same samples prepared for p38 analysis. Surprisingly, *Cyld*^{-/-}-BMDCs showed reduced JNK activation upon WA(pYV) infection (MOI = 5) at 30min post infection (with 23% phospho-JNK of total JNK) compared to *Cyld*^{+/-}-BMDCs (with 46% phospho-JNK) (Fig.36A). However, *Cyld*^{-/-}cells sustained their maximal JNK activation level until 60 minutes post infection, whereas in *Cyld*^{+/-}-cells the JNK activation level decreased rapidly after 30 min

(Fig.36A). Finally, JNK activation reached the ground level at 90 min post infection, in both $Cyld^{-/-}$- and $Cyld^{+/-}$-BMDCs.

In the case of infection with the mutant strain WA(pYVΔYopP) (MOI = 16), unexpectedly, both $Cyld^{-/-}$- and $Cyld^{+/-}$- BMDCs showed lower and late JNK activation compared to infection with strain WA(pYV) (Fig.36B). It is not clear whether this is due to the higher MOI of WA(pYVΔYopP) (MOI = 16) compared to that of WA(pYV) (MOI = 5). However, again $Cyld^{-/-}$-cells show reduced JNK activation during the whole analysed infection time (Fig.36B).

3.10 CYLD contribution to YopP-mediated NF-κB-suppression

Another prominent cellular target of *Yersinia* YopP is IKK complex which is involved in NF-κB activation. The effector protein YopP has been shown to interfere with NF-κB activation by blockade of IKKβ, resulting in attenuated transcription of immune response genes (Mukherjee et al., 2006; Zhou et al., 2005a). Because CYLD has also been shown to regulate negatively NF-κB signalling (Brummelkamp et al., 2003; Kovalenko et al., 2003; Salhi et al., 2004; Yoshida et al., 2005), we wondered whether YopP-mediated suppression of NF-κB would be altered in $Cyld^{-/-}$ cells.

Our pilot experiments that were performed with splenocytes being infected with *Y. enterocolitica* at different MOIs (5 to 100) for up to 150 min indicated that p65 NF-κB member was not significantly activated with lower MOI (<50) (see exemplary result for MOI = 20; Fig.37). Therefore, in the following experiments, we infected the splenocytes with MOI ≥ 50.

Splenocytes were infected with *Y. enterocolitica* WA(pYV) (MOI = 90) or mutant WA(pYVΔYopP) (MOI = 80) and the activation of p65 and c-Rel were analyzed using TransAM NF-κB family kit (Active Motif) (see chapter 2.2.3.8.). The results indicated that $Cyld^{-/-}$ cells show increased p65 activation upon infection with WA(pYV) or mutant WA(pYVΔYopP) at 30min post infection compared to $Cyld^{+/-}$ cells (Fig.38). However, the difference in NF-κB activity was reduced from ca. 40% to ca. 15% when $Cyld^{-/-}$ and $Cyld^{+/-}$ cells were infected with WA(pAV) (Fig.38A) and mutant WA(pYVΔYopP) (Fig.38B), respectively.

The analysis of another member of the NF-κB family, c-Rel, indicated that it did not show any significant activation for both $Cyld^{-/-}$ and $Cyld^{+/-}$ cells upon *Yersinia* infection (Fig.39).

In conclusion, YopP-mediated inactivation of NF-κB is dependent, at least to some extent, on CYLD.
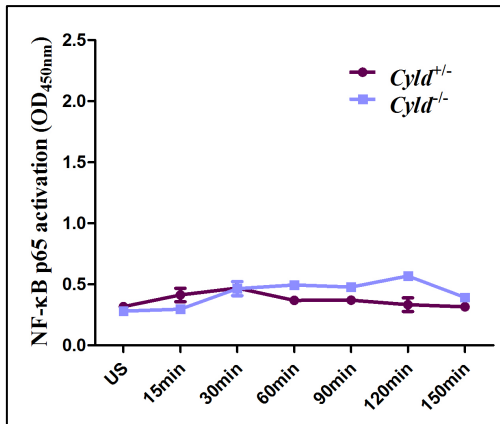
Fig. 37. No significant activation of NF-κB member, p65, in both *Cyld^{-/-}* and *Cyld^{+/-}* splenocytes upon *Yersinia* infection at low MOI (<50). Splenocytes were infected *in vitro* with *Y. enterocolitica* at MOI = 20 for different time points. Similar amount of whole cell extracts were subjected to p65 activation assay using TransAM NF-κB family kit. Results are shown as % of total p65. US: unstimulated cells.

Fig. 38. *Cyld^{-/-}* cells show increased p65 activation upon infection with WA(pYV) *or* mutant WA(pYVΔYopP). Splenocytes were infected *in vitro* with **WA(pYV)** at MOI = 90 **(A)** or **WA(pYVΔYopP**) at MOI = 80 **(B)** for different time points. Similar amount of whole cell extracts were subjected to p65 activation assay using TransAM NF-κB family kit. Results are given as % of total p65. US: unstimulated cells.
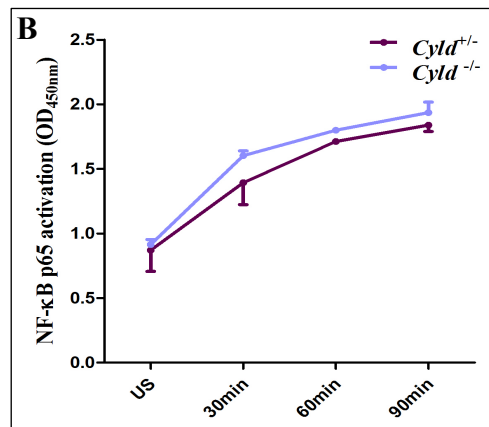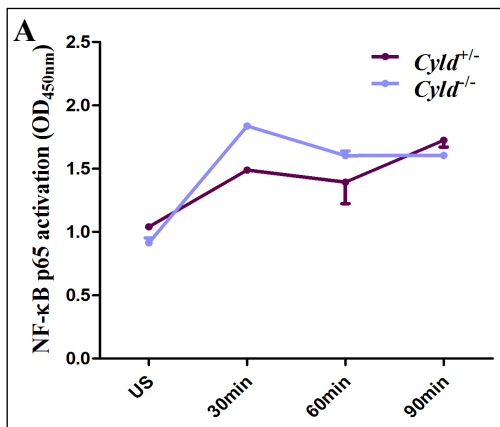

Fig. 39. No significant activation of c-Rel in both *Cyld^{-/-}* and *Cyld^{+/-}* splenocytes upon *Yersinia* infection. Splenocytes were infected *in vitro* with WA(pYV) at MOI = 90 **(A)** or WA(pYVΔYopP) at MOI = 80 **(B)** for different time points. Similar amount of whole cell extracts were subjected to c-Rel activation assay using TransAM NF-κB family kit. Results are given as % of total c-Rel. US: unstimulated cells.
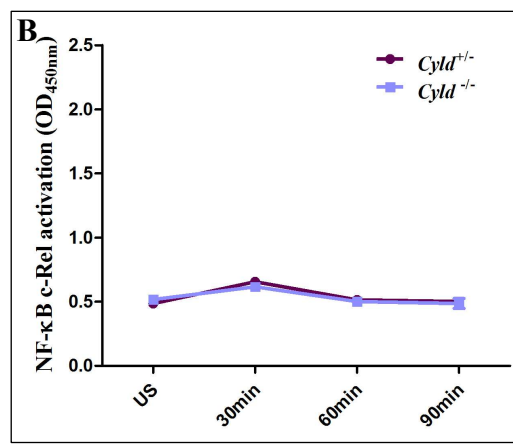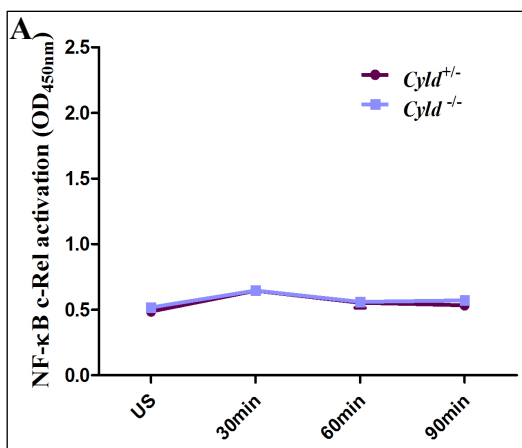
3.11 Yops are translocated with similar efficiency into $Cyld^{+/-}$ and $Cyld^{/-}$ cells

The results shown above clearly demonstrate that Yops-mediated inhibition of immune defence mechanisms, such as phagocytosis, oxidative burst, NF-κB and p38, are attenuated in CYLD-deficient cells. This attenuation of Yop effector function could be due to decreased Yop translocation rate in $Cyld^{/-}$ cells. To investigate this possibility, we performed a translocation assay using a ß-lactamase reporter system (see chapter 2.2.3.15). For this assay, the coding sequence of TEM-ß-lactamase was fused with the 3' end of *yopH* gene sequence and 3' end of *yopP* gene sequence, respectively, and cloned into plasmid pACYC184. The reporter constructs (designated as pYopH-Bla or pYopP-Bla) were then transformed into *Y. enterocolitica* mutants WA(pYVΔYopH), WA(pYVΔYopP) and the secretion deficient mutant WA(pYVΔLcrD) (the reporter constructs and the reporter *Yersinia* strains were generated by Hicham Bouabe, unpublished data). The Ysc-T3SS defect mutant WA(pYVΔLcrD, pYopH-Bla) strain, is known to be highly phagocytosed and was used as control to confirm the translocation-dependent reporter activity of Yop-Bla.

Using the ß-lactamase FRET-substrate, CCF4-AM, the injection of Yop-Bla proteins into host cells can be detected by FACS analysis based on a shift from green to blue fluorescence (see 2.2.3.15., Fig.11).
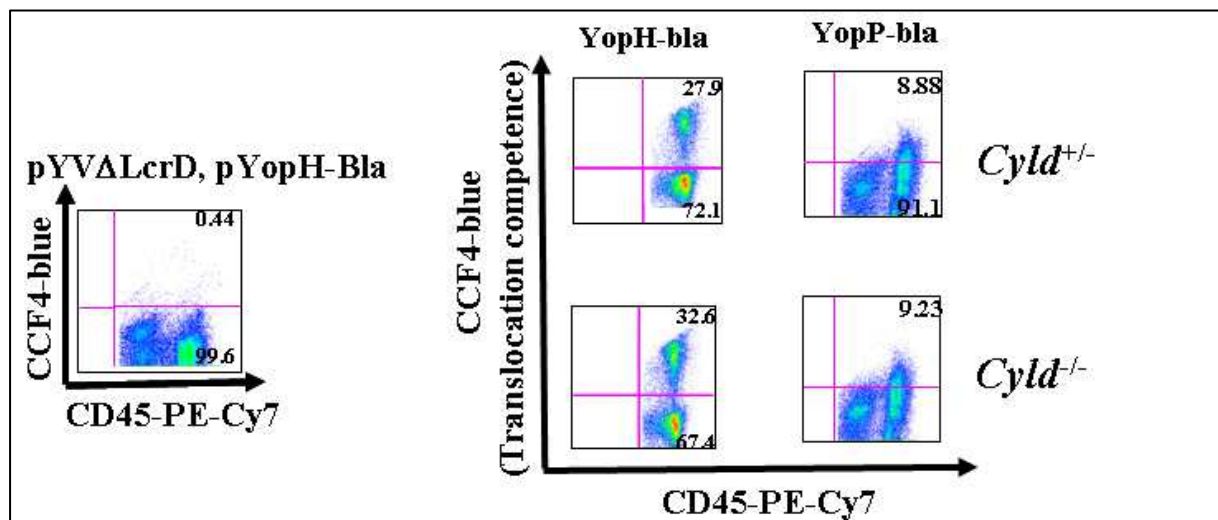
Splenocytes from $Cyld^{+/-}$ and $Cyld^{/-}$ mice were infected with WA(pYVΔYopH, pYopH-Bla) (here denoted as strain YopH-Bla), WA(pYVΔYopP, pYopP-Bla (strain YopP-Bla) or WA(pYVΔLcrD, pYopH-Bla) at MOI = 20 for 60 min. Splenocytes were then loaded with CCF4-AM, stained with antibodies against immune cell surface markers and analyzed by FACS.

As shown in Figure. 40, similar cell numbers were injected by strain YopH-Bla or YopP-Bla in both $Cyld^{+/-}$ and $Cyld^{/-}$ splenocytes (Fig.40a). Furthermore, the quanification of Bla-reporter acitivity by calculating the ratio of blue to green fluorescenc (indirect parameter of the amount of Bla-protein whitin a cell) revealed no differences in the efficiency of YopH-Bla and YopP-Bla translocation in both $Cyld^{+/-}$ and $Cyld^{/-}$ splenocytes (Fig.40B).

The infection of splenocytes with the Ysc-T3SS deficient control strain did show any blue fluorescence demonstrating that the measured activity of the Yop-Bla reporter strains were Ysc-T3SS-translocation-dependent.

In conclusion, the impaired ability of Yops to inhibit optimally cell defense mechanisms in CYLD-deficient cells is not due to decreased translocation of these effectors into host cells.

(A)

(B)
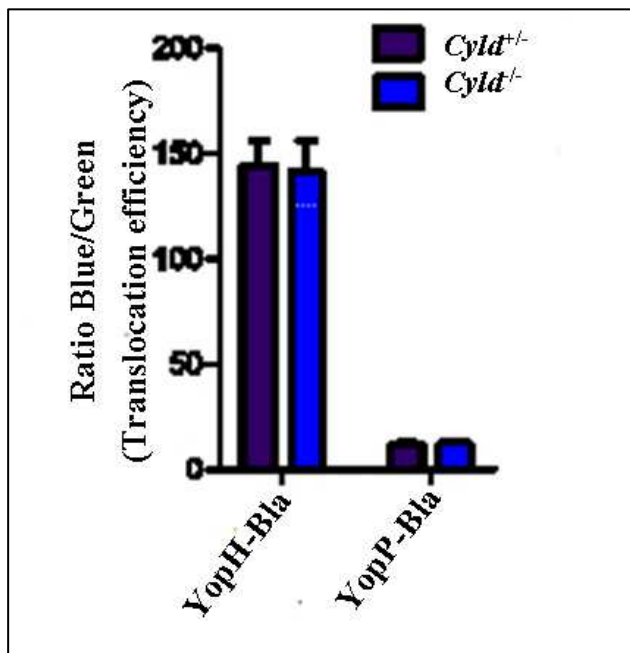
Fig. 40. YopP- and YopH-Bla fusions are translocated with similar efficiency into *Cyld*^{+/-}- and *Cyld*^{-/-} splenocytes. Splenocytes from *Cyld*^{+/-} and *Cyld*^{-/-} mice were infected with strain YopH-Bla, strain YopP-Bla or Ysc-T3SS deficient control strain WA(pYVΔLcrD) at MOI = 20 for 60 min. Splenocytes were then loaded with CCF4-AM, stained with antibodies against leukocyte marker (CD45) and analyzed by FACS. **(A)** Dot plots showing the percentage of Yop-Bla[+] splenocytes gated on the leukocyte marker CD45. **(B)** Quantification of Yop-Bla translocation in the Bla+ populations by measuring the ratio of blue to green fluorescence (blue/green), and then normalization (blue cells) to the corresponding Bla[-] population.

4. Discussion

Recent studies have identified the tumor suppressor CYLD as a negative regulator for NF-κB signalling by deubiquitinating TRAFs (TRAF2; TRAF6; TRAF7) and IKK-γ subunit (Brummelkamp et al., 2003; Kovalenko et al., 2003; Yoshida et al., 2005). CYLD was also shown to inhibit the activation of the mitogen-activated protein kinases (MAPKs), JNK and p38 (Reiley et al. 2004; Yoshida et al. 2005).

Interestingly, many pathogens have also evolved virulence proteins that selectively target pathways of NF-κB and MAPKs, allowing them to interfere with the transcription of immune response genes. For instance, YopP from *Yersinia enterocolitica* (YopJ in *Y. pestis* and *Y. pseudotuberculosis*) and their functional related proteins, such as VopA from *Vibrio parahaemolyticus*, AvrA and SseL from *Salmonellae*, AopP of *Aeromonas salmonicida* and AvrRxv of the phytopathogenic bacterium *Xanthamonas campestris pv. vesicatori*, have also been shown to inhibit the activation of NF-κB and/or MAPKs, such as p38 and JNK (Bonshtien et al., 2005; Du and Galan, 2009; Fehr et al., 2006; Hotson and Mudgett, 2004; Jones et al., 2008; Le Negrate et al., 2008; Mittal et al., 2006; Mukherjee et al., 2006; Orth et al., 1999; Palmer et al., 1999; Trosky et al., 2004; Zhou et al., 2005b).

Moreover, many pathogens, such as pathogenic *Yersinia* spp. and *Salmonella* spp were reported to exploit or modulate the ubiquitination machinery of the host cells (Angot et al., 2007; Hentschke et al., 2007; Hicks and Galan, 2010; Munro et al., 2007).

Thus, considering the overlapping functions of CYLD and virulence factors, it is worthwhile to explore whether the tumor suppressor gene, *Cyld*, is beneficial or detrimental to bacterial infections.

Therefore, in this study, we investigated the role of CYLD in regulation of innate immune responses to the enteric pathogen, *Yersinia enterocolitica*.

4.1 *Cyld⁻/⁻* mice show enhanced resistance specifically to *Yersinia enterocolitica*

We found that the susceptibility of *Cyld⁻/⁻* mice to *Salmonella* Typhimurium infection was comparable (P>0.05) to that of *Cyld⁺/⁻* mice after both oral and *i.p.* infection. This finding indicates that, under our experimental conditions, CYLD seems not to play a significant role in *Salmonella* mouse infection. However, when we analysed the influence of CYLD on mouse resistance against *Y. enterocolitica*, we found that *Cyld⁻/⁻* mice cleared more efficiently the bacteria in liver and spleen compared to *Cyld⁺/⁻* mice, after both oral and i.p. infection. Interestingly, there was no significant difference (P = 0.57) in yersiniae load in the Peyer's

patches (PPs) of $Cyld^{-/-}$ mice and control littermates after oral infection. Thus CYLD seems not to be required for defense against *Yersinia* in the PPs. This might due to the low expression of CYLD in the intestine (Massoumi et al., 2006), which includes gut-associated lymphoid tissue (GALT), such as PPs. Furthermore, we found that the colonization phenotype in spleen and liver were reproducible independent of the infection route (i.p. or oral), which indicates that the decreased colonization of spleen and liver in CYLD-deficient mice in the case of oral infection, is not because of the diminished disseminating capability of *Yersinia* from intestine/PPs to spleen or liver during the early infection course.

The increased *Yersinia* clearance in $Cyld^{-/-}$ mice was not associated with increased recruitment of leukocytes (e.g. neutrophil, monocytes) to the infection site (see chapter 3.3). Furthermore, the amounts of proinflammatory cytokines, such as TNF-α, in the serum of the $Cyld^{+/-}$ and $Cyld^{-/-}$ mice 1 day post-infection, and in the supernatants of LPS-stimulated $Cyld^{+/-}$ - and $Cyld^{-/-}$ BMDCs were comparable (Fig.29 and Fig.32). Thus, CYLD-deficiency does not result per se in a higher inflammation and stronger defence mechanism. This conclusion is supported by our finding that WT and $Cyld^{-/-}$ mice showed similar susceptibility to *Salmonella* Typhimurium infection. Furthermore, Srokowski et al. who used the same $Cyld^{-/-}$ mouse strain as we used could also not detect any alterations of the immune system (Srokowski et al., 2009). These findings stand in contrast to other knockout mouse models of CYLD that display e.g. alterations of the immune system including hyper-induction of IFNα in virus infected DCs (Zhang et al., 2008) as well as protection from infections (Lim et al., 2007).

These discrepancies may be due to the gene targeting strategies used by the corresponding investigators to generate the *Cyld* knockout mouse models (summarized in the introduction part: chapter 1.5.4). One consequence of the different targeting strategies may be the expression of different short fragments of CYLD protein or "new" splice variants instead of the deletion of the complete *Cyld* gene. For instance, a recently generated mouse strain that expresses solely a splice variant of CYLD lacking exons 7 and 8, displays, in contrary to mice lacking the fulllength CYLD, a hyperactive phenotype in DCs, enhanced activity of NF-κB and production of proinflammatory, and a dramatic expansion of mature B lymphocyte populations in all peripheral lymphoid organs (Hovelmeyer et al., 2007; Srokowski et al., 2009).

Taking together, the explanation of the improved resistance of $Cyld^{-/-}$ mice does not rely on an intrinsic enhanced immune response. Rather we suggest that *Yersinia* exhibits reduced ability to counteract the host defence mechanisms in the absence of CYLD.

4.2 CYLD promotes Yops-mediated anti-host functions

Yersinia is an extracellular multiplying bacterium that ensures its extracellular growth by injecting virulence proteins (Yops) into host cells via Ysc-T3SS, which interfere with several signaling pathways, such as MAPK cascades and RhoGTPases, resulting in the inhibition of phagocytosis, oxidative burst and cytokine production (Heesemann et al., 2006).

Because of the improved pathogen-specific resistance of $Cyld^{-/-}$ mice to *Yersinia* infection, we speculated that Yop-mediated anti-host functions are impaired in $Cyld^{-/-}$ cells. To address this question, we compared several well-known Yops-mediated anti-host functions in $Cyld^{-/-}$ and $Cyld^{+/-}$ cells.

4.2.1 CYLD is required for Yops-mediated inhibition of phagocytosis

We performed *in vitro* phagocytosis assay and found that $Cyld^{-/-}$ PECs show higher phagocytic capability (ca. 3 times more than $Cyld^{+/-}$ PECs) to *Y. enterocolitica* and display more efficient intracellular killing of internalized *Y. enterocolitica*. *In vivo* phagocytosis assay confirmed these *in vitro* findings. Thus, Yops-mediated inhibition of phagocytosis seems to be attenuated in the absence of CYLD. In order to analyze directly the contribution of CYLD to the anti-phagocytosis effect of a given Yop, we investigated the capability of $Cyld^{-/-}$ and $Cyld^{+/-}$ PECs to phagocytose *Y. enterocolitica* strain that lack YopH (chapter 3.5, Fig.18), an effector protein which is known to inhibit phagocytosis (Bliska and Black, 1995; Fallman et al., 2002; Persson et al., 1997; Rosqvist et al., 1988). Interestingly, although the phagocytosis of strain WA(pYVΔYopH) was higher by both $Cyld^{-/-}$ and $Cyld^{+/-}$ PECs compared to strain WA(pYV), $Cyld^{-/-}$ PECs phagocytosed only about two times more compared to $Cyld^{+/-}$ PECs. In contrast, WA(pYV) was phagocytosed about 3 times more by $Cyld^{-/-}$ PECs compared to $Cyld^{+/-}$ PECs (chapter 3.5, Fig.18A). Thus, the anti-phagocytosis effect of YopH seemed to be higher in $Cyld^{+/-}$ PECs compared to $Cyld^{-/-}$ PECs (chapter 3.5, Fig.18B), which indicates that CYLD might support YopH-mediated anti-phagocytosis effect. However, as WA(pYVΔYopH) were not phagocytosed similarly by $Cyld^{-/-}$ PECs and $Cyld^{+/-}$ PECs, the impairment of the anti-phagocytosis effect seems also ascribed to other *Yersinia* effectors (e.g. YopE, YopO, YopT) who might also contribute to this phagocytosis phenotype in the absence of CYLD. The contribution of YopE, YopO and YopT to the inhibition of phagocytosis has already been reported by several groups (Grosdent et al., 2002; Rosqvist et al., 1990). In further studies, the contribution of CYLD to the anti-phagocytosis effects of other Yops than YopH should be investigated by performing phagocytosis assays with Yop-mutants lacking e.g. YopE, YopO and/or YopT.

4.2.2 CYLD is required for Yops-mediated inhibition of oxidative burst

Another very important characteristic of *Yersinia* virulence mediated by Yops is the inhibition of the production of reactive oxygen and nitrogen species (ROS/RNS) by host cells, such as macrophages and neutrophils (Allen, 2003; Hartland et al., 1994; Lian and Pai, 1985; Ruckdeschel et al., 1996).

The analysis of oxidative burst response by two independent methods (chemiluminometric and fluorimetric probe that enable to detect intra- and extracellular ROS/RNS products; chapter 3.6.1 and 3.6.2) revealed that CYLD-deficient cells show significantly higher and extended respiratory burst response (both intra- and extracellular ROS/RNS products) to *Y. enterocolitica* infection compared to $Cyld^{+/-}$ cells. In accordance with these results, internalized *Yersinia* bacteria were killed almost two times more efficiently in $Cyld^{-/-}$ than WT PECs (Fig.20). In contrast, results acquired with other pathogenic bacteria such as *L. monocytogenes* or *Salmonella* Typhimurium showed similar level of oxidative burst response by either $Cyld^{+/-}$ or $Cyld^{-/-}$ cells. Thus, the improved oxidative burst activity in $Cyld^{-/-}$ cells seems not to be an intrinsic effect of CYLD-deficiency, rather CYLD seems to be specifically involved in the negative regulation of cellular oxidative burst activity during *Yersinia* infection by promoting Yops-mediated inhibition of oxidative burst.

In order to examine this assumption, we investigated the capability of ROS production of $Cyld^{+/-}$ and $Cyld^{-/-}$ cells during infection with *Y. enterocolitica* strains that lack the effector proteins YopH or YopP. It is already known that the protein tyrosine phosphatase YopH contribute to the inhibition of oxidative burst (Bliska and Black, 1995; Green et al., 1995; Ruckdeschel et al., 1996). Furthermore, because CYLD (deubiquitinase) and YopP (acetyltransferase) show overlapping functions e.g. as negative regulators of MAPK (Reiley et al., 2004; Yoshida et al., 2005; Zhou et al., 2005a) and MAPKs are known to be involved in the activation of oxidative burst (Brown et al., 2004; El Benna et al., 1996a; El Benna et al., 1996b; Laroux et al., 2005; Sakamoto et al., 2007; Yamamori et al., 2002), YopP is also suggested to be involved in the inhibition of ROS production by blocking the MAPK pathways (Visser et al., 1999). Interestingly, $Cyld^{+/-}$ and $Cyld^{-/-}$ cells displayed similar respiratory burst response to the infection with both *Yersinia* mutants (ΔYopH or ΔYopP), which persisted even beyond 40 min post-infection in comparison to ROS production by $Cyld^{+/-}$ cells infected with strain WA(pYV) (Fig.26 and Fig.28). Thus, the presence of Yops alone is not sufficient to inhibit completely oxidative burst by *Yersinia enterocolitica*, rather CYLD protein is necessary for Yops-mediated inhibition of ROS production.

However, it is not clear whether the attenuated inhibition of ROS-production in $Cyld^{-/-}$ cells is a direct effect of altered Yops-function in the inhibition of oxidative burst or a secondary effect of the improved phagocytosis ability of $Cyld^{-/-}$ to *Yersinia*. It is generally accepted that phagocytosis is accompanied by the release of ROS (Johnston et al., 1976; Root et al., 1975; Root and Metcalf, 1977; Sbarra et al., 1976). But because YopP was also involved in the inhibition of oxidative burst (Fig.28B) and *Y. enterocolitica* strain lacking YopP was phagocytosed as efficient as the WA(pYV) parental strain (data was not shown but see: Grosdent et al., 2002), we suggest that the stimulation/inhibition of oxidative burst by *Yersinia* is, at least partly, independent of the phagocytosis process. This suggestion is supported by studies that showed some cases of phagocytosis-independent oxidative burst activities (Gordon and Hart, 1994; Wright and Silverstein, 1983; Yamamoto and Johnston, 1984).

4.2.3 CYLD is required for Yops-mediated inhibition of NF-κB and MAPK activation and cytokine production

Yersinia enterocolitica is known to inhibit signaling pathways such as NF-κB and MAPK, and to attenuate cytokine production, mainly via YopP (Navarro et al., 2005; Ruckdeschel et al., 1997). To further validate the assumption that CYLD promotes Yop-mediated inhibition of host defence mechanisms, we cheeked NF-κB and p38 activation as well as cytokine production by $Cyld^{-/-}$ and $Cyld^{+/-}$ cells during *Yersinia* infection as further arguments.

Kinetic studies of p38 phosphorylation and NF-κB activation during *Y. enterocolitica* infection revealed that $Cyld^{-/-}$ cells showed higher p38 activation at 30 min and 60 min post infection compared to $Cyld^{+/-}$ cells (Fig.34A). We could rule out a nonspecific intrinsic effect of CYLD to attenuate p38 signaling because infection with *S. typhimurium* resulted in similar activation level of p38 in $Cyld^{-/-}$ and WT cells (Fig.35). However, when we determined YopP-mediated inhibition of p38 activation by comparing the ratios of WA(pYV)-dependent to WA(pYVΔYopP)-dependent inhibition of p38 phosphorylation between $Cyld^{+/-}$ and $Cyld^{-/-}$ cells, we found that YopP-mediated inactivation of p38 is higher in $Cyld^{+/-}$ cells (about 20%) compared to $Cyld^{-/-}$ cells (Fig.34B). Furthermore, the difference in NF-κB activity between $Cyld^{+/-}$ and $Cyld^{-/-}$ cells was reduced, from ca. 40% to ca. 15%, when the cells were infected with *Y. enterocolitica*-ΔYopP (Fig.38). Because the elimination of YopP did not result in equal activation level of p38 and NF-κB in $Cyld^{+/-}$ and $Cyld^{-/-}$ cells, we suggest that either other "YopP-independent" *Yersinia* factors also contributes to the inhibition of p38 and NF-κB, at least in the context of CYLD-deficiency. It is also likely that CYLD acts together with

YopP to mediate additive suppression of p38 and NF-κB. The later suggestion is supported by published data showing that CYLD negatively regulate PAMPs-dependent activation of both NF-κB and p38 MAPK pathways (Yoshida et al., 2005).

MAPK cascades are the most intensively studied objectives of signal transduction pathways that induce the expression of cytokines (Johnson and Lapadat, 2002; Kyriakis and Avruch, 2001). Thus, we wondered whether the differential activation of p38 in $Cyld^{+/-}$ and $Cyld^{-/-}$ cells during *Yersinia* infection would result in differences in their cytokine production level. Interestingly, while $Cyld^{+/-}$ and $Cyld^{-/-}$ cells showed similar production level of TNF-α after infection with *Y. enterocolitica* (Fig.30A), the production of MCP-1 was decreased and that of IL-12/IL-23p40 increased in $Cyld^{-/-}$ cells compared to $Cyld^{+/-}$ cells (Fig.30B and Fig.31A). Furthermore, tyrosine phosphorylation of signal transducer and activator of transcription (STAT)-4 and IFNγ production were enhanced in $Cyld^{-/-}$ cells, compared to $Cyld^{+/-}$ cells (Fig.31B). STAT4 provides a direct link between IL-12 receptor and cytokine-induced gene transcription (Watford et al., 2003; Wurster et al., 2000). An early target of IL-12 is the cytokine IFNγ (Lund et al., 2004; Watford et al., 2003).

How can this differential expression profile of MCP-1, IL-12 and TNF-α by $Cyld^{-/-}$ and WT cells be explained?

The MAPKs are differentially involved in the induction of cytokine synthesis (Salojin and Oravecz, 2007; Zhang et al., 2009; Zhang and Dong, 2005). For instance, p38 and c-Jun N-terminal Kinase (JNK) cooperatively induce the expression of TNF-α (Comalada et al., 2003; Das et al., 2009; Hoffmeyer et al., 1999; Lee et al., 1994; Srivastava et al., 1999; Swantek et al., 1999; Swantek et al., 1997; Wysk et al., 1999), whereas MCP-1 is induced by JNK but not p38 (Arndt et al., 2004; Gao et al., 2009; Nakayama et al., 2001; Xiao and Chodosh, 2005) (summarized in Fig.41).

Furthermore, recent studies have demonstrated that signaling pathways do not work independently, but instead exhibit "cross-talks" (Dumont et al., 2001; Huang et al., 2009). For example, it has been shown that activated p38 inhibits the activation of JNK e.g. by activating phosphatases, such as protein phosphatase 2A (PP2A), which in turn inactivates the upstream kinases, MKK4 and MKK7, of the JNK cascade (Fig.41) (Avdi et al., 2002; Hui et al., 2007; Saldeen and Welsh, 2004).
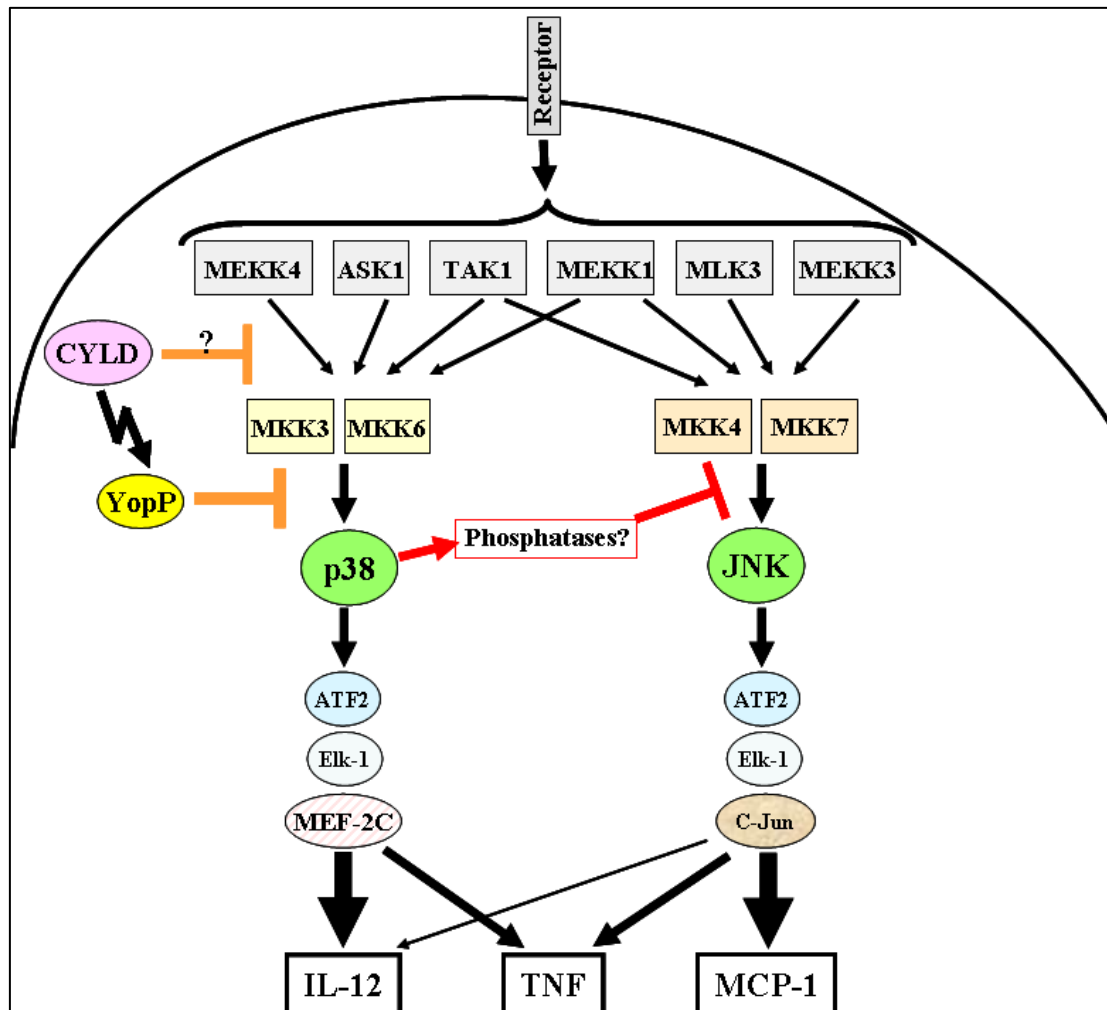
Fig. 41. Cross-signaling between Jun N-terminal kinase (JNK) and p38 mitogen-activated protein kinases (MAPKs) pathways and their regulation of cytokine production (modified e.g from (Avdi et al., 2002; Wagner and Nebreda, 2009; Zhang and Dong, 2005). The signal cascades of p38 and JNK are activated by several stimuli, including microbial patterns (e.g. LPS), environmental stresses (e.g. ultraviolet irradiation, heat and osmotic shock, toxins), growth factors and inflammatory cytokines. The different upstream activators of JNK and p38 MAPKs, such as MAP1K, MAP3K, MAP4K, ASK1 and TAK1 are depicted. p38 is activated by the upstream MKK3 and MKK6 kinases, whereas JNK can be activated by the upstream MKK4 and MKK7 kinases. p38 and JNK activate the transcription factors, ATF2, Elk-1, MEF-2C and/or C-Jun. JNK and p38 are cooperatively involved in the induction of TNF production while MCP-1 is upregulated by JNK but not by p38. The contribution of p38 to IL-12 is more significant than that of JNK. The p38 and JNK pathways are the targets of *Yersinia* effector protein YopP. The inhibitions of p38 and JNK pathways by CYLD is controversial (our own data, and (Massoumi et al., 2006; Reiley et al., 2004; Yoshida et al., 2005).
TAK1: transforming growth factor β-activated kinase 1; ATF2: activating transcription factor 2; ASK1: apoptosis signal-regulating kinase 1; MEF-2C: myocyte-specific enhancer factor 2; Elk-1: ets-like gene-1; MKK: Mitogen-activated protein kinase kinase; MEKK: MAP/Erk kinase kinase.

Interestingly, in accordance with these published studies, we also found that the increased activation of p38 was accompanied with decreased JNK activity in our *Yersinia*-infected *Cyld*^{-/-} DCs (Fig.34 and Fig.36). Since it is JNK but not p38 that is involved in MCP-1 induction, as mentioned above, the reduced MCP-1 production by *Cyld*^{-/-} DCs can be explained by their attenuated JNK signalling.

In the case of TNF-α, although *Cyld*^{-/-} DCs showed increased p38 activation, this did not result in enhanced TNF production, compared to *Cyld*^{+/-} cells. Keeping in mind that both p38

and JNK are involved in the induction of TNF-α production, the similar production level of TNF-α suggests that p38-induced TNF-α production in $Cyld^{-/-}$ cells is lowered out by the simultaneous attenuated JNK activity.

In the case of IL-12, although, depending on stimuli and experimental conditions, JNK has also been shown to contribute to IL-12 production (Dobreva et al., 2008, 2009; Kim et al., 2005; Ma et al., 2004), p38 seems to play the major role in the induction of IL-12. This is supported by *in vivo* studies on mice deficient in the Mkk3 gene, one of the two specific MAPK kinases (MAPKKs) that activate p38. Despite normal expression level and activation of JNK, Mkk3-deficient mice were defective in IL-12 production by macrophages and dendritic cells (Lu et al., 1999). Moreover, it was shown that JNK even negatively regulates LPS-induced IL-12 production in human macrophages (Utsugi et al., 2003). Considering these published data, we suggest that the improved production of IL-12 by our *Yersinia*-infected $Cyld^{-/-}$ DCs is due to the enhanced p38 activation.

Taking together, the present data strongly suggest that several virulence mechanisms, such as inhibition of phagocytosis, oxidative burst, MAPK-signaling and cytokine production, mediated by *Y. enterocolitica* are impaired in CYLD-deficient background. Thus, functional CYLD seems to be required for Yops-mediated anti-host functions.

4.3 Model for enhanced host defence against *Y. enterocolitica* in $Cyld^{-/-}$-mice

The presented data enabled us to propose an integrated model of the defense system used by host cells to counteract the *Y. enterocolitica* infection in the absence of CYLD (Fig.42). For the sake of convenience, all immune defense mechanisms (phagocytosis, oxidative burst, p38 signaling, and cytokine production) are depicted in one model cell. However, one should note that the depicted immune defenses mechanisms in Fig. 42 are executed by different immune cell types.

Upon *Yersinia* infection, innate immune cells such as macrophages and PMNs sense *Yersinia* through e.g. integrins (for example ß1-integrin) (Deuretzbacher et al., 2009; Falkow et al., 1992; Gustavsson et al., 2002; Weidow et al., 2000) and/or PRRs such as TLRs (Inohara et al., 2002; O'Neill, 2000), and transduce signaling cascades inside the cells to mobilize antimicrobial functions.

Very early defence mechanisms initiated by immune cells are phagocytosis of invading bacteria and production of bactericidal ROS. However *Yersinia enterocolitica* injects within few minutes after contact with the immune cells several effector proteins (Yops) through Ysc-T3SS into the cytosol of host cells to counteract the defense responses. The inhibition of

phagocytosis and oxidative burst are the most important counteractions initiated by *Yersinia* to evade its killing and ensure its extracellular survival. Yops, such as YopE and YopH, mediate the anti-phagocytosis effect and inhibition of oxidative burst. However, these Yersinia effectors seem not able to inhibit optimally phagocytosis, oxidative burst and MAPK pathways in *Cyld*^{-/-} cells.

One mechanism that could lead to the enhanced activation of NADPH oxidase and subsequently higher production of ROS might be the enhanced p38 activation in the *Yersinia*-infected *Cyld*^{-/-} cells. This is supported by published data that showed the involvement of p38 in the phosphorylation and activation of NADPH oxidase (Brown et al., 2004; El Benna et al., 1996b; Laroux et al., 2005; Sakamoto et al., 2006; Singh et al., 2009; Yamamori et al., 2002), and by our data that could show that YopP-deficient *Yersinia* lost the ability to inhibit p38 activation (Fig.34A, and (Palmer et al., 1998; Palmer et al., 1999; Ruckdeschel et al., 1997) and ROS production (Fig.28B).

In the late course of infection, the killing of *Yersinia* can be further improved by the MAPK (e.g. p38)/IL-12/STAT4/IFNγ-Axis. The elevated activation of p38 in *Cyld*^{-/-} cells induces higher production of IL-12, which acts through its IL-12R and the downstream transcription factor STAT4 to induce the production IFN-γ (Cho et al., 1996; Morinobu et al., 2002; Zhang and Kaplan, 2000). The activity of STAT4 can be further enhanced through serine phosphorylation by p38 (Morinobu et al., 2002; Visconti et al., 2000; Zhang and Kaplan, 2000). IFN-γ can prime cells expressing IFNγ receptor and its downstream transcription factor STAT1 for further IL-12 production (Boehm et al., 1997; Trinchieri, 1995; Yoshida et al., 1994). p38 could be also involved in the optimal activation of STAT1 by phosphorylating critical serine residues (Bode et al., 1999; Goh et al., 1999; Kovarik et al., 1999; Ramsauer et al., 2002).

As a consequence, these p38/IL-12/STAT4/IFNγ-axis would result in establishing of a T helper cell (Th) 1-based immune response associated with cell-mediated immunity to kill internalized bacteria by inducing IFNγ–response genes, such as 2'-5'oligoadenylate synthetase (OAS), PKR, iNOS, NRAMP1, phox complex (NADPH oxidase), Mx proteins and IRGs (Boehm et al., 1997; Taylor et al., 2007; Trinchieri, 1995). The importance of the IL-12/IFNγ-mediated immune response to protect mice against *Yersinia* infection has already been verified (Bohn and Autenrieth, 1996; Bohn et al., 1998; Hein et al., 2001).
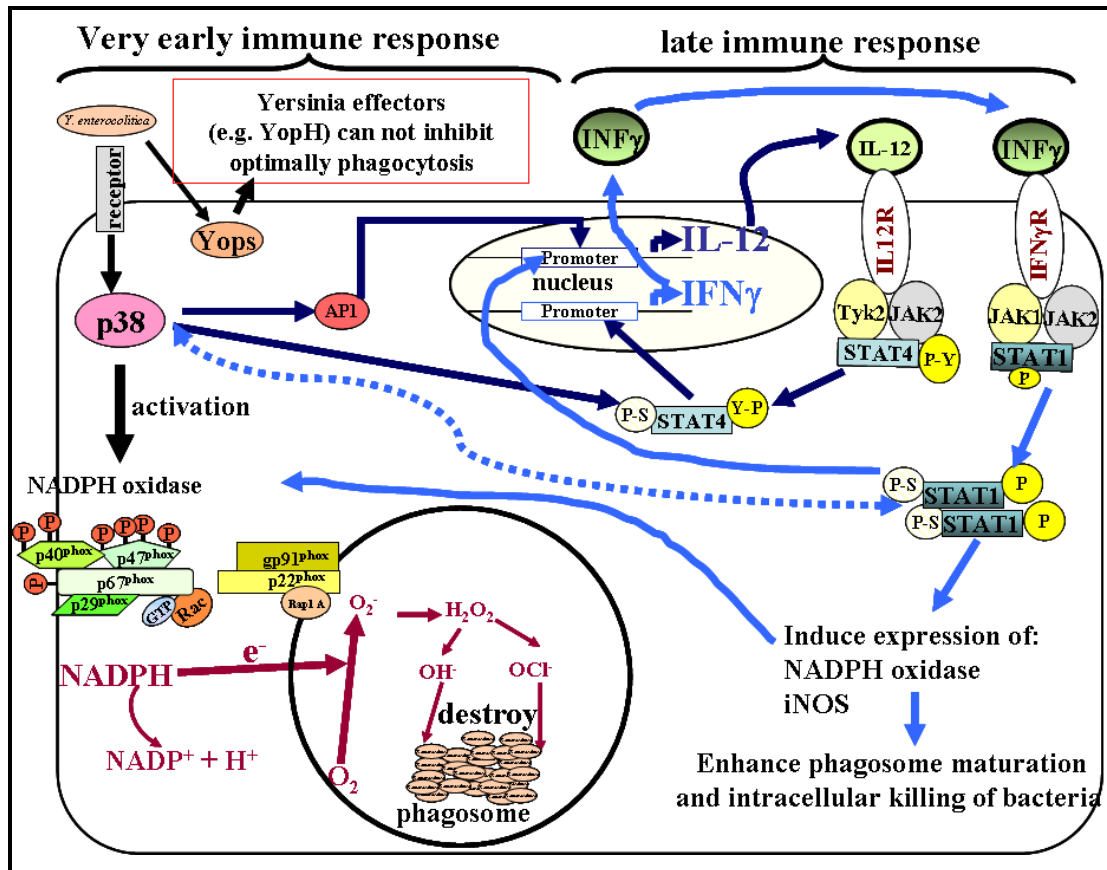
Fig. 42. Model for enhanced defence against *Y. enterocolitica* under conditions of CYLD deficiency. For details see text in 4.3.

4.4 Outlook: How could CYLD contribute to Yops-mediated anti-host functions?

A large body of evidence generated in this study clearly indicates that CYLD seems to be needed for Yops to enhance those anti-host functions. The translocation assay using a ß-lactamase reporter system (Fig.40) revealed that the impaired ability of Yops to inhibit optimally cell defense mechanisms in *Cyld^{/-}* cells is not due to the decreased translocation rate of Yops (at least the analysed YopH-Bla and YopP-Bla) into host cells.

But how could CYLD contribute to Yop-mediated anti-host functions?

There are at least two hypothetical scenarios on how CYLD could do that. However, both scenarios presuppose that, at least, some Yops are K48- and/or K63-polyubiquitinated.

The first possible scenario could be that the deubiquitinase CYLD could remove the Ub-chains from the K48-polyubiquitinated Yops which were marked for degradation and therefore enhance their half life time ($t_{1/2}$). This hypothesis is based on two considerations: (i) it was shown that YopE of strain WA(pYV) is K48-ubiquitinated and degraded by the proteasome in the target cell (Ruckdeschel et al., 2006); (ii) CYLD has recently been shown

to possess a deubiquitinase activity also towards K48-polyubiquitin chains (Reiley et al., 2006).

The second possibility could be that a subset of Yops becomes K63-polyubiquitinated after their translocation resulting in e.g. altered and unfavourable subcellular localization, which does not allow them to optimally interact with their cellular targets and exert their anti-host functions. CYLD could remove the K63-polyubiquitin chains and restore favourable subcellular localization of Yops enabling them to reach optimally their host targets. K63-polyubiquitination is known to mediate e.g. subcellular protein trafficking (Sun, 2008). Furthermore, it has been shown that virulence factor, such as SopB of *Salmonella*, diversifies its function according to its ubiquitination state-dependent subcellular localization (Patel et al., 2009).

5. Summary

Recent studies have identified the tumor suppressor CYLD as a key regulator of NF-κB, a transcription factor that promotes cell survival and oncogenesis, as well as host defence to infection. In the present study, we investigated the role of tumor suppressor CYLD in regulation of innate immune responses of mice to *Y. enterocolitica* infection and for comparison to *Salmonella* Typhimurium infection. *Yersinia* is an extracellular multiplying bacterium that ensures its extracellular growth by injecting virulence proteins (Yops) into host cells by the injectisome Ysc-T3SS, which interfere with several signaling pathways (such as MAPK and NF-κB cascades), resulting in the inhibition of phagocytosis, oxidative burst and cytokine production. In contrast, *Salmonella* Typhimurium is endowed with 2 T3SS which inject effector proteins to induce pathogen uptake and intracellular replication.

Surprisingly, we found that $Cyld^{-/-}$ mice were more resistant to *Y. enterocolitica* than $Cyld^{+/-}$ mice in contrast to *Salmonella* Typimurium infection which appeared to be CYLD-independent. These results suggest that CYLD acts as a detrimental factor for host survival during early *Y. enterocolitica* infection.

Furthermore, we showed that Yops-mediated inhibition of host defense mechanisms, such as phagocytosis, oxidative burst, NF-κB, cytokine production and p38 activation is attenuated in $Cyld^{-/-}$-phagocytic cells in respect of $Cyld^{+/-}$ cells.

Taken together, this study provides for the first time, an empirical demonstration of a pathogen-specific contribution of a tumor suppressor gene and its encoded protein, respectively, CYLD, to infection susceptibility in a manner that seems to be independent of its tumor suppression mechanism. This is another example of the extraordinary complexity of the pathogen/host cell interactions.

6. Zusammenfassung

Der Tumorsuppressor CYLD ist ein wichtiger Regulator für Transkriptionsfaktoren, die für Zellüberleben, Onkogenese und Wirtsabwehr gegen Infektionserreger verantwortlich sind. In der vorliegenden Arbeit wurde die Rolle des Tumorsuppressorproteins CYLD bei der Regulation der angeborenen Wirtsabwehr gegen *Yersinia enterocolitica* und *Salmonella* Typhimurium im experimentellen Mausinfektionsmodell untersucht. *Y. enterocolitica* ist ein extrazellulär replizierender Erreger, der mittels seines Ysc-T3SS (Injektiosom) *Yersinia* outer proteins (Yop) in kontaktierte Wirtszellen „injiziert" und über die Yop-Effektorwirkung die Wirtszell-Signaltransduktionswege kontrolliert (z. B. MAP-Kinase Wege, NF-κB Kaskaden). Auf diese Weise inhibieren Yersinien Phagozytose, Suerstoffradikalbildung (ROS) und proinflammatorische Zytokinfreisetzung. Im Vergleich dazu nutzt *Salmonella* Typhimurium zwei T3SS und die Injektion von Effektorproteinen, um internalisiert zu werden und im Phagosom intrazellulär zu replizieren. Vergleichende Infektionsversuche mit Yersinien und Salmonellen in *Cyld*$^{+/-}$- und *Cyld*$^{-/-}$-Mäusen ergaben ein überraschendes Ergebnis: Cyld$^{-/-}$-Mäuse erwiesen sich als infektionsresistenter für *Yersinia* als Cyld$^{+/-}$-Mäuse. Dagegen zeigten *Cyld*$^{+/-}$- und *Cyld*$^{-/-}$-Mäuse für Salmonellen keinen Unterschied im Infektionsverlauf. Diese Ergebnisse weisen darauf hin, dass CYLD in der Initialphase der *Yersinia*-Infektion die Wirkung der Yop-Effektoren unterstützt. Diese Hypothese konnte durch die Ergebnisse der vergleichenden Phagozytenrate, ROS-Generierung, NF-κB- und p38Kinase-Aktivierung verifiziert werden.

Zusammenfassend zeigen diese Untersuchungen erstmalig, wie das Tumorsuppressorprotein CYLD zusammen mit den *Yersinia* Effektorproteinen die Infektionsempfänglichkeit des Wirtes zum Vorteil des Erregers beeinflusst. Darüber hinaus konnte der CYLD-Effekt als *Yersinia*-spezifisch identifiziert werden.

7. References

Achtman, M., Zurth, K., Morelli, G., Torrea, G., Guiyoule, A., and Carniel, E. (1999). Yersinia pestis, the cause of plague, is a recently emerged clone of Yersinia pseudotuberculosis. Proc Natl Acad Sci U S A *96*, 14043-14048.

Adhikari, A., Xu, M., and Chen, Z.J. (2007). Ubiquitin-mediated activation of TAK1 and IKK. Oncogene *26*, 3214-3226.

Ago, T., Nunoi, H., Ito, T., and Sumimoto, H. (1999). Mechanism for phosphorylation-induced activation of the phagocyte NADPH oxidase protein p47(phox). Triple replacement of serines 303, 304, and 328 with aspartates disrupts the SH3 domain-mediated intramolecular interaction in p47(phox), thereby activating the oxidase. J Biol Chem *274*, 33644-33653.

Akasaki, T., Koga, H., and Sumimoto, H. (1999). Phosphoinositide 3-kinase-dependent and - independent activation of the small GTPase Rac2 in human neutrophils. J Biol Chem *274*, 18055-18059.

Allen, L.A. (2003). Mechanisms of pathogenesis: evasion of killing by polymorphonuclear leukocytes. Microbes Infect *5*, 1329-1335.

Allen, R.C., and Loose, L.D. (1976). Phagocytic activation of a luminol-dependent chemiluminescence in rabbit alveolar and peritoneal macrophages. Biochem Biophys Res Commun *69*, 245-252.

Alonso, A., Bottini, N., Bruckner, S., Rahmouni, S., Williams, S., Schoenberger, S.P., and Mustelin, T. (2004). Lck dephosphorylation at Tyr-394 and inhibition of T cell antigen receptor signaling by Yersinia phosphatase YopH. J Biol Chem *279*, 4922-4928.

Angot, A., Vergunst, A., Genin, S., and Peeters, N. (2007). Exploitation of eukaryotic ubiquitin signaling pathways by effectors translocated by bacterial type III and type IV secretion systems. PLoS Pathog *3*, e3.

Annunziata, C.M., Davis, R.E., Demchenko, Y., Bellamy, W., Gabrea, A., Zhan, F., Lenz, G., Hanamura, I., Wright, G., Xiao, W.*, et al.* (2007). Frequent engagement of the classical and alternative NF-kappaB pathways by diverse genetic abnormalities in multiple myeloma. Cancer Cell *12*, 115-130.

Arndt, P.G., Suzuki, N., Avdi, N.J., Malcolm, K.C., and Worthen, G.S. (2004). Lipopolysaccharide-induced c-Jun NH2-terminal kinase activation in human neutrophils: role of phosphatidylinositol 3-Kinase and Syk-mediated pathways. J Biol Chem *279*, 10883-10891.

Avdi, N.J., Malcolm, K.C., Nick, J.A., and Worthen, G.S. (2002). A role for protein phosphatase-2A in p38 mitogen-activated protein kinase-mediated regulation of the c-Jun NH(2)-terminal kinase pathway in human neutrophils. J Biol Chem *277*, 40687-40696.

Bacon, C.M., McVicar, D.W., Ortaldo, J.R., Rees, R.C., O'Shea, J.J., and Johnston, J.A. (1995a). Interleukin 12 (IL-12) induces tyrosine phosphorylation of JAK2 and TYK2: differential use of Janus family tyrosine kinases by IL-2 and IL-12. J Exp Med *181*, 399-404.

Bacon, C.M., Petricoin, E.F., 3rd, Ortaldo, J.R., Rees, R.C., Larner, A.C., Johnston, J.A., and O'Shea, J.J. (1995b). Interleukin 12 induces tyrosine phosphorylation and activation of STAT4 in human lymphocytes. Proc Natl Acad Sci U S A *92*, 7307-7311.

Bao, S., Beagley, K.W., France, M.P., Shen, J., and Husband, A.J. (2000). Interferon-gamma plays a critical role in intestinal immunity against Salmonella typhimurium infection. Immunology *99*, 464-472.

Barz, C., Abahji, T.N., Trulzsch, K., and Heesemann, J. (2000). The Yersinia Ser/Thr protein kinase YpkA/YopO directly interacts with the small GTPases RhoA and Rac-1. FEBS Lett *482*, 139-143.

Beinke, S., and Ley, S.C. (2004). Functions of NF-kappaB1 and NF-kappaB2 in immune cell biology. Biochem J *382*, 393-409.

Belich, M.P., Salmeron, A., Johnston, L.H., and Ley, S.C. (1999). TPL-2 kinase regulates the proteolysis of the NF-kappaB-inhibitory protein NF-kappaB1 p105. Nature *397*, 363-368.

Biggs, P.J., Chapman, P., Lakhani, S.R., Burn, J., and Stratton, M.R. (1996). The cylindromatosis gene (cyld1) on chromosome 16q may be the only tumour suppressor gene involved in the development of cylindromas. Oncogene *12*, 1375-1377.

Biggs, P.J., Wooster, R., Ford, D., Chapman, P., Mangion, J., Quirk, Y., Easton, D.F., Burn, J., and Stratton, M.R. (1995). Familial cylindromatosis (turban tumour syndrome) gene localised to chromosome 16q12-q13: evidence for its role as a tumour suppressor gene. Nat Genet *11*, 441-443.

Bignell, G.R., Warren, W., Seal, S., Takahashi, M., Rapley, E., Barfoot, R., Green, H., Brown, C., Biggs, P.J., Lakhani, S.R.*, et al.* (2000). Identification of the familial cylindromatosis tumour-suppressor gene. Nat Genet *25*, 160-165.

Bishop, D.K., and Hinrichs, D.J. (1987). Adoptive transfer of immunity to Listeria monocytogenes. The influence of in vitro stimulation on lymphocyte subset requirements. J Immunol *139*, 2005-2009.

Black, D.S., and Bliska, J.B. (1997). Identification of p130Cas as a substrate of Yersinia YopH (Yop51), a bacterial protein tyrosine phosphatase that translocates into mammalian cells and targets focal adhesions. EMBO J *16*, 2730-2744.

Black, D.S., and Bliska, J.B. (2000). The RhoGAP activity of the Yersinia pseudotuberculosis cytotoxin YopE is required for antiphagocytic function and virulence. Mol Microbiol *37*, 515-527.

Bliska, J.B., and Black, D.S. (1995). Inhibition of the Fc receptor-mediated oxidative burst in macrophages by the Yersinia pseudotuberculosis tyrosine phosphatase. Infect Immun *63*, 681-685.

Bode, J.G., Nimmesgern, A., Schmitz, J., Schaper, F., Schmitt, M., Frisch, W., Haussinger, D., Heinrich, P.C., and Graeve, L. (1999). LPS and TNFalpha induce SOCS3 mRNA and inhibit IL-6-induced activation of STAT3 in macrophages. FEBS Lett *463*, 365-370.

Boehm, U., Klamp, T., Groot, M., and Howard, J.C. (1997). Cellular responses to interferon-gamma. Annu Rev Immunol *15*, 749-795.

Bohn, E., and Autenrieth, I.B. (1996). IL-12 is essential for resistance against Yersinia enterocolitica by triggering IFN-gamma production in NK cells and CD4+ T cells. J Immunol *156*, 1458-1468.

Bohn, E., Schmitt, E., Bielfeldt, C., Noll, A., Schulte, R., and Autenrieth, I.B. (1998). Ambiguous role of interleukin-12 in Yersinia enterocolitica infection in susceptible and resistant mouse strains. Infect Immun *66*, 2213-2220.

Boland, A., and Cornelis, G.R. (1998). Role of YopP in suppression of tumor necrosis factor alpha release by macrophages during Yersinia infection. Infect Immun *66*, 1878-1884.

Boland, A., Sory, M.P., Iriarte, M., Kerbourch, C., Wattiau, P., and Cornelis, G.R. (1996). Status of YopM and YopN in the Yersinia Yop virulon: YopM of Y.enterocolitica is internalized inside the cytosol of PU5-1.8 macrophages by the YopB, D, N delivery apparatus. EMBO J *15*, 5191-5201.

Bonshtien, A., Lev, A., Gibly, A., Debbie, P., Avni, A., and Sessa, G. (2005). Molecular properties of the Xanthomonas AvrRxv effector and global transcriptional changes determined by its expression in resistant tomato plants. Mol Plant Microbe Interact *18*, 300-310.

Bottone, E.J. (1997). Yersinia enterocolitica: the charisma continues. Clin Microbiol Rev *10*, 257-276.

Briheim, G., Follin, P., Sandstedt, S., and Dahlgren, C. (1989). Relationship between intracellularly and extracellularly generated oxygen metabolites from primed polymorphonuclear leukocytes differs from that obtained from nonprimed cells. Inflammation *13*, 455-464.

Brodsky, I.E., Palm, N.W., Sadanand, S., Ryndak, M.B., Sutterwala, F.S., Flavell, R.A., Bliska, J.B., and Medzhitov, R. A Yersinia effector protein promotes virulence by preventing inflammasome recognition of the type III secretion system. Cell Host Microbe *7*, 376-387.

Brown, G.E., Stewart, M.Q., Bissonnette, S.A., Elia, A.E., Wilker, E., and Yaffe, M.B. (2004). Distinct ligand-dependent roles for p38 MAPK in priming and activation of the neutrophil NADPH oxidase. J Biol Chem *279*, 27059-27068.

Brubaker, R.R. (1991). Factors promoting acute and chronic diseases caused by yersiniae. Clin Microbiol Rev *4*, 309-324.

Brubaker, R.R. (2003). Interleukin-10 and inhibition of innate immunity to Yersiniae: roles of Yops and LcrV (V antigen). Infect Immun *71*, 3673-3681.

Brummelkamp, T.R., Nijman, S.M., Dirac, A.M., and Bernards, R. (2003). Loss of the cylindromatosis tumour suppressor inhibits apoptosis by activating NF-kappaB. Nature *424*, 797-801.

Buchmeier, N.A., and Schreiber, R.D. (1985). Requirement of endogenous interferon-gamma production for resolution of Listeria monocytogenes infection. Proc Natl Acad Sci U S A *82*, 7404-7408.

Caamano, J.H., Rizzo, C.A., Durham, S.K., Barton, D.S., Raventos-Suarez, C., Snapper, C.M., and Bravo, R. (1998). Nuclear factor (NF)-kappa B2 (p100/p52) is required for normal splenic microarchitecture and B cell-mediated immune responses. J Exp Med *187*, 185-196.

Carniel, E. (2001). The Yersinia high-pathogenicity island: an iron-uptake island. Microbes Infect *3*, 561-569.

Chen, F., Sugiura, Y., Myers, K.G., Liu, Y., and Lin, W. Ubiquitin carboxyl-terminal hydrolase L1 is required for maintaining the structure and function of the neuromuscular junction. Proc Natl Acad Sci U S A *107*, 1636-1641.

Chen, F.E., Huang, D.B., Chen, Y.Q., and Ghosh, G. (1998). Crystal structure of p50/p65 heterodimer of transcription factor NF-kappaB bound to DNA. Nature *391*, 410-413.

Chen, Z.J. (2005). Ubiquitin signalling in the NF-kappaB pathway. Nat Cell Biol *7*, 758-765.

Cho, S.S., Bacon, C.M., Sudarshan, C., Rees, R.C., Finbloom, D., Pine, R., and O'Shea, J.J. (1996). Activation of STAT4 by IL-12 and IFN-alpha: evidence for the involvement of ligand-induced tyrosine and serine phosphorylation. J Immunol *157*, 4781-4789.

Chua, A.O., Chizzonite, R., Desai, B.B., Truitt, T.P., Nunes, P., Minetti, L.J., Warrier, R.R., Presky, D.H., Levine, J.F., Gately, M.K., and et al. (1994). Expression cloning of a human IL-12 receptor component. A new member of the cytokine receptor superfamily with strong homology to gp130. J Immunol *153*, 128-136.

Clark, M.A., Hirst, B.H., and Jepson, M.A. (1998). M-cell surface beta1 integrin expression and invasin-mediated targeting of Yersinia pseudotuberculosis to mouse Peyer's patch M cells. Infect Immun *66*, 1237-1243.

Comalada, M., Xaus, J., Valledor, A.F., Lopez-Lopez, C., Pennington, D.J., and Celada, A. (2003). PKC epsilon is involved in JNK activation that mediates LPS-induced TNF-alpha, which induces apoptosis in macrophages. Am J Physiol Cell Physiol *285*, C1235-1245.

Cornelis, G.R. (2002). The Yersinia Ysc-Yop 'type III' weaponry. Nat Rev Mol Cell Biol *3*, 742-752.

Cornelis, G.R., Biot, T., Lambert de Rouvroit, C., Michiels, T., Mulder, B., Sluiters, C., Sory, M.P., Van Bouchaute, M., and Vanooteghem, J.C. (1989). The Yersinia yop regulon. Mol Microbiol *3*, 1455-1459.

Cui, Y.D., Inanami, O., Yamamori, T., Niwa, K., Nagahata, H., and Kuwabara, M. (2000). FMLP-induced formation of F-actin in HL60 cells is dependent on PI3-K but not on intracellular Ca2+, PKC, ERK or p38 MAPK. Inflamm Res *49*, 684-691.

Das, M., Sabio, G., Jiang, F., Rincon, M., Flavell, R.A., and Davis, R.J. (2009). Induction of hepatitis by JNK-mediated expression of TNF-alpha. Cell *136*, 249-260.

Denecker, G., Declercq, W., Geuijen, C.A., Boland, A., Benabdillah, R., van Gurp, M., Sory, M.P., Vandenabeele, P., and Cornelis, G.R. (2001). Yersinia enterocolitica YopP-induced apoptosis of macrophages involves the apoptotic signaling cascade upstream of bid. J Biol Chem *276*, 19706-19714.

Denecker, G., Totemeyer, S., Mota, L.J., Troisfontaines, P., Lambermont, I., Youta, C., Stainier, I., Ackermann, M., and Cornelis, G.R. (2002). Effect of low- and high-virulence Yersinia enterocolitica strains on the inflammatory response of human umbilical vein endothelial cells. Infect Immun *70*, 3510-3520.

Depaolo, R.W., Tang, F., Kim, I., Han, M., Levin, N., Ciletti, N., Lin, A., Anderson, D., Schneewind, O., and Jabri, B. (2008). Toll-like receptor 6 drives differentiation of tolerogenic dendritic cells and contributes to LcrV-mediated plague pathogenesis. Cell Host Microbe *4*, 350-361.

Dessein, R., Gironella, M., Vignal, C., Peyrin-Biroulet, L., Sokol, H., Secher, T., Lacas-Gervais, S., Gratadoux, J.J., Lafont, F., Dagorn, J.C*., et al.* (2009). Toll-like receptor 2 is critical for induction of Reg3 beta expression and intestinal clearance of Yersinia pseudotuberculosis. Gut *58*, 771-776.

Deuretzbacher, A., Czymmeck, N., Reimer, R., Trulzsch, K., Gaus, K., Hohenberg, H., Heesemann, J., Aepfelbacher, M., and Ruckdeschel, K. (2009). Beta1 integrin-dependent engulfment of Yersinia enterocolitica by macrophages is coupled to the activation of autophagy and suppressed by type III protein secretion. J Immunol *183*, 5847-5860.

Dobreva, Z.G., Stanilova, S.A., and Miteva, L.D. (2008). Differences in the inducible gene expression and protein production of IL-12p40, IL-12p70 and IL-23: involvement of p38 and JNK kinase pathways. Cytokine *43*, 76-82.

Dobreva, Z.G., Stanilova, S.A., and Miteva, L.D. (2009). The influence of JNK and P38 MAPK inhibition on IL-12P40 and IL-23 production depending on IL12B promoter polymorphism. Cell Mol Biol Lett *14*, 609-621.

Du, F., and Galan, J.E. (2009). Selective inhibition of type III secretion activated signaling by the Salmonella effector AvrA. PLoS Pathog *5*, e1000595.

Dukuzumuremyi, J.M., Rosqvist, R., Hallberg, B., Akerstrom, B., Wolf-Watz, H., and Schesser, K. (2000). The Yersinia protein kinase A is a host factor inducible RhoA/Rac-binding virulence factor. J Biol Chem *275*, 35281-35290.

Dumont, J.E., Pecasse, F., and Maenhaut, C. (2001). Crosstalk and specificity in signalling. Are we crosstalking ourselves into general confusion? Cell Signal *13*, 457-463.

Ea, C.K., Deng, L., Xia, Z.P., Pineda, G., and Chen, Z.J. (2006). Activation of IKK by TNFalpha requires site-specific ubiquitination of RIP1 and polyubiquitin binding by NEMO. Mol Cell *22*, 245-257.

Edman, D.C., Pollock, M.B., and Hall, E.R. (1968). Listeria monocytogenes L forms. I. Induction maintenance, and biological characteristics. J Bacteriol *96*, 352-357.

Edwards, J.P., Zhang, X., Frauwirth, K.A., and Mosser, D.M. (2006). Biochemical and functional characterization of three activated macrophage populations. J Leukoc Biol *80*, 1298-1307.

El Benna, J., Faust, R.P., Johnson, J.L., and Babior, B.M. (1996a). Phosphorylation of the respiratory burst oxidase subunit p47phox as determined by two-dimensional phosphopeptide mapping. Phosphorylation by protein kinase C, protein kinase A, and a mitogen-activated protein kinase. J Biol Chem *271*, 6374-6378.

El Benna, J., Han, J., Park, J.W., Schmid, E., Ulevitch, R.J., and Babior, B.M. (1996b). Activation of p38 in stimulated human neutrophils: phosphorylation of the oxidase component p47phox by p38 and ERK but not by JNK. Arch Biochem Biophys *334*, 395-400.

Falkow, S., Isberg, R.R., and Portnoy, D.A. (1992). The interaction of bacteria with mammalian cells. Annu Rev Cell Biol *8*, 333-363.

Fallman, M., Andersson, K., Hakansson, S., Magnusson, K.E., Stendahl, O., and Wolf-Watz, H. (1995). Yersinia pseudotuberculosis inhibits Fc receptor-mediated phagocytosis in J774 cells. Infect Immun *63*, 3117-3124.

Fallman, M., Deleuil, F., and McGee, K. (2002). Resistance to phagocytosis by Yersinia. Int J Med Microbiol *291*, 501-509.

Fehr, D., Casanova, C., Liverman, A., Blazkova, H., Orth, K., Dobbelaere, D., Frey, J., and Burr, S.E. (2006). AopP, a type III effector protein of Aeromonas salmonicida, inhibits the NF-kappaB signalling pathway. Microbiology *152*, 2809-2818.

Feng, S., Chen, J.K., Yu, H., Simon, J.A., and Schreiber, S.L. (1994). Two binding orientations for peptides to the Src SH3 domain: development of a general model for SH3-ligand interactions. Science *266*, 1241-1247.

Franzoso, G., Carlson, L., Poljak, L., Shores, E.W., Epstein, S., Leonardi, A., Grinberg, A., Tran, T., Scharton-Kersten, T., Anver, M.*, et al.* (1998). Mice deficient in nuclear factor (NF)-kappa B/p52 present with defects in humoral responses, germinal center reactions, and splenic microarchitecture. J Exp Med *187*, 147-159.

Freitas, M., Lima, J.L., and Fernandes, E. (2009). Optical probes for detection and quantification of neutrophils' oxidative burst. A review. Anal Chim Acta *649*, 8-23.

Friedman, C.S., O'Donnell, M.A., Legarda-Addison, D., Ng, A., Cardenas, W.B., Yount, J.S., Moran, T.M., Basler, C.F., Komuro, A., Horvath, C.M.*, et al.* (2008). The tumour suppressor CYLD is a negative regulator of RIG-I-mediated antiviral response. EMBO Rep *9*, 930-936.

Fueller, F., and Schmidt, G. (2008). The polybasic region of Rho GTPases defines the cleavage by Yersinia enterocolitica outer protein T (YopT). Protein Sci *17*, 1456-1462.

Gao, J., Huo, L., Sun, X., Liu, M., Li, D., Dong, J.T., and Zhou, J. (2008). The tumor suppressor CYLD regulates microtubule dynamics and plays a role in cell migration. J Biol Chem *283*, 8802-8809.

Gao, Y.J., Zhang, L., Samad, O.A., Suter, M.R., Yasuhiko, K., Xu, Z.Z., Park, J.Y., Lind, A.L., Ma, Q., and Ji, R.R. (2009). JNK-induced MCP-1 production in spinal cord astrocytes contributes to central sensitization and neuropathic pain. J Neurosci *29*, 4096-4108.

Gemski, P., Lazere, J.R., Casey, T., and Wohlhieter, J.A. (1980). Presence of a virulence-associated plasmid in Yersinia pseudotuberculosis. Infect Immun *28*, 1044-1047.

Geng, J.G. (2001). Directional migration of leukocytes: their pathological roles in inflammation and strategies for development of anti-inflammatory therapies. Cell Res *11*, 85-88.

Genovese, F., Mancuso, G., Cuzzola, M., Biondo, C., Beninati, C., Delfino, D., and Teti, G. (1999). Role of IL-10 in a neonatal mouse listeriosis model. J Immunol *163*, 2777-2782.

Ghosh, S., and Karin, M. (2002). Missing pieces in the NF-kappaB puzzle. Cell *109 Suppl*, S81-96.

Gilmore, T.D., and Herscovitch, M. (2006). Inhibitors of NF-kappaB signaling: 785 and counting. Oncogene *25*, 6887-6899.

Goh, K.C., Haque, S.J., and Williams, B.R. (1999). p38 MAP kinase is required for STAT1 serine phosphorylation and transcriptional activation induced by interferons. EMBO J *18*, 5601-5608.

Gong, B., and Leznik, E. (2007). The role of ubiquitin C-terminal hydrolase L1 in neurodegenerative disorders. Drug News Perspect *20*, 365-370.

Gordon, A.H., and Hart, P.D. (1994). Stimulation or inhibition of the respiratory burst in cultured macrophages in a mycobacterium model: initial stimulation is followed by inhibition after phagocytosis. Infect Immun *62*, 4650-4651.

Green, S.P., Hartland, E.L., Robins-Browne, R.M., and Phillips, W.A. (1995). Role of YopH in the suppression of tyrosine phosphorylation and respiratory burst activity in murine macrophages infected with Yersinia enterocolitica. J Leukoc Biol *57*, 972-977.

Grosdent, N., Maridonneau-Parini, I., Sory, M.P., and Cornelis, G.R. (2002). Role of Yops and adhesins in resistance of Yersinia enterocolitica to phagocytosis. Infect Immun *70*, 4165-4176.

Groves, E., Rittinger, K., Amstutz, M., Berry, S., Holden, D.W., Cornelis, G.R., and Caron, E. Sequestering of Rac by the Yersinia effector YopO blocks Fcgamma receptor-mediated phagocytosis. J Biol Chem *285*, 4087-4098.

Guan, K.L., and Dixon, J.E. (1990). Protein tyrosine phosphatase activity of an essential virulence determinant in Yersinia. Science *249*, 553-556.

Guler, M.L., Gorham, J.D., Hsieh, C.S., Mackey, A.J., Steen, R.G., Dietrich, W.F., and Murphy, K.M. (1996). Genetic susceptibility to Leishmania: IL-12 responsiveness in TH1 cell development. Science *271*, 984-987.

Gustavsson, A., Armulik, A., Brakebusch, C., Fassler, R., Johansson, S., and Fallman, M. (2002). Role of the beta1-integrin cytoplasmic tail in mediating invasin-promoted internalization of Yersinia. J Cell Sci *115*, 2669-2678.

Haase, R., Richter, K., Pfaffinger, G., Courtois, G., and Ruckdeschel, K. (2005). Yersinia outer protein P suppresses TGF-beta-activated kinase-1 activity to impair innate immune signaling in Yersinia enterocolitica-infected cells. J Immunol *175*, 8209-8217.

Hacker, H., Redecke, V., Blagoev, B., Kratchmarova, I., Hsu, L.C., Wang, G.G., Kamps, M.P., Raz, E., Wagner, H., Hacker, G.*, et al.* (2006). Specificity in Toll-like receptor signalling through distinct effector functions of TRAF3 and TRAF6. Nature *439*, 204-207.

Haglund, K., Di Fiore, P.P., and Dikic, I. (2003). Distinct monoubiquitin signals in receptor endocytosis. Trends Biochem Sci *28*, 598-603.

Hakansson, S., Schesser, K., Persson, C., Galyov, E.E., Rosqvist, R., Homble, F., and Wolf-Watz, H. (1996). The YopB protein of Yersinia pseudotuberculosis is essential for the translocation of Yop effector proteins across the target cell plasma membrane and displays a contact-dependent membrane disrupting activity. EMBO J *15*, 5812-5823.

Hamid, N., Gustavsson, A., Andersson, K., McGee, K., Persson, C., Rudd, C.E., and Fallman, M. (1999). YopH dephosphorylates Cas and Fyn-binding protein in macrophages. Microb Pathog *27*, 231-242.

Hamrick, T.S., Havell, E.A., Horton, J.R., and Orndorff, P.E. (2000). Host and bacterial factors involved in the innate ability of mouse macrophages to eliminate internalized unopsonized Escherichia coli. Infect Immun *68*, 125-132.

Han, J., Lee, J.D., Bibbs, L., and Ulevitch, R.J. (1994). A MAP kinase targeted by endotoxin and hyperosmolarity in mammalian cells. Science *265*, 808-811.

Hanski, C., Kutschka, U., Schmoranzer, H.P., Naumann, M., Stallmach, A., Hahn, H., Menge, H., and Riecken, E.O. (1989). Immunohistochemical and electron microscopic study of interaction of Yersinia enterocolitica serotype O8 with intestinal mucosa during experimental enteritis. Infect Immun *57*, 673-678.

Hartland, E.L., Green, S.P., Phillips, W.A., and Robins-Browne, R.M. (1994). Essential role of YopD in inhibition of the respiratory burst of macrophages by Yersinia enterocolitica. Infect Immun *62*, 4445-4453.

Hayden, M.S., and Ghosh, S. (2004). Signaling to NF-kappaB. Genes Dev *18*, 2195-2224.

Heesemann, J., Gross, U., Schmidt, N., and Laufs, R. (1986). Immunochemical analysis of plasmid-encoded proteins released by enteropathogenic Yersinia sp. grown in calcium-deficient media. Infect Immun *54*, 561-567.

Heesemann, J., and Laufs, R. (1983). Construction of a mobilizable Yersinia enterocolitica virulence plasmid. J Bacteriol *155*, 761-767.

Heesemann, J., Sing, A., and Trulzsch, K. (2006). Yersinia's stratagem: targeting innate and adaptive immune defense. Curr Opin Microbiol *9*, 55-61.

Hein, J., Sing, A., Di Genaro, M.S., and Autenrieth, I.B. (2001). Interleukin-12 and interleukin-18 are indispensable for protective immunity against enteropathogenic Yersinia. Microb Pathog *31*, 195-199.

Hellerbrand, C., Bumes, E., Bataille, F., Dietmaier, W., Massoumi, R., and Bosserhoff, A.K. (2007). Reduced expression of CYLD in human colon and hepatocellular carcinomas. Carcinogenesis *28*, 21-27.

Hem, A., Smith, A.J., and Solberg, P. (1998). Saphenous vein puncture for blood sampling of the mouse, rat, hamster, gerbil, guinea pig, ferret and mink. Lab Anim *32*, 364-368.

Hentschke, M., Trulzsch, K., Heesemann, J., Aepfelbacher, M., and Ruckdeschel, K. (2007). Serogroup-related escape of Yersinia enterocolitica YopE from degradation by the ubiquitin-proteasome pathway. Infect Immun *75*, 4423-4431.

Hershko, A., and Ciechanover, A. (1998). The ubiquitin system. Annu Rev Biochem *67*, 425-479.

Hicke, L., and Dunn, R. (2003). Regulation of membrane protein transport by ubiquitin and ubiquitin-binding proteins. Annu Rev Cell Dev Biol *19*, 141-172.

Hicke, L., Schubert, H.L., and Hill, C.P. (2005). Ubiquitin-binding domains. Nat Rev Mol Cell Biol *6*, 610-621.

Hicks, S.W., and Galan, J.E. Hijacking the host ubiquitin pathway: structural strategies of bacterial E3 ubiquitin ligases. Curr Opin Microbiol *13*, 41-46.

Hinz, M., Stilmann, M., Arslan, S.C., Khanna, K.K., Dittmar, G., and Scheidereit, C. A cytoplasmic ATM-TRAF6-cIAP1 module links nuclear DNA damage signaling to ubiquitin-mediated NF-kappaB activation. Mol Cell *40*, 63-74.

Hochstrasser, M. (1995). Ubiquitin, proteasomes, and the regulation of intracellular protein degradation. Curr Opin Cell Biol *7*, 215-223.

Hoffmeyer, A., Grosse-Wilde, A., Flory, E., Neufeld, B., Kunz, M., Rapp, U.R., and Ludwig, S. (1999). Different mitogen-activated protein kinase signaling pathways cooperate to regulate tumor necrosis factor alpha gene expression in T lymphocytes. J Biol Chem *274*, 4319-4327.

Hoiseth, S.K., and Stocker, B.A. (1981). Aromatic-dependent Salmonella typhimurium are non-virulent and effective as live vaccines. Nature *291*, 238-239.

Holmstrom, A., Petterson, J., Rosqvist, R., Hakansson, S., Tafazoli, F., Fallman, M., Magnusson, K.E., Wolf-Watz, H., and Forsberg, A. (1997). YopK of Yersinia pseudotuberculosis controls translocation of Yop effectors across the eukaryotic cell membrane. Mol Microbiol *24*, 73-91.

Hoover, D.L., and Nacy, C.A. (1984). Macrophage activation to kill Leishmania tropica: defective intracellular killing of amastigotes by macrophages elicited with sterile inflammatory agents. J Immunol *132*, 1487-1493.

Hotson, A., and Mudgett, M.B. (2004). Cysteine proteases in phytopathogenic bacteria: identification of plant targets and activation of innate immunity. Curr Opin Plant Biol *7*, 384-390.

Hovelmeyer, N., Wunderlich, F.T., Massoumi, R., Jakobsen, C.G., Song, J., Worns, M.A., Merkwirth, C., Kovalenko, A., Aumailley, M., Strand, D.*, et al.* (2007). Regulation of B cell homeostasis and activation by the tumor suppressor gene CYLD. J Exp Med *204*, 2615-2627.

Huang, G., Shi, L.Z., and Chi, H. (2009). Regulation of JNK and p38 MAPK in the immune system: signal integration, propagation and termination. Cytokine *48*, 161-169.

Hueck, C.J. (1998). Type III protein secretion systems in bacterial pathogens of animals and plants. Microbiol Mol Biol Rev *62*, 379-433.

Hui, L., Bakiri, L., Stepniak, E., and Wagner, E.F. (2007). p38alpha: a suppressor of cell proliferation and tumorigenesis. Cell Cycle *6*, 2429-2433.

Inohara, N., Ogura, Y., and Nunez, G. (2002). Nods: a family of cytosolic proteins that regulate the host response to pathogens. Curr Opin Microbiol *5*, 76-80.

Isberg, R.R., Hamburger, Z., and Dersch, P. (2000). Signaling and invasin-promoted uptake via integrin receptors. Microbes Infect *2*, 793-801.

Isberg, R.R., and Leong, J.M. (1990). Multiple beta 1 chain integrins are receptors for invasin, a protein that promotes bacterial penetration into mammalian cells. Cell *60*, 861-871.

Jacobson, N.G., Szabo, S.J., Weber-Nordt, R.M., Zhong, Z., Schreiber, R.D., Darnell, J.E., Jr., and Murphy, K.M. (1995). Interleukin 12 signaling in T helper type 1 (Th1) cells involves tyrosine phosphorylation of signal transducer and activator of transcription (Stat)3 and Stat4. J Exp Med *181*, 1755-1762.

Janot, L., Secher, T., Torres, D., Maillet, I., Pfeilschifter, J., Quesniaux, V.F., Landmann, R., Ryffel, B., and Erard, F. (2008). CD14 works with toll-like receptor 2 to contribute to recognition and control of Listeria monocytogenes infection. J Infect Dis *198*, 115-124.

Jin, W., Chang, M., Paul, E.M., Babu, G., Lee, A.J., Reiley, W., Wright, A., Zhang, M., You, J., and Sun, S.C. (2008). Deubiquitinating enzyme CYLD negatively regulates RANK signaling and osteoclastogenesis in mice. J Clin Invest *118*, 1858-1866.

Jin, W., Reiley, W.R., Lee, A.J., Wright, A., Wu, X., Zhang, M., and Sun, S.C. (2007). Deubiquitinating enzyme CYLD regulates the peripheral development and naive phenotype maintenance of B cells. J Biol Chem *282*, 15884-15893.

Johnson, G.L., and Lapadat, R. (2002). Mitogen-activated protein kinase pathways mediated by ERK, JNK, and p38 protein kinases. Science *298*, 1911-1912.

Johnston, R.B., Jr., Lehmeyer, J.E., and Guthrie, L.A. (1976). Generation of superoxide anion and chemiluminescence by human monocytes during phagocytosis and on contact with surface-bound immunoglobulin G. J Exp Med *143*, 1551-1556.

Jones, R.M., Wu, H., Wentworth, C., Luo, L., Collier-Hyams, L., and Neish, A.S. (2008). Salmonella AvrA Coordinates Suppression of Host Immune and Apoptotic Defenses via JNK Pathway Blockade. Cell Host Microbe *3*, 233-244.

Kampik, D., Schulte, R., and Autenrieth, I.B. (2000). Yersinia enterocolitica invasin protein triggers differential production of interleukin-1, interleukin-8, monocyte chemoattractant protein 1, granulocyte-macrophage colony-stimulating factor, and tumor necrosis factor alpha in epithelial cells: implications for understanding the early cytokine network in Yersinia infections. Infect Immun *68*, 2484-2492.

Keats, J.J., Fonseca, R., Chesi, M., Schop, R., Baker, A., Chng, W.J., Van Wier, S., Tiedemann, R., Shi, C.X., Sebag, M.*, et al.* (2007). Promiscuous mutations activate the noncanonical NF-kappaB pathway in multiple myeloma. Cancer Cell *12*, 131-144.

Kikuchi, H., Fujinawa, T., Kuribayashi, F., Nakanishi, A., Imajoh-Ohmi, S., Goto, M., and Kanegasaki, S. (1994). Induction of essential components of the superoxide generating system in human monoblastic leukemia U937 cells. J Biochem *116*, 742-746.

Kim, L., Del Rio, L., Butcher, B.A., Mogensen, T.H., Paludan, S.R., Flavell, R.A., and Denkers, E.Y. (2005). p38 MAPK autophosphorylation drives macrophage IL-12 production during intracellular infection. J Immunol *174*, 4178-4184.

Koga, H., Terasawa, H., Nunoi, H., Takeshige, K., Inagaki, F., and Sumimoto, H. (1999). Tetratricopeptide repeat (TPR) motifs of p67(phox) participate in interaction with the small GTPase Rac and activation of the phagocyte NADPH oxidase. J Biol Chem *274*, 25051-25060.

Koornhof, H.J., Smego, R.A., Jr., and Nicol, M. (1999). Yersiniosis. II: The pathogenesis of Yersinia infections. Eur J Clin Microbiol Infect Dis *18*, 87-112.

Kovalenko, A., Chable-Bessia, C., Cantarella, G., Israel, A., Wallach, D., and Courtois, G. (2003). The tumour suppressor CYLD negatively regulates NF-kappaB signalling by deubiquitination. Nature *424*, 801-805.

Kovarik, P., Stoiber, D., Eyers, P.A., Menghini, R., Neininger, A., Gaestel, M., Cohen, P., and Decker, T. (1999). Stress-induced phosphorylation of STAT1 at Ser727 requires p38 mitogen-activated protein kinase whereas IFN-gamma uses a different signaling pathway. Proc Natl Acad Sci U S A *96*, 13956-13961.

Krump, E., Sanghera, J.S., Pelech, S.L., Furuya, W., and Grinstein, S. (1997). Chemotactic peptide N-formyl-met-leu-phe activation of p38 mitogen-activated protein kinase (MAPK) and MAPK-activated protein kinase-2 in human neutrophils. J Biol Chem *272*, 937-944.

Kuhnert, P., Hacker, J., Muhldorfer, I., Burnens, A.P., Nicolet, J., and Frey, J. (1997). Detection system for Escherichia coli-specific virulence genes: absence of virulence determinants in B and C strains. Appl Environ Microbiol *63*, 703-709.

Kuribayashi, F., Nunoi, H., Wakamatsu, K., Tsunawaki, S., Sato, K., Ito, T., and Sumimoto, H. (2002). The adaptor protein p40(phox) as a positive regulator of the superoxide-producing phagocyte oxidase. EMBO J *21*, 6312-6320.

Kyriakis, J.M., and Avruch, J. (2001). Mammalian mitogen-activated protein kinase signal transduction pathways activated by stress and inflammation. Physiol Rev *81*, 807-869.

Lal, A.S., Clifton, A.D., Rouse, J., Segal, A.W., and Cohen, P. (1999). Activation of the neutrophil NADPH oxidase is inhibited by SB 203580, a specific inhibitor of SAPK2/p38. Biochem Biophys Res Commun *259*, 465-470.

Laroux, F.S., Romero, X., Wetzler, L., Engel, P., and Terhorst, C. (2005). Cutting edge: MyD88 controls phagocyte NADPH oxidase function and killing of gram-negative bacteria. J Immunol *175*, 5596-5600.

Laskowski-Arce, M.A., and Orth, K. (2007). The elusive activity of the Yersinia protein kinase A kinase domain is revealed. Trends Microbiol *15*, 437-440.

Lawrence, T., Bebien, M., Liu, G.Y., Nizet, V., and Karin, M. (2005). IKKalpha limits macrophage NF-kappaB activation and contributes to the resolution of inflammation. Nature *434*, 1138-1143.

Lax, A.J., and Thomas, W. (2002). How bacteria could cause cancer: one step at a time. Trends Microbiol *10*, 293-299.

Le Negrate, G., Faustin, B., Welsh, K., Loeffler, M., Krajewska, M., Hasegawa, P., Mukherjee, S., Orth, K., Krajewski, S., Godzik, A*., et al.* (2008). Salmonella secreted factor L deubiquitinase of Salmonella typhimurium inhibits NF-kappaB, suppresses IkappaBalpha ubiquitination and modulates innate immune responses. J Immunol *180*, 5045-5056.

Lee, J.C., Prabhakar, U., Griswold, D.E., Dunnington, D., Young, P.R., and Badger, A. (1994). Low-molecular-weight TNF biosynthesis inhibitors: strategies and prospectives. Circ Shock *44*, 97-103.

Lee, M.S., and Kim, Y.J. (2007). Signaling pathways downstream of pattern-recognition receptors and their cross talk. Annu Rev Biochem *76*, 447-480.

Lenardo, M., Pierce, J.W., and Baltimore, D. (1987). Protein-binding sites in Ig gene enhancers determine transcriptional activity and inducibility. Science *236*, 1573-1577.

Li, Q., Van Antwerp, D., Mercurio, F., Lee, K.F., and Verma, I.M. (1999). Severe liver degeneration in mice lacking the IkappaB kinase 2 gene. Science *284*, 321-325.

Lian, C.J., and Pai, C.H. (1985). Inhibition of human neutrophil chemiluminescence by plasmid-mediated outer membrane proteins of Yersinia enterocolitica. Infect Immun *49*, 145-151.

Lim, J.H., Ha, U.H., Woo, C.H., Xu, H., and Li, J.D. (2008). CYLD is a crucial negative regulator of innate immune response in Escherichia coli pneumonia. Cell Microbiol *10*, 2247-2256.

Lim, J.H., Jono, H., Koga, T., Woo, C.H., Ishinaga, H., Bourne, P., Xu, H., Ha, U.H., and Li, J.D. (2007). Tumor suppressor CYLD acts as a negative regulator for non-typeable Haemophilus influenza-induced inflammation in the middle ear and lung of mice. PLoS One *2*, e1032.

Liu, Y.C., Penninger, J., and Karin, M. (2005). Immunity by ubiquitylation: a reversible process of modification. Nat Rev Immunol *5*, 941-952.

Lu, H.T., Yang, D.D., Wysk, M., Gatti, E., Mellman, I., Davis, R.J., and Flavell, R.A. (1999). Defective IL-12 production in mitogen-activated protein (MAP) kinase kinase 3 (Mkk3)-deficient mice. EMBO J *18*, 1845-1857.

Lund, R.J., Chen, Z., Scheinin, J., and Lahesmaa, R. (2004). Early target genes of IL-12 and STAT4 signaling in th cells. J Immunol *172*, 6775-6782.

Luo, Y., and Dorf, M.E. (2001). Isolation of mouse neutrophils. Curr Protoc Immunol *Chapter 3*, Unit 3 20.

Lutz, M.B., Kukutsch, N., Ogilvie, A.L., Rossner, S., Koch, F., Romani, N., and Schuler, G. (1999). An advanced culture method for generating large quantities of highly pure dendritic cells from mouse bone marrow. J Immunol Methods *223*, 77-92.

Ma, W., Gee, K., Lim, W., Chambers, K., Angel, J.B., Kozlowski, M., and Kumar, A. (2004). Dexamethasone inhibits IL-12p40 production in lipopolysaccharide-stimulated human monocytic cells by down-regulating the activity of c-Jun N-terminal kinase, the activation protein-1, and NF-kappa B transcription factors. J Immunol *172*, 318-330.

Ma, X., Chow, J.M., Gri, G., Carra, G., Gerosa, F., Wolf, S.F., Dzialo, R., and Trinchieri, G. (1996). The interleukin 12 p40 gene promoter is primed by interferon gamma in monocytic cells. J Exp Med *183*, 147-157.

MacMicking, J., Xie, Q.W., and Nathan, C. (1997). Nitric oxide and macrophage function. Annu Rev Immunol *15*, 323-350.

Mahoney, D.J., Cheung, H.H., Mrad, R.L., Plenchette, S., Simard, C., Enwere, E., Arora, V., Mak, T.W., Lacasse, E.C., Waring, J., and Korneluk, R.G. (2008). Both cIAP1 and cIAP2 regulate TNFalpha-mediated NF-kappaB activation. Proc Natl Acad Sci U S A *105*, 11778-11783.

Makarova, K.S., Aravind, L., and Koonin, E.V. (2000). A novel superfamily of predicted cysteine proteases from eukaryotes, viruses and Chlamydia pneumoniae. Trends Biochem Sci *25*, 50-52.

Massoumi, R., Chmielarska, K., Hennecke, K., Pfeifer, A., and Fassler, R. (2006). Cyld inhibits tumor cell proliferation by blocking Bcl-3-dependent NF-kappaB signaling. Cell *125*, 665-677.

Massoumi, R., Kuphal, S., Hellerbrand, C., Haas, B., Wild, P., Spruss, T., Pfeifer, A., Fassler, R., and Bosserhoff, A.K. (2009). Down-regulation of CYLD expression by Snail promotes tumor progression in malignant melanoma. J Exp Med *206*, 221-232.

Massoumi, R., and Paus, R. (2007). Cylindromatosis and the CYLD gene: new lessons on the molecular principles of epithelial growth control. Bioessays *29*, 1203-1214.

McCoy, M.W., Marre, M.L., Lesser, C.F., and Mecsas, J. The C-terminal tail of Yersinia pseudotuberculosis YopM is critical for interacting with RSK1 and for virulence. Infect Immun *78*, 2584-2598.

McDonald, C., Vacratsis, P.O., Bliska, J.B., and Dixon, J.E. (2003). The yersinia virulence factor YopM forms a novel protein complex with two cellular kinases. J Biol Chem *278*, 18514-18523.

McLaughlin-Drubin, M.E., and Munger, K. (2008). Viruses associated with human cancer. Biochim Biophys Acta *1782*, 127-150.

McLeish, K.R., Knall, C., Ward, R.A., Gerwins, P., Coxon, P.Y., Klein, J.B., and Johnson, G.L. (1998). Activation of mitogen-activated protein kinase cascades during priming of human neutrophils by TNF-alpha and GM-CSF. J Leukoc Biol *64*, 537-545.

McNamara, D., and El-Omar, E. (2008). Helicobacter pylori infection and the pathogenesis of gastric cancer: a paradigm for host-bacterial interactions. Dig Liver Dis *40*, 504-509.

McPhee, J.B., Mena, P., and Bliska, J.B. Delineation of regions of the Yersinia YopM protein required for interaction with the RSK1 and PRK2 host kinases and their requirement for interleukin-10 production and virulence. Infect Immun *78*, 3529-3539.

Mebius, R.E., and Kraal, G. (2005). Structure and function of the spleen. Nat Rev Immunol *5*, 606-616.

Mittal, R., Peak-Chew, S.Y., and McMahon, H.T. (2006). Acetylation of MEK2 and I kappa B kinase (IKK) activation loop residues by YopJ inhibits signaling. Proc Natl Acad Sci U S A *103*, 18574-18579.

Monnazzi, L.G., Carlos, I.Z., and de Medeiros, B.M. (2004). Influence of Yersinia pseudotuberculosis outer proteins (Yops) on interleukin-12, tumor necrosis factor alpha and nitric oxide production by peritoneal macrophages. Immunol Lett *94*, 91-98.

Morinobu, A., Gadina, M., Strober, W., Visconti, R., Fornace, A., Montagna, C., Feldman, G.M., Nishikomori, R., and O'Shea, J.J. (2002). STAT4 serine phosphorylation is critical for IL-12-induced IFN-gamma production but not for cell proliferation. Proc Natl Acad Sci U S A *99*, 12281-12286.

Mukherjee, S., Hao, Y.H., and Orth, K. (2007). A newly discovered post-translational modification--the acetylation of serine and threonine residues. Trends Biochem Sci *32*, 210-216.

Mukherjee, S., Keitany, G., Li, Y., Wang, Y., Ball, H.L., Goldsmith, E.J., and Orth, K. (2006). Yersinia YopJ acetylates and inhibits kinase activation by blocking phosphorylation. Science *312*, 1211-1214.

Munro, P., Flatau, G., and Lemichez, E. (2007). Bacteria and the ubiquitin pathway. Curr Opin Microbiol *10*, 39-46.

Naeger, L.K., McKinney, J., Salvekar, A., and Hoey, T. (1999). Identification of a STAT4 binding site in the interleukin-12 receptor required for signaling. J Biol Chem *274*, 1875-1878.

Nagy, A., Rossant, J., Nagy, R., Abramow-Newerly, W., and Roder, J.C. (1993). Derivation of completely cell culture-derived mice from early-passage embryonic stem cells. Proc Natl Acad Sci U S A *90*, 8424-8428.

Nakanishi, A., Imajoh-Ohmi, S., Fujinawa, T., Kikuchi, H., and Kanegasaki, S. (1992). Direct evidence for interaction between COOH-terminal regions of cytochrome b558 subunits and cytosolic 47-kDa protein during activation of an O(2-)-generating system in neutrophils. J Biol Chem *267*, 19072-19074.

Nakayama, K., Furusu, A., Xu, Q., Konta, T., and Kitamura, M. (2001). Unexpected transcriptional induction of monocyte chemoattractant protein 1 by proteasome inhibition: involvement of the c-Jun N-terminal kinase-activator protein 1 pathway. J Immunol *167*, 1145-1150.

Navarro, L., Alto, N.M., and Dixon, J.E. (2005). Functions of the Yersinia effector proteins in inhibiting host immune responses. Curr Opin Microbiol *8*, 21-27.

Navarro, L., Koller, A., Nordfelth, R., Wolf-Watz, H., Taylor, S., and Dixon, J.E. (2007). Identification of a molecular target for the Yersinia protein kinase A. Mol Cell *26*, 465-477.

Netea, M.G., Kullberg, B.J., and Van der Meer, J.W. (2004). Proinflammatory cytokines in the treatment of bacterial and fungal infections. BioDrugs *18*, 9-22.

Neyt, C., and Cornelis, G.R. (1999). Insertion of a Yop translocation pore into the macrophage plasma membrane by Yersinia enterocolitica: requirement for translocators YopB and YopD, but not LcrG. Mol Microbiol *33*, 971-981.

Nick, J.A., Avdi, N.J., Gerwins, P., Johnson, G.L., and Worthen, G.S. (1996). Activation of a p38 mitogen-activated protein kinase in human neutrophils by lipopolysaccharide. J Immunol *156*, 4867-4875.

Nick, J.A., Avdi, N.J., Young, S.K., Knall, C., Gerwins, P., Johnson, G.L., and Worthen, G.S. (1997). Common and distinct intracellular signaling pathways in human neutrophils utilized by platelet activating factor and FMLP. J Clin Invest *99*, 975-986.

Nijman, S.M., Luna-Vargas, M.P., Velds, A., Brummelkamp, T.R., Dirac, A.M., Sixma, T.K., and Bernards, R. (2005). A genomic and functional inventory of deubiquitinating enzymes. Cell *123*, 773-786.

Nishida, E., and Gotoh, Y. (1993). The MAP kinase cascade is essential for diverse signal transduction pathways. Trends Biochem Sci *18*, 128-131.

Nishikori, M., Ohno, H., Haga, H., and Uchiyama, T. (2005). Stimulation of CD30 in anaplastic large cell lymphoma leads to production of nuclear factor-kappaB p52, which is associated with hyperphosphorylated Bcl-3. Cancer Sci *96*, 487-497.

O'Neill, L. (2000). The Toll/interleukin-1 receptor domain: a molecular switch for inflammation and host defence. Biochem Soc Trans *28*, 557-563.

Offermanns, S., Toombs, C.F., Hu, Y.H., and Simon, M.I. (1997). Defective platelet activation in G alpha(q)-deficient mice. Nature *389*, 183-186.

Oganesyan, G., Saha, S.K., Guo, B., He, J.Q., Shahangian, A., Zarnegar, B., Perry, A., and Cheng, G. (2006). Critical role of TRAF3 in the Toll-like receptor-dependent and -independent antiviral response. Nature *439*, 208-211.

Orth, K., Palmer, L.E., Bao, Z.Q., Stewart, S., Rudolph, A.E., Bliska, J.B., and Dixon, J.E. (1999). Inhibition of the mitogen-activated protein kinase kinase superfamily by a Yersinia effector. Science *285*, 1920-1923.

Palmer, L.E., Hobbie, S., Galan, J.E., and Bliska, J.B. (1998). YopJ of Yersinia pseudotuberculosis is required for the inhibition of macrophage TNF-alpha production and downregulation of the MAP kinases p38 and JNK. Mol Microbiol *27*, 953-965.

Palmer, L.E., Pancetti, A.R., Greenberg, S., and Bliska, J.B. (1999). YopJ of Yersinia spp. is sufficient to cause downregulation of multiple mitogen-activated protein kinases in eukaryotic cells. Infect Immun *67*, 708-716.

Patel, J.C., Hueffer, K., Lam, T.T., and Galan, J.E. (2009). Diversification of a Salmonella virulence protein function by ubiquitin-dependent differential localization. Cell *137*, 283-294.

Paxian, S., Merkle, H., Riemann, M., Wilda, M., Adler, G., Hameister, H., Liptay, S., Pfeffer, K., and Schmid, R.M. (2002). Abnormal organogenesis of Peyer's patches in mice deficient for NF-kappaB1, NF-kappaB2, and Bcl-3. Gastroenterology *122*, 1853-1868.

Perkins, N.D. (2006). Post-translational modifications regulating the activity and function of the nuclear factor kappa B pathway. Oncogene *25*, 6717-6730.

Perkins, N.D. (2007). Integrating cell-signalling pathways with NF-kappaB and IKK function. Nat Rev Mol Cell Biol *8*, 49-62.

Perkins, N.D., and Gilmore, T.D. (2006). Good cop, bad cop: the different faces of NF-kappaB. Cell Death Differ *13*, 759-772.

Persson, C., Carballeira, N., Wolf-Watz, H., and Fallman, M. (1997). The PTPase YopH inhibits uptake of Yersinia, tyrosine phosphorylation of p130Cas and FAK, and the associated accumulation of these proteins in peripheral focal adhesions. EMBO J *16*, 2307-2318.

Pickart, C.M., and Eddins, M.J. (2004). Ubiquitin: structures, functions, mechanisms. Biochim Biophys Acta *1695*, 55-72.

Presky, D.H., Yang, H., Minetti, L.J., Chua, A.O., Nabavi, N., Wu, C.Y., Gately, M.K., and Gubler, U. (1996). A functional interleukin 12 receptor complex is composed of two beta-type cytokine receptor subunits. Proc Natl Acad Sci U S A *93*, 14002-14007.

Putzker, M., Sauer, H., and Sobe, D. (2001). Plague and other human infections caused by Yersinia species. Clin Lab *47*, 453-466.

Ramsauer, K., Sadzak, I., Porras, A., Pilz, A., Nebreda, A.R., Decker, T., and Kovarik, P. (2002). p38 MAPK enhances STAT1-dependent transcription independently of Ser-727 phosphorylation. Proc Natl Acad Sci U S A *99*, 12859-12864.

Raz, E., Zlokarnik, G., Tsien, R.Y., and Driever, W. (1998). beta-lactamase as a marker for gene expression in live zebrafish embryos. Dev Biol *203*, 290-294.

Regamey, A., Hohl, D., Liu, J.W., Roger, T., Kogerman, P., Toftgard, R., and Huber, M. (2003). The tumor suppressor CYLD interacts with TRIP and regulates negatively nuclear factor kappaB activation by tumor necrosis factor. J Exp Med *198*, 1959-1964.

Reiley, W., Zhang, M., and Sun, S.C. (2004). Negative regulation of JNK signaling by the tumor suppressor CYLD. J Biol Chem *279*, 55161-55167.

Reiley, W.W., Jin, W., Lee, A.J., Wright, A., Wu, X., Tewalt, E.F., Leonard, T.O., Norbury, C.C., Fitzpatrick, L., Zhang, M., and Sun, S.C. (2007). Deubiquitinating enzyme CYLD negatively regulates the ubiquitin-dependent kinase Tak1 and prevents abnormal T cell responses. J Exp Med *204*, 1475-1485.

Reiley, W.W., Zhang, M., Jin, W., Losiewicz, M., Donohue, K.B., Norbury, C.C., and Sun, S.C. (2006). Regulation of T cell development by the deubiquitinating enzyme CYLD. Nat Immunol *7*, 411-417.

Rest, R.F. (1994). Measurement of human neutrophil respiratory burst activity during phagocytosis of bacteria. Methods Enzymol *236*, 119-136.

Roos, D., de Boer, M., Kuribayashi, F., Meischl, C., Weening, R.S., Segal, A.W., Ahlin, A., Nemet, K., Hossle, J.P., Bernatowska-Matuszkiewicz, E., and Middleton-Price, H. (1996). Mutations in the X-linked and autosomal recessive forms of chronic granulomatous disease. Blood *87*, 1663-1681.

Root, R.K., Metcalf, J., Oshino, N., and Chance, B. (1975). H2O2 release from human granulocytes during phagocytosis. I. Documentation, quantitation, and some regulating factors. J Clin Invest *55*, 945-955.

Root, R.K., and Metcalf, J.A. (1977). H2O2 release from human granulocytes during phagocytosis. Relationship to superoxide anion formation and cellular catabolism of H2O2: studies with normal and cytochalasin B-treated cells. J Clin Invest *60*, 1266-1279.

Roppenser, B. ,Roder, A. ,Hentschke, M. ,Ruckdeschel, K. ,Aepfelbacher, M. (2009). Yersinia enterocolitica differentially modulates RhoG activity in host cells. J Cell Sci *122*, 696-705.

Rosqvist, R., Bolin, I., and Wolf-Watz, H. (1988). Inhibition of phagocytosis in Yersinia pseudotuberculosis: a virulence plasmid-encoded ability involving the Yop2b protein. Infect Immun *56*, 2139-2143.

Rosqvist, R., Forsberg, A., Rimpilainen, M., Bergman, T., and Wolf-Watz, H. (1990). The cytotoxic protein YopE of Yersinia obstructs the primary host defence. Mol Microbiol *4*, 657-667.

Rosqvist, R., Forsberg, A., and Wolf-Watz, H. (1991). Intracellular targeting of the Yersinia YopE cytotoxin in mammalian cells induces actin microfilament disruption. Infect Immun *59*, 4562-4569.

Ruckdeschel, K., Machold, J., Roggenkamp, A., Schubert, S., Pierre, J., Zumbihl, R., Liautard, J.P., Heesemann, J., and Rouot, B. (1997). Yersinia enterocolitica promotes deactivation of

macrophage mitogen-activated protein kinases extracellular signal-regulated kinase-1/2, p38, and c-Jun NH2-terminal kinase. Correlation with its inhibitory effect on tumor necrosis factor-alpha production. J Biol Chem *272*, 15920-15927.

Ruckdeschel, K., Harb, S., Roggenkamp, A., Hornef, M., Zumbihl, R., Kohler, S., Heesemann, J., and Rouot, B. (1998). Yersinia enterocolitica impairs activation of transcription factor NF-kappaB: involvement in the induction of programmed cell death and in the suppression of the macrophage tumor necrosis factor alpha production. J Exp Med *187*, 1069-1079.

Ruckdeschel, K., Pfaffinger, G., Trulzsch, K., Zenner, G., Richter, K., Heesemann, J., and Aepfelbacher, M. (2006). The proteasome pathway destabilizes Yersinia outer protein E and represses its antihost cell activities. J Immunol *176*, 6093-6102.

Ruckdeschel, K., Roggenkamp, A., Schubert, S., and Heesemann, J. (1996). Differential contribution of Yersinia enterocolitica virulence factors to evasion of microbicidal action of neutrophils. Infect Immun *64*, 724-733.

Sakai, A., Koga, T., Lim, J.H., Jono, H., Harada, K., Szymanski, E., Xu, H., Kai, H., and Li, J.D. (2007). The bacterium, nontypeable Haemophilus influenzae, enhances host antiviral response by inducing Toll-like receptor 7 expression: evidence for negative regulation of host anti-viral response by CYLD. FEBS J *274*, 3655-3668.

Sakamoto, K., Kuribayashi, F., Nakamura, M., and Takeshige, K. (2006). Involvement of p38 MAP kinase in not only activation of the phagocyte NADPH oxidase induced by formyl-methionyl-leucyl-phenylalanine but also determination of the extent of the activity. J Biochem *140*, 739-745.

Sakamoto, K., Tominaga, Y., Yamauchi, K., Nakatsu, Y., Sakumi, K., Yoshiyama, K., Egashira, A., Kura, S., Yao, T., Tsuneyoshi, M.*, et al.* (2007). MUTYH-null mice are susceptible to spontaneous and oxidative stress induced intestinal tumorigenesis. Cancer Res *67*, 6599-6604.

Sakharov, P.P., Gudkova, E.I., Polshkova, V.N., and Fudel, T.N. (1961). [Studies on the transformation activity in streptomycin-resistant and pathogenic microbes.]. Biull Eksp Biol Med *52*, 80-84.

Saldeen, J., and Welsh, N. (2004). p38 MAPK inhibits JNK2 and mediates cytokine-activated iNOS induction and apoptosis independently of NF-KB translocation in insulin-producing cells. Eur Cytokine Netw *15*, 47-52.

Salhi, A., Bornholdt, D., Oeffner, F., Malik, S., Heid, E., Happle, R., and Grzeschik, K.H. (2004). Multiple familial trichoepithelioma caused by mutations in the cylindromatosis tumor suppressor gene. Cancer Res *64*, 5113-5117.

Salojin, K., and Oravecz, T. (2007). Regulation of innate immunity by MAPK dual-specificity phosphatases: knockout models reveal new tricks of old genes. J Leukoc Biol *81*, 860-869.

Sauvonnet, N., Lambermont, I., van der Bruggen, P., and Cornelis, G.R. (2002). YopH prevents monocyte chemoattractant protein 1 expression in macrophages and T-cell proliferation through inactivation of the phosphatidylinositol 3-kinase pathway. Mol Microbiol *45*, 805-815.

Sbarra, A.J., Selvaraj, R.J., Paul, B.B., Poskitt, P.K., Zgliczynski, J.M., Mitchell, G.W., Jr., and Louis, F. (1976). Biochemical, functional, and structural aspects of phagocytosis. Int Rev Exp Pathol *16*, 249-271.

Schubert, S., Rakin, A., and Heesemann, J. (2004). The Yersinia high-pathogenicity island (HPI): evolutionary and functional aspects. Int J Med Microbiol *294*, 83-94.

Schulte, R., Wattiau, P., Hartland, E.L., Robins-Browne, R.M., and Cornelis, G.R. (1996). Differential secretion of interleukin-8 by human epithelial cell lines upon entry of virulent or nonvirulent Yersinia enterocolitica. Infect Immun *64*, 2106-2113.

Sen, R., and Baltimore, D. (1986). Inducibility of kappa immunoglobulin enhancer-binding protein Nf-kappa B by a posttranslational mechanism. Cell *47*, 921-928.

Setsukinai, K., Urano, Y., Kakinuma, K., Majima, H.J., and Nagano, T. (2003). Development of novel fluorescence probes that can reliably detect reactive oxygen species and distinguish specific species. J Biol Chem *278*, 3170-3175.

Shao, F., Merritt, P.M., Bao, Z., Innes, R.W., and Dixon, J.E. (2002). A Yersinia effector and a Pseudomonas avirulence protein define a family of cysteine proteases functioning in bacterial pathogenesis. Cell *109*, 575-588.

Siebers, A., and Finlay, B.B. (1996). M cells and the pathogenesis of mucosal and systemic infections. Trends Microbiol *4*, 22-29.

Simonet, M., Richard, S., and Berche, P. (1990). Electron microscopic evidence for in vivo extracellular localization of Yersinia pseudotuberculosis harboring the pYV plasmid. Infect Immun *58*, 841-845.

Sing, A., Rost, D., Tvardovskaia, N., Roggenkamp, A., Wiedemann, A., Kirschning, C.J., Aepfelbacher, M., and Heesemann, J. (2002). Yersinia V-antigen exploits toll-like receptor 2 and CD14 for interleukin 10-mediated immunosuppression. J Exp Med *196*, 1017-1024.

Singh, A., Zarember, K.A., Kuhns, D.B., and Gallin, J.I. (2009). Impaired priming and activation of the neutrophil NADPH oxidase in patients with IRAK4 or NEMO deficiency. J Immunol *182*, 6410-6417.

Smego, R.A., Frean, J., and Koornhof, H.J. (1999). Yersiniosis I: microbiological and clinicoepidemiological aspects of plague and non-plague Yersinia infections. Eur J Clin Microbiol Infect Dis *18*, 1-15.

Smith, J.A., and Weidemann, M.J. (1993). Further characterization of the neutrophil oxidative burst by flow cytometry. J Immunol Methods *162*, 261-268.

Songsungthong, W., Higgins, M.C., Rolan, H.G., Murphy, J.L., and Mecsas, J. ROS-inhibitory activity of YopE is required for full virulence of Yersinia in mice. Cell Microbiol.

Sory, M.P., and Cornelis, G.R. (1994). Translocation of a hybrid YopE-adenylate cyclase from Yersinia enterocolitica into HeLa cells. Mol Microbiol *14*, 583-594.

Spinner, J.L., Seo, K.S., O'Loughlin, J.L., Cundiff, J.A., Minnich, S.A., Bohach, G.A., and Kobayashi, S.D. Neutrophils are resistant to Yersinia YopJ/P-induced apoptosis and are protected from ROS-mediated cell death by the type III secretion system. PLoS One *5*, e9279.

Srivastava, S., Weitzmann, M.N., Cenci, S., Ross, F.P., Adler, S., and Pacifici, R. (1999). Estrogen decreases TNF gene expression by blocking JNK activity and the resulting production of c-Jun and JunD. J Clin Invest *104*, 503-513.

Srokowski, C.C., Masri, J., Hovelmeyer, N., Krembel, A.K., Tertilt, C., Strand, D., Mahnke, K., Massoumi, R., Waisman, A., and Schild, H. (2009). Naturally occurring short splice variant of CYLD positively regulates dendritic cell function. Blood *113*, 5891-5895.

Stall, A.M., Farinas, M.C., Tarlinton, D.M., Lalor, P.A., Herzenberg, L.A., and Strober, S. (1988). Ly-1 B-cell clones similar to human chronic lymphocytic leukemias routinely develop in older normal mice and young autoimmune (New Zealand Black-related) animals. Proc Natl Acad Sci U S A *85*, 7312-7316.

Stegmeier, F., Sowa, M.E., Nalepa, G., Gygi, S.P., Harper, J.W., and Elledge, S.J. (2007). The tumor suppressor CYLD regulates entry into mitosis. Proc Natl Acad Sci U S A *104*, 8869-8874.

Stice, L.L., Vaziri, C., and Faller, D.V. (1999). Regulation of platelet-derived growth factor signaling by activated p21Ras. Front Biosci *4*, D72-86.

Stokes, A., Wakano, C., Koblan-Huberson, M., Adra, C.N., Fleig, A., and Turner, H. (2006). TRPA1 is a substrate for de-ubiquitination by the tumor suppressor CYLD. Cell Signal *18*, 1584-1594.

Stuart, L.M., and Ezekowitz, R.A. (2005). Phagocytosis: elegant complexity. Immunity *22*, 539-550.

Sumimoto, H., Kage, Y., Nunoi, H., Sasaki, H., Nose, T., Fukumaki, Y., Ohno, M., Minakami, S., and Takeshige, K. (1994). Role of Src homology 3 domains in assembly and activation of the phagocyte NADPH oxidase. Proc Natl Acad Sci U S A *91*, 5345-5349.

Sun, S.C. (2008). Deubiquitylation and regulation of the immune response. Nat Rev Immunol *8*, 501-511.

Sun, S.C., and Ley, S.C. (2008). New insights into NF-kappaB regulation and function. Trends Immunol *29*, 469-478.

Swantek, J.L., Christerson, L., and Cobb, M.H. (1999). Lipopolysaccharide-induced tumor necrosis factor-alpha promoter activity is inhibitor of nuclear factor-kappaB kinase-dependent. J Biol Chem *274*, 11667-11671.

Swantek, J.L., Cobb, M.H., and Geppert, T.D. (1997). Jun N-terminal kinase/stress-activated protein kinase (JNK/SAPK) is required for lipopolysaccharide stimulation of tumor necrosis factor alpha (TNF-alpha) translation: glucocorticoids inhibit TNF-alpha translation by blocking JNK/SAPK. Mol Cell Biol *17*, 6274-6282.

Sweet, C.R., Conlon, J., Golenbock, D.T., Goguen, J., and Silverman, N. (2007). YopJ targets TRAF proteins to inhibit TLR-mediated NF-kappaB, MAPK and IRF3 signal transduction. Cell Microbiol *9*, 2700-2715.

Szabo, S.J., Dighe, A.S., Gubler, U., and Murphy, K.M. (1997). Regulation of the interleukin (IL)-12R beta 2 subunit expression in developing T helper 1 (Th1) and Th2 cells. J Exp Med *185*, 817-824.

Takahashi, M., Rapley, E., Biggs, P.J., Lakhani, S.R., Cooke, D., Hansen, J., Blair, E., Hofmann, B., Siebert, R., Turner, G.*, et al.* (2000). Linkage and LOH studies in 19 cylindromatosis families show no evidence of genetic heterogeneity and refine the CYLD locus on chromosome 16q12-q13. Hum Genet *106*, 58-65.

Takeshige, K., Ito, T., and Sumimoto, H. (1996). Activation of the phagocyte NADPH oxidase. J Toxicol Sci *21*, 291-292.

Tanaka, M., Fuentes, M.E., Yamaguchi, K., Durnin, M.H., Dalrymple, S.A., Hardy, K.L., and Goeddel, D.V. (1999). Embryonic lethality, liver degeneration, and impaired NF-kappa B activation in IKK-beta-deficient mice. Immunity *10*, 421-429.

Taylor, G.A., Feng, C.G., and Sher, A. (2007). Control of IFN-gamma-mediated host resistance to intracellular pathogens by immunity-related GTPases (p47 GTPases). Microbes Infect *9*, 1644-1651.

Thiefes, A., Wolf, A., Doerrie, A., Grassl, G.A., Matsumoto, K., Autenrieth, I., Bohn, E., Sakurai, H., Niedenthal, R., Resch, K., and Kracht, M. (2006). The Yersinia enterocolitica effector YopP inhibits host cell signalling by inactivating the protein kinase TAK1 in the IL-1 signalling pathway. EMBO Rep *7*, 838-844.

Torres, D., Barrier, M., Bihl, F., Quesniaux, V.J., Maillet, I., Akira, S., Ryffel, B., and Erard, F. (2004). Toll-like receptor 2 is required for optimal control of Listeria monocytogenes infection. Infect Immun *72*, 2131-2139.

Trasak, C., Zenner, G., Vogel, A., Yuksekdag, G., Rost, R., Haase, I., Fischer, M., Israel, L., Imhof, A., Linder, S.*, et al.* (2007). Yersinia protein kinase YopO is activated by a novel G-actin binding process. J Biol Chem *282*, 2268-2277.

Trinchieri, G. (1995). Interleukin-12: a proinflammatory cytokine with immunoregulatory functions that bridge innate resistance and antigen-specific adaptive immunity. Annu Rev Immunol *13*, 251-276.

Tripp, C.S., Gately, M.K., Hakimi, J., Ling, P., and Unanue, E.R. (1994). Neutralization of IL-12 decreases resistance to Listeria in SCID and C.B-17 mice. Reversal by IFN-gamma. J Immunol *152*, 1883-1887.

Tripp, C.S., Wolf, S.F., and Unanue, E.R. (1993). Interleukin 12 and tumor necrosis factor alpha are costimulators of interferon gamma production by natural killer cells in severe combined immunodeficiency mice with listeriosis, and interleukin 10 is a physiologic antagonist. Proc Natl Acad Sci U S A *90*, 3725-3729.

Trompouki, E., Hatzivassiliou, E., Tsichritzis, T., Farmer, H., Ashworth, A., and Mosialos, G. (2003). CYLD is a deubiquitinating enzyme that negatively regulates NF-kappaB activation by TNFR family members. Nature *424*, 793-796.

Trompouki, E., Tsagaratou, A., Kosmidis, S.K., Dolle, P., Qian, J., Kontoyiannis, D.L., Cardoso, W.V., and Mosialos, G. (2009). Truncation of the catalytic domain of the cylindromatosis tumor suppressor impairs lung maturation. Neoplasia *11*, 469-476.

Trosky, J.E., Mukherjee, S., Burdette, D.L., Roberts, M., McCarter, L., Siegel, R.M., and Orth, K. (2004). Inhibition of MAPK signaling pathways by VopA from Vibrio parahaemolyticus. J Biol Chem *279*, 51953-51957.

Trulzsch, K., Oellerich, M.F., and Heesemann, J. (2007). Invasion and dissemination of Yersinia enterocolitica in the mouse infection model. Adv Exp Med Biol *603*, 279-285.

Trulzsch, K., Sporleder, T., Igwe, E.I., Russmann, H., and Heesemann, J. (2004). Contribution of the major secreted yops of Yersinia enterocolitica O:8 to pathogenicity in the mouse infection model. Infect Immun *72*, 5227-5234.

Unanue, E.R. (1997). Inter-relationship among macrophages, natural killer cells and neutrophils in early stages of Listeria resistance. Curr Opin Immunol *9*, 35-43.

Utsugi, M., Dobashi, K., Ishizuka, T., Masubuchi, K., Shimizu, Y., Nakazawa, T., and Mori, M. (2003). C-Jun-NH2-terminal kinase mediates expression of connective tissue growth factor induced by transforming growth factor-beta1 in human lung fibroblasts. Am J Respir Cell Mol Biol *28*, 754-761.

Verma, K., Mandal, S., and Kapila, K. (1995). Cystic change in lymph nodes with metastatic squamous cell carcinoma. Acta Cytol *39*, 478-480.

Viboud, G.I., and Bliska, J.B. (2005). Yersinia outer proteins: role in modulation of host cell signaling responses and pathogenesis. Annu Rev Microbiol *59*, 69-89.

Viboud, G.I., Mejia, E., and Bliska, J.B. (2006). Comparison of YopE and YopT activities in counteracting host signalling responses to Yersinia pseudotuberculosis infection. Cell Microbiol *8*, 1504-1515.

Visconti, R., Gadina, M., Chiariello, M., Chen, E.H., Stancato, L.F., Gutkind, J.S., and O'Shea, J.J. (2000). Importance of the MKK6/p38 pathway for interleukin-12-induced STAT4 serine phosphorylation and transcriptional activity. Blood *96*, 1844-1852.

Visser, L.G., Annema, A., and van Furth, R. (1995). Role of Yops in inhibition of phagocytosis and killing of opsonized Yersinia enterocolitica by human granulocytes. Infect Immun *63*, 2570-2575.

Visser, L.G., Seijmonsbergen, E., Nibbering, P.H., van den Broek, P.J., and van Furth, R. (1999). Yops of Yersinia enterocolitica inhibit receptor-dependent superoxide anion production by human granulocytes. Infect Immun *67*, 1245-1250.

Von Pawel-Rammingen, U., Telepnev, M.V., Schmidt, G., Aktories, K., Wolf-Watz, H., and Rosqvist, R. (2000). GAP activity of the Yersinia YopE cytotoxin specifically targets the Rho

pathway: a mechanism for disruption of actin microfilament structure. Mol Microbiol *36*, 737-748.

Wagner, E.F., and Nebreda, A.R. (2009). Signal integration by JNK and p38 MAPK pathways in cancer development. Nat Rev Cancer *9*, 537-549.

Warschkau, H., Yu, H., and Kiderlen, A.F. (1998). Activation and suppression of natural cellular immune functions by Pneumocystis carinii. Immunobiology *198*, 343-360.

Watford, W.T., Hissong, B.D., Bream, J.H., Kanno, Y., Muul, L., and O'Shea, J.J. (2004). Signaling by IL-12 and IL-23 and the immunoregulatory roles of STAT4. Immunol Rev *202*, 139-156.

Watford, W.T., Moriguchi, M., Morinobu, A., and O'Shea, J.J. (2003). The biology of IL-12: coordinating innate and adaptive immune responses. Cytokine Growth Factor Rev *14*, 361-368.

Weidow, C.L., Black, D.S., Bliska, J.B., and Bouton, A.H. (2000). CAS/Crk signalling mediates uptake of Yersinia into human epithelial cells. Cell Microbiol *2*, 549-560.

Weisbrich, A., Honnappa, S., Jaussi, R., Okhrimenko, O., Frey, D., Jelesarov, I., Akhmanova, A., and Steinmetz, M.O. (2007). Structure-function relationship of CAP-Gly domains. Nat Struct Mol Biol *14*, 959-967.

Whitmarsh, A.J., and Davis, R.J. (1996). Transcription factor AP-1 regulation by mitogen-activated protein kinase signal transduction pathways. J Mol Med *74*, 589-607.

Wickstrom, S.A., Masoumi, K.C., Khochbin, S., Fassler, R., and Massoumi, R. CYLD negatively regulates cell-cycle progression by inactivating HDAC6 and increasing the levels of acetylated tubulin. EMBO J *29*, 131-144.

Wright, A., Reiley, W.W., Chang, M., Jin, W., Lee, A.J., Zhang, M., and Sun, S.C. (2007). Regulation of early wave of germ cell apoptosis and spermatogenesis by deubiquitinating enzyme CYLD. Dev Cell *13*, 705-716.

Wright, S.D., and Silverstein, S.C. (1983). Receptors for C3b and C3bi promote phagocytosis but not the release of toxic oxygen from human phagocytes. J Exp Med *158*, 2016-2023.

Wu, C.J., Conze, D.B., Li, T., Srinivasula, S.M., and Ashwell, J.D. (2006). Sensing of Lys 63-linked polyubiquitination by NEMO is a key event in NF-kappaB activation [corrected]. Nat Cell Biol *8*, 398-406.

Wurster, A.L., Tanaka, T., and Grusby, M.J. (2000). The biology of Stat4 and Stat6. Oncogene *19*, 2577-2584.

Wysk, M., Yang, D.D., Lu, H.T., Flavell, R.A., and Davis, R.J. (1999). Requirement of mitogen-activated protein kinase kinase 3 (MKK3) for tumor necrosis factor-induced cytokine expression. Proc Natl Acad Sci U S A *96*, 3763-3768.

Xiao, J., and Chodosh, J. (2005). JNK regulates MCP-1 expression in adenovirus type 19-infected human corneal fibroblasts. Invest Ophthalmol Vis Sci *46*, 3777-3782.

Xue, L., Igaki, T., Kuranaga, E., Kanda, H., Miura, M., and Xu, T. (2007). Tumor suppressor CYLD regulates JNK-induced cell death in Drosophila. Dev Cell *13*, 446-454.

Yamamori, T., Inanami, O., Nagahata, H., Cui, Y., and Kuwabara, M. (2000). Roles of p38 MAPK, PKC and PI3-K in the signaling pathways of NADPH oxidase activation and phagocytosis in bovine polymorphonuclear leukocytes. FEBS Lett *467*, 253-258.

Yamamori, T., Inanami, O., Sumimoto, H., Akasaki, T., Nagahata, H., and Kuwabara, M. (2002). Relationship between p38 mitogen-activated protein kinase and small GTPase Rac for the activation of NADPH oxidase in bovine neutrophils. Biochem Biophys Res Commun *293*, 1571-1578.

Yamamoto, K., and Johnston, R.B., Jr. (1984). Dissociation of phagocytosis from stimulation of the oxidative metabolic burst in macrophages. J Exp Med *159*, 405-416.

Yamamoto, M., Okamoto, T., Takeda, K., Sato, S., Sanjo, H., Uematsu, S., Saitoh, T., Yamamoto, N., Sakurai, H., Ishii, K.J.*, et al.* (2006). Key function for the Ubc13 E2 ubiquitin-conjugating enzyme in immune receptor signaling. Nat Immunol *7*, 962-970.

Yamauchi, A., Yu, L., Potgens, A.J., Kuribayashi, F., Nunoi, H., Kanegasaki, S., Roos, D., Malech, H.L., Dinauer, M.C., and Nakamura, M. (2001). Location of the epitope for 7D5, a monoclonal antibody raised against human flavocytochrome b558, to the extracellular peptide portion of primate gp91phox. Microbiol Immunol *45*, 249-257.

Yanisch-Perron, C., Vieira, J., and Messing, J. (1985). Improved M13 phage cloning vectors and host strains: nucleotide sequences of the M13mp18 and pUC19 vectors. Gene *33*, 103-119.

Yao, T., Mecsas, J., Healy, J.I., Falkow, S., and Chien, Y. (1999). Suppression of T and B lymphocyte activation by a Yersinia pseudotuberculosis virulence factor, yopH. J Exp Med *190*, 1343-1350.

Yoshida, A., Koide, Y., Uchijima, M., and Yoshida, T.O. (1994). IFN-gamma induces IL-12 mRNA expression by a murine macrophage cell line, J774. Biochem Biophys Res Commun *198*, 857-861.

Yoshida, H., Jono, H., Kai, H., and Li, J.D. (2005). The tumor suppressor cylindromatosis (CYLD) acts as a negative regulator for toll-like receptor 2 signaling via negative cross-talk with TRAF6 AND TRAF7. J Biol Chem *280*, 41111-41121.

Yu, L., Zhen, L., and Dinauer, M.C. (1997). Biosynthesis of the phagocyte NADPH oxidase cytochrome b558. Role of heme incorporation and heterodimer formation in maturation and stability of gp91phox and p22phox subunits. J Biol Chem *272*, 27288-27294.

Zarnegar, B., He, J.Q., Oganesyan, G., Hoffmann, A., Baltimore, D., and Cheng, G. (2004). Unique CD40-mediated biological program in B cell activation requires both type 1 and type 2 NF-kappaB activation pathways. Proc Natl Acad Sci U S A *101*, 8108-8113.

Zarnegar, B.J., Wang, Y., Mahoney, D.J., Dempsey, P.W., Cheung, H.H., He, J., Shiba, T., Yang, X., Yeh, W.C., Mak, T.W.*, et al.* (2008). Noncanonical NF-kappaB activation requires

coordinated assembly of a regulatory complex of the adaptors cIAP1, cIAP2, TRAF2 and TRAF3 and the kinase NIK. Nat Immunol *9*, 1371-1378.

Zhang, J., Stirling, B., Temmerman, S.T., Ma, C.A., Fuss, I.J., Derry, J.M., and Jain, A. (2006). Impaired regulation of NF-kappaB and increased susceptibility to colitis-associated tumorigenesis in CYLD-deficient mice. J Clin Invest *116*, 3042-3049.

Zhang, M., Wu, X., Lee, A.J., Jin, W., Chang, M., Wright, A., Imaizumi, T., and Sun, S.C. (2008). Regulation of IkappaB kinase-related kinases and antiviral responses by tumor suppressor CYLD. J Biol Chem *283*, 18621-18626.

Zhang, S., and Kaplan, M.H. (2000). The p38 mitogen-activated protein kinase is required for IL-12-induced IFN-gamma expression. J Immunol *165*, 1374-1380.

Zhang, Y., Reynolds, J.M., Chang, S.H., Martin-Orozco, N., Chung, Y., Nurieva, R.I., and Dong, C. (2009). MKP-1 is necessary for T cell activation and function. J Biol Chem *284*, 30815-30824.

Zhang, Y.L., and Dong, C. (2005). MAP kinases in immune responses. Cell Mol Immunol *2*, 20-27.

Zhang, Z., Harms, E., and Van Etten, R.L. (1994). Asp129 of low molecular weight protein tyrosine phosphatase is involved in leaving group protonation. J Biol Chem *269*, 25947-25950.

Zhong, S., Fields, C.R., Su, N., Pan, Y.X., and Robertson, K.D. (2007). Pharmacologic inhibition of epigenetic modifications, coupled with gene expression profiling, reveals novel targets of aberrant DNA methylation and histone deacetylation in lung cancer. Oncogene *26*, 2621-2634.

Zhou, H., Monack, D.M., Kayagaki, N., Wertz, I., Yin, J., Wolf, B., and Dixit, V.M. (2005a). Yersinia virulence factor YopJ acts as a deubiquitinase to inhibit NF-kappa B activation. J Exp Med *202*, 1327-1332.

Zhou, J., Li, Y., Liang, P., Yuan, W., Ye, X., Zhu, C., Cheng, Y., Wang, Y., Li, G., Wu, X., and Liu, M. (2005b). A novel six-transmembrane protein hhole functions as a suppressor in MAPK signaling pathways. Biochem Biophys Res Commun *333*, 344-352.

Zou, J., Presky, D.H., Wu, C.Y., and Gubler, U. (1997). Differential associations between the cytoplasmic regions of the interleukin-12 receptor subunits beta1 and beta2 and JAK kinases. J Biol Chem *272*, 6073-6077.

Zumbihl, R., Aepfelbacher, M., Andor, A., Jacobi, C.A., Ruckdeschel, K., Rouot, B., and Heesemann, J. (1999). The cytotoxin YopT of Yersinia enterocolitica induces modification and cellular redistribution of the small GTP-binding protein RhoA. J Biol Chem *274*, 29289-29293.

8. ABBREVIATIONS

α Anti

Amp ampicillin

APC allophycocyanin

BCR B cell receptor

ß-me ß-mercaptoethanol

bp base pair

BSA bovine serum albumin

°C temperature in degrees Celsius

Ca Calcium

CD cluster of differentiation

CFU Colony Forming Units

CO_2 Carbon dioxide

Conz. Concentration

cpm counts per minute

Cre site-specific recombinase (causes recombination)

C region constant region

dH_2O Distilled Water

dNTP desoxyribonucleotide-triphosphate

DMEM Dulbecco's modified Eagle medium

DMSO Dimethyl sulfoxide

DNA desoxyribonucleic acid

ds double-stranded

EDTA ethylene-diaminetetraacetic acid

e.g. Example

EGTA Ethylene glycol tetraacetic acid

ERK Extracellular signal-regulated kinases

et al. And others

EtBr ethidium bromide

FACS Fluorescence-activated cell sorting

FBS Fetal bovine serum

FCS Fetal calf serum

FITC Fluorescein isothiocyanate

FSC Forward scatter

g gram

GMFI Geometric Mean Fluorescence Intensity

h hour/s

i.e. That is

Ig Immunoglobulin

i.p. intraperitoneally

IPTG Isopropyl β-D-1-thiogalactopyranoside

JNK c-Jun N-terminal kinases

kb kilobase

kD/ kDa kilodalton

l liter

LB Luria-Bertani medium

loxP recognition sequence for Cre (locus of x-ing over of phage P1)

m milli (10^{-3})

M Molar (mol/l)

mAb Monoclonal antibodies

MHC major histocompatibility locus

mg Milligram

min minute

ml milliliter

mM millimolar

MOI Multiplicity Of Infection

MW Molecular weight

μl microliter

μM micromolar

NaCl sodium chloride

NaOH sodium hydroxide

neo neomycin resistance gene

nm Nanometer

OD Optical density

% percent

PBS phosphate buffered saline

PCR polymerase chain reaction

PE phycoerythrine

PFA Paraformaldehyde

PMN Polymorphonuclear leukocytes

rpm Revolution per minute

RT Room temperature

RNA ribonucleic acid

RU relative units

sec Seconds

SDS sodium dodecyl sulfate

ss single-stranded

SSC sodium chloride/ sodium citrate buffer

TAE Tris-acetic acid-EDTA buffer

Taq Pol polymerase from *Thermus aquaticus*

TCR T cell receptor

TE Tris-EDTA buffer

TEMED Tetramethylethylenediamine

TRIS Tris-(hydroxymethyl)-aminomethane

TRIS-HCl Tris-(hydroxymethyl)-aminomethane-hydrochloride

TWEEN polyoxyethylene-sorbitan-monolaureate

µ Micro

U units

µg Microgram

µl Microlitre

UV ultraviolet

V Volts

Vol volume

v/v Volume percent

WT Wild-type

w/v Weight per volume

w/w Weight percent

9. ACKNOWLEDGEMENTS

10. Publications

1. Hicham Bouabe, **<u>Yunying Liu</u>**,Markus Moser, Michael R. Bösl and Jürgen Heesemann (2011) Novel highly sensitive IL-10-beta-lactamase reporter mouse reveals cells of the innate immune system as a substantial source of IL-10 in vivo. J. Immunol. 187(6):3165-76.

2. **<u>YunYing Liu</u>**, Ramin Massoumi, Reinhard Fässler, Jürgen Heesemann, Hicham Bouabe (2012) Contribution of the tumor suppressor CYLD to susceptibility to *Yersinia enterocolitica* infection by promoting Yops-mediated anti-host functions (manuscript in revision).

11. Curriculum Vitae

Personal information:

Name: Yunying Liu

Gender: Female

Date of Birth: 18.07.1979

Birth place: Qingdao, Shandong Province, P.R. China

Nationality: Chinese

Education:

Sep 2007- Mar 2010: **Ph.D. thesis** in Max-von-Pettenkofer-Institute, Ludwig-Maximilians-University (Munich, Germany) under the Sandwich PhD-Programme between the LMU-Munich and "Chinese Scholarship Council".
The title of the Ph.D. thesis is: "**The role of the Tumor suppressor CYLD in *Yersinia enterocolitica* infection**".

Sep 2003-Sep 2007: **Master-PhD study (Medical Microbiology)**, School of Medicine, Zhejiang University, Hangzhou, P.R. China
The title of the Master-PhD thesis is: "**Pathogenesis of Leptospirosis: Interaction of *Leptospira interrogans* with *in vitro* cultured Mammalian cells**".

Sep 1998-July 2003: **Bachelor of medicine (Clinical medicine)**, School of Medicine, Qingdao University, Qingdao, P.R. China

Sep 1994-July 1998: **High school**, Jiaozhou erzhong, P.R. China